

平成 23 年度

修 士 論 文

Fundamental Study on Dynamic Behaviors of the Parthenon Athens

指導教員 花里利一 教授

三重大学大学院工学研究科
建築学専攻

大村真理子

Fundamental Study on Dynamic Behaviors of the Parthenon Athens

Contents

| | | |
|-----------|--|----|
| Chapter 1 | Introduction | 3 |
| 1.1 | Abstract | 3 |
| 1.2 | Background | 3 |
| 1.3 | Purpose | 3 |
| 1.4 | Past Studies | 4 |
| 1.5 | Damage Caused by the Past Earthquakes | 5 |
| Chapter 2 | Microtremor Measurement and Earthquake Monitoring | 7 |
| 2.1 | Microtremor Measurement | 7 |
| 2.2 | Earthquake Monitoring | 15 |
| 2.3 | Concluding Remarks | 15 |
| Chapter 3 | Simulation of the Ground Motion at the base of the Acropolis hill | 17 |
| 3.1 | Introduction | 17 |
| 3.2 | Overviews of the Past earthquakes | 17 |
| 3.3 | Target Acceleration Response Spectra and Phases | 19 |
| 3.4 | Simulated Earthquake Motions | 23 |
| 3.5 | Concluding Remarks | 23 |
| Chapter 4 | Shake Table Tests on a Simplified Miniature Model of the Parthenon | 26 |
| 4.1 | Introduction | 26 |
| 4.2 | Phase 1 | 26 |
| 4.2.1 | Model Description | 26 |
| 4.2.2 | Experimental Setup | 29 |
| 4.2.3 | Exciting Input Motions | 30 |
| 4.2.4 | Results | 32 |
| 4.3 | Phase 2 | 36 |
| 4.3.1 | Suggestions of Reinforcement | 36 |
| 4.3.2 | Model Description | 36 |
| 4.3.3 | Experimental Setup | 36 |
| 4.3.4 | Seismic Input Motions | 36 |
| 4.3.5 | Results | 39 |
| 4.4 | Concluding remarks | 52 |

| | | |
|----------------------|--|------------|
| Chapter 5 | Structural Analysis | 53 |
| 5.1 | Introduction..... | 53 |
| 5.2 | Analysis Model | 53 |
| 5.3 | Identification of the Model Parameters..... | 55 |
| 5.4 | Seismic Input Ground Motion..... | 57 |
| 5.5 | Analysis Results..... | 62 |
| 5.5.1 | Mechanical Reason of Residual Displacement | 65 |
| 5.6 | Concluding Remarks..... | 66 |
| Chapter 6 | Conclusions | 67 |
| 6.1 | Summary of the Study | 67 |
| 6.2 | Future Studies | 68 |
| Acknowledgment | | 69 |
| References..... | | 70 |
| Appendix..... | | Appendix 1 |

Chapter 1 Introduction

1.1 Abstract

This thesis describes field survey, experiments and analysis in order to understand the dynamic behavior of the Parthenon on the Acropolis in Athens.

The natural frequencies of the colonnades of the monument were evaluated as the fundamental characteristics based on micro-tremor measurements. Furthermore, one earthquake was recorded in 2010 by accelerographs installed by the authors; however, it was too small to study the topographical effect of the Acropolis hill where the monument is standing.

The ground motions at the foot of the Acropolis hill were simulated and used for shake table tests and seismic response analysis of the monument. The ground accelerations of the Corinth earthquake of 1981 and Athens earthquake of 1999 were simulated and these motions were used for structural analysis.

Shaking table tests were carried out with the simplified miniature model of the monument. As results, residual displacement pattern of the monument caused by Corinth earthquake was successfully reproduced. Furthermore, the mechanisms of the displacement pattern were discussed.

Finally, equivalent linear analysis was conducted. As results, the behavior of the Parthenon was discussed.

1.2 Background

The Parthenon Athens has survived against many earthquakes during its long history; about 25 centuries despite Greece is located in a seismic region around the Mediterranean coast. Accordingly, it seems that the monument has excellent seismic performance. However, it was damaged slightly by the recent earthquakes. In addition, its dynamic performance was not known well. It is necessary to study and understand the dynamic behavior of the monument for the restoration and preservation process.

International collaborative research had been established with the National Technical University of Athens (NTUA) since 2008. The prediction of the seismic response of the monument and the proposal of the reinforce technique is main purpose of this research. The seismographs were installed at the base and on the beams of the Parthenon in Sep. 2008 to observe the behaviors of the Parthenon under seismic motions. However, useful record to study the seismic performance of the monument or topographical effect of the Acropolis hill where the monument is standing has not been recorded yet.

1.3 Purpose

The scope of the present international collaborative research is to study the dynamic behaviors of the Parthenon Athens toward the proposal for the anti-seismic structural restoration. Although it has structurally survived for 25 centuries against earthquakes, the recent large earthquake caused the significant damage with the residual displacement to the entablature. In the present research, therefore,

the mechanical reason of such damage was demonstrated from an earthquake point of view, as it would be expected that the outcome of this study could give useful knowledge to the restoration project ongoing.

1.4 Past Studies

1980s, Hanazato et.al conducted Seismic response analysis of the Parthenon's columns in order to study their feasibility to safely withstand anticipated earthquake ground motions [1, 2 and 3]. The masonry columns were firstly modeled by using lumped mass system with both translational and rotational degrees of freedom. Three types of models were used for the analysis. The parameters for the analysis model were identified from the microtremor analysis of Temple of Olympian Zeus Athens [4]. As results, the natural periods of the Parthenon's columns were estimated. Then, liner response analysis was performed to examine the earthquake resistant capacity against the synthetic ground motions corresponding to return period of 100 and 1000 years [5]. The analytical results indicate that the Parthenon is not enough safe against the anticipated ground motions derived probabilistically for both return periods. However, the columns of the monument have fundamental periods; which are longer than the predominant periods, of the ground motions; 0.10s and it was concluded that the integrity of the Parthenon may be owed to the fact that the frequency characteristics of the earthquake motions at the top of the Acropolis hill did not coincide with those of the monument [1, 2 and 3]. Moreover, the experiments by Y. Mabuchi et al. indicated that replacing old timber shear keys inserted between marble drums by new ones is enough for restoration [6]. And the result has been referred to in present restoration project.

G. C. Manos presented results and conclusions from experimental study that examines the dynamic response of rigid bodies, representing simple models of ancient columns or colonnades with or without the insertion of wires made of shape memory alloy (SMA) [7]. As results, the dynamic performance of the models structures, that is of the single column, of the model colonnade with two columns and of the model colonnade with four columns, exhibited similar trends, in terms of stability. Furthermore, it was concluded that the insertion of the SMA wires had a noticeable favorable influence on the stability of the model formations. The model structures with the insertion of the SMA wires developed stable response at amplitudes higher than those at which the models without SMA wires had already overturned.

H. P. Mousakis et al. reported experimental results concerning the earthquake response of marble model which was 1:3 scale of the column of the Parthenon [8]. It was found that the behavior of such a multi-drum marble column is very sensitive; the response of the model varied according to even trivial perturbation of the geometry, small changes of the initial conditions or input motion characteristics. Then, Numerical prediction of the earthquake response of a multi-drum marble model of a classical column was performed using the distinct element method by Papantonopoulos et al. [9]. The results were compared with above-mentioned experimental data and showed that the distinct element method

can capture the main features of the response quite well. It was confirmed that the method can be used with confidence in the restoration process of ancient monuments to estimate the response to expected earthquake motions.

Caddemi S. et al. evaluated the seismic risk of the Concordia temple in Agrigento (Italy) [10]. A general methodology to assess the seismic vulnerability, to be applied also to any kind of structure composed of stone blocks was proposed. The vulnerability assessment has been conducted by equivalent nonlinear static analyses along the principal directions of the structure and the subsequent identification of equivalent single degree of freedom system. Furthermore, the seismic vulnerability has been expressed both in a deterministic and a probabilistic context, the first by means of the evaluation of risk coefficient and the latter by evaluating the severe damage probability.

1.5 Damage Caused by the Past Earthquakes

The deformation of the monument caused by the Athens earthquake of 1999 and the Corinth earthquake of 1981 is mentioned here. According to reference [11 and 12], after the earthquake of 1999, *“the width of the crack in the exterior south architrave block of the SW corner, caused by the earthquake of February 24, 1981 was increased.”* And after the earthquake of 1981, *“The entablatures of the four corners were expanded outside (Fig. 1-1). The cracks in the marble and the gaps in the marble blocks were extended. Extension of the gap in the NE marble blocks which was unstable before; maximum length of 2.5cm (1 in Fig. 1-1). The NE corner column revolved horizontally and inclined. The SE corner column (2 in Fig. 1-1) revolved vertically. The entablature of the NW corner (3 in Fig. 1-1) and the SW corner (4 in Fig. 1-1) had gaps. Two bronze elements for joints, inserted at the 1973 restoration work, were cracked. The horizontally expansion on the upper part of the beams (6 in Fig. 1-1) were maximum length of 36mm. The 5th column from the SE (7 in Fig. 1-1) inclined outside. The gap on the vertical joint of the member of the architrave. Many slippages and marks of revolution on the drums of the colonnade, it was found extended cracks which were before on some of them.”*

The following figs show the deformation of the monument after the earthquakes of 1981.

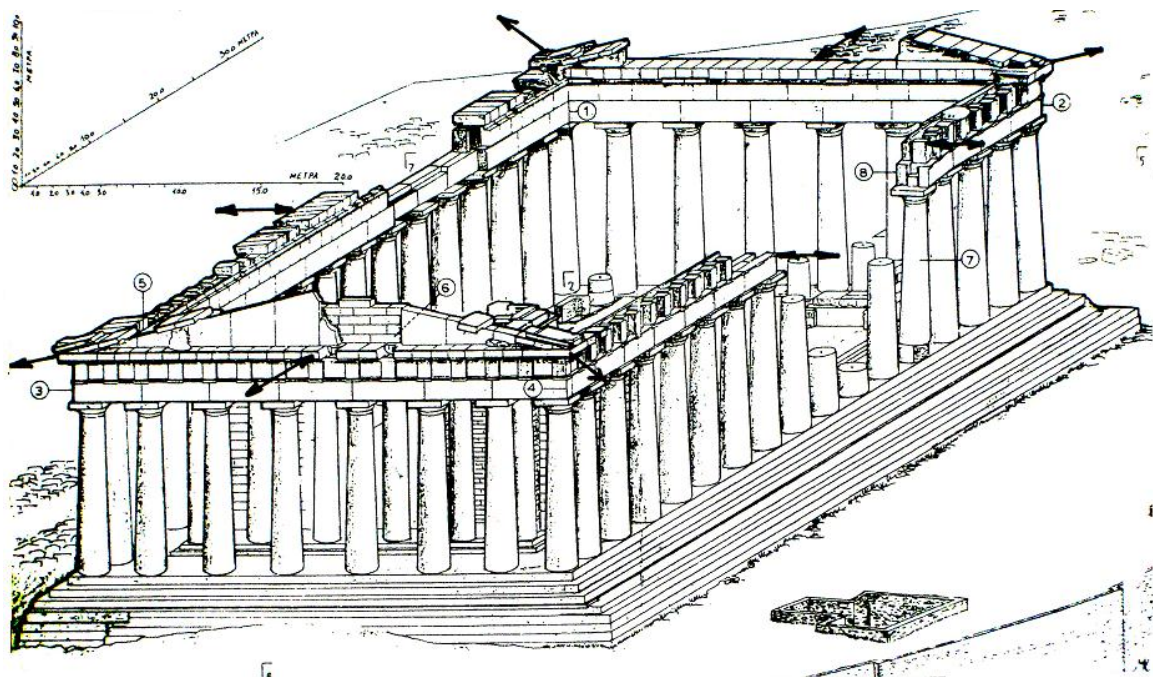


Fig. 1-1 Axonometric projection of the Parthenon [12]

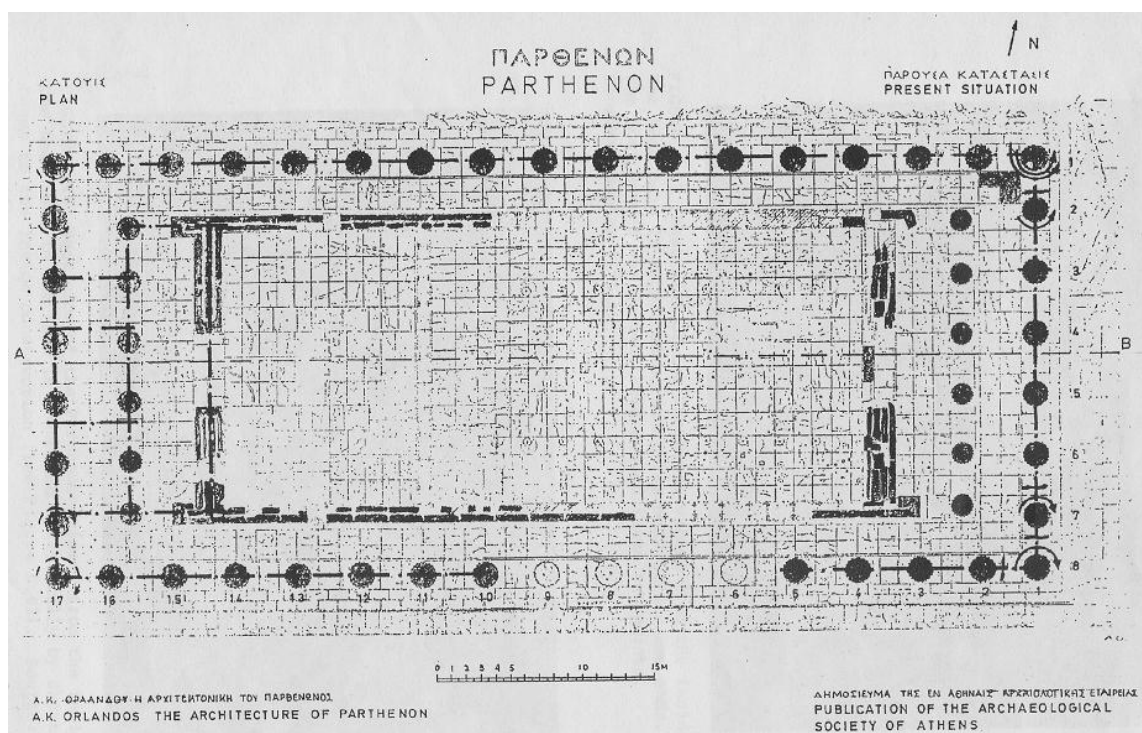


Fig. 1-2 The Parthenon after the earthquakes of 1981 [11]

“The arcs with arrows indicate rotations of the top in relation to the bottom. The lines indicate cracks of the head beams after the recent earthquakes. The dotted and dashed lines indicate horizontal beams at the top.”

Chapter 2 Microtremor Measurement and Earthquake Monitoring

2.1 Microtremor Measurement

Measurements of microtremor were carried out by using a total of 6 microtremor sensors, shown in Fig.2-1. Sampling duration was 60 seconds for each record with sampling frequency of 100 Hz. A portable monitoring equipment of SPC-51A (Tokyo Sokushin Co., Ltd.) was used in the present research.

Fig.2-2 shows the arrangements of the micro-tremor sensors at the west, east and north colonnades. A sensor of CH1 was placed on the base, while the other sensors from CH2 to 6 were arranged the top of the frieze. Transfer functions from the base to the top of the beam were calculated to obtain the natural frequencies in both in-plane and out-of-plane directions.

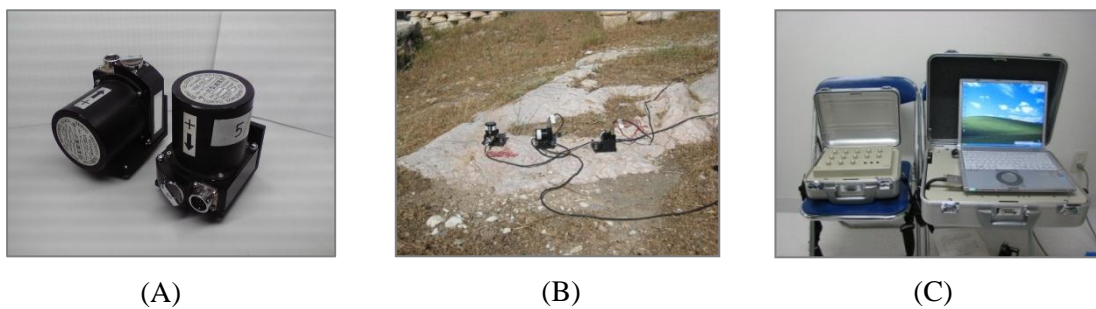


Fig. 2-1 A, B) Microtremor sensors, and C) Recording unit

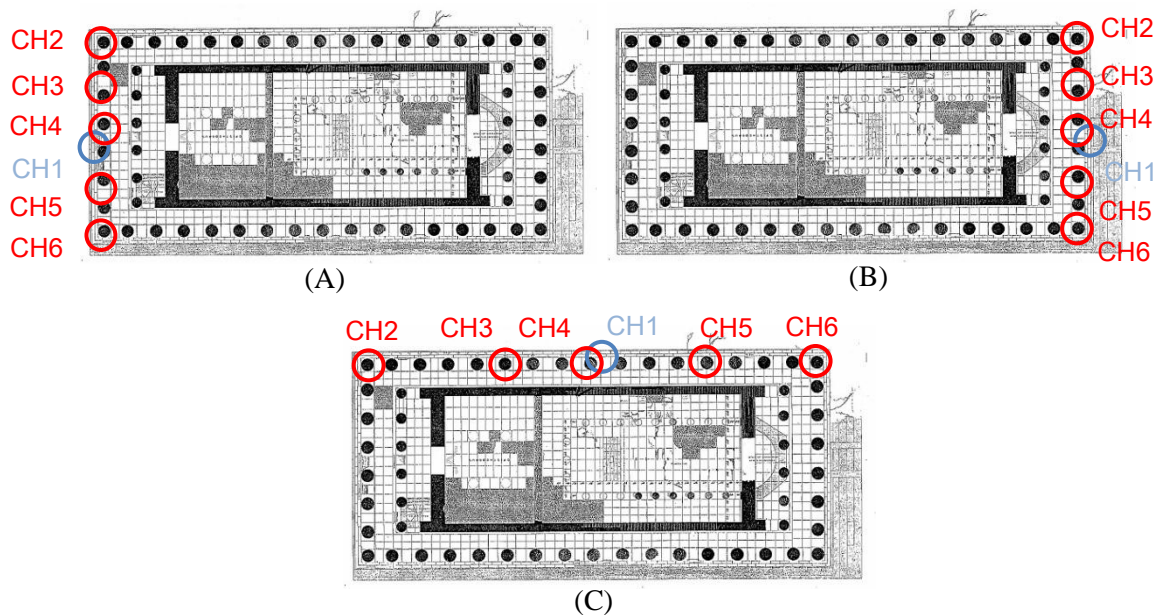


Fig. 2-2 Arrangement of the microtremor sensors at A) the west colonnade, B) the east colonnade, and C) the north colonnade

Figs.2-3 shows the transfer function at the west colonnade in its in-plane direction. It can be recognized that the natural frequency of the west colonnade is about 3.3 Hz in this direction. On the other hand, spectral peaks, shown in Figs.2-4, were affected by the sensor's location in out-of-plane direction. In these figures, there found a predominant peak at 2.4 Hz in the spectra observed at the measuring points in the middle (CH3, 4 and 5) of the west colonnade.

It can be found in Figs.2-5 that the natural frequency of the east colonnade was 3.7 Hz in in-plane direction. The natural frequency of this colonnade in out-of-plane direction was also found to be 2.7 Hz shown in Figs.2-6.

Transfer function of the micro tremor records at the north colonnade showed that the natural frequency was 3.7 Hz for the in-plane behavior, shown in Figs.2-7. On the other hand, the natural frequency for the out of-plane behavior was not observed clearly, shown in Figs.2-8.

The past study conducted by Hanazato *et al.* [1, 2 and 3] showed that the natural frequencies of the west colonnades were 1.7Hz and 3.7Hz, in out-of plane and in plane directions, respectively. The measured natural frequency in in-plane direction is in roughly agreement with the past analytical study. On the other hand, there was significant difference in natural frequencies in out-of plane directions between the analysis and the measurement. Hence, its reason was discussed as the followings. Uniform deformation of the beam in out-of plane direction was assumed in the analysis model introduced in the past study. In this assumption, the effect of the constraint at the both corners connecting perpendicularly to the neighboring colonnades was ignored. However, the actual behaviors (natural frequency and mode) of the colonnades were structurally affected by the boundary conditions at the both corners. Such difference in the boundary condition caused difference in the natural frequencies.

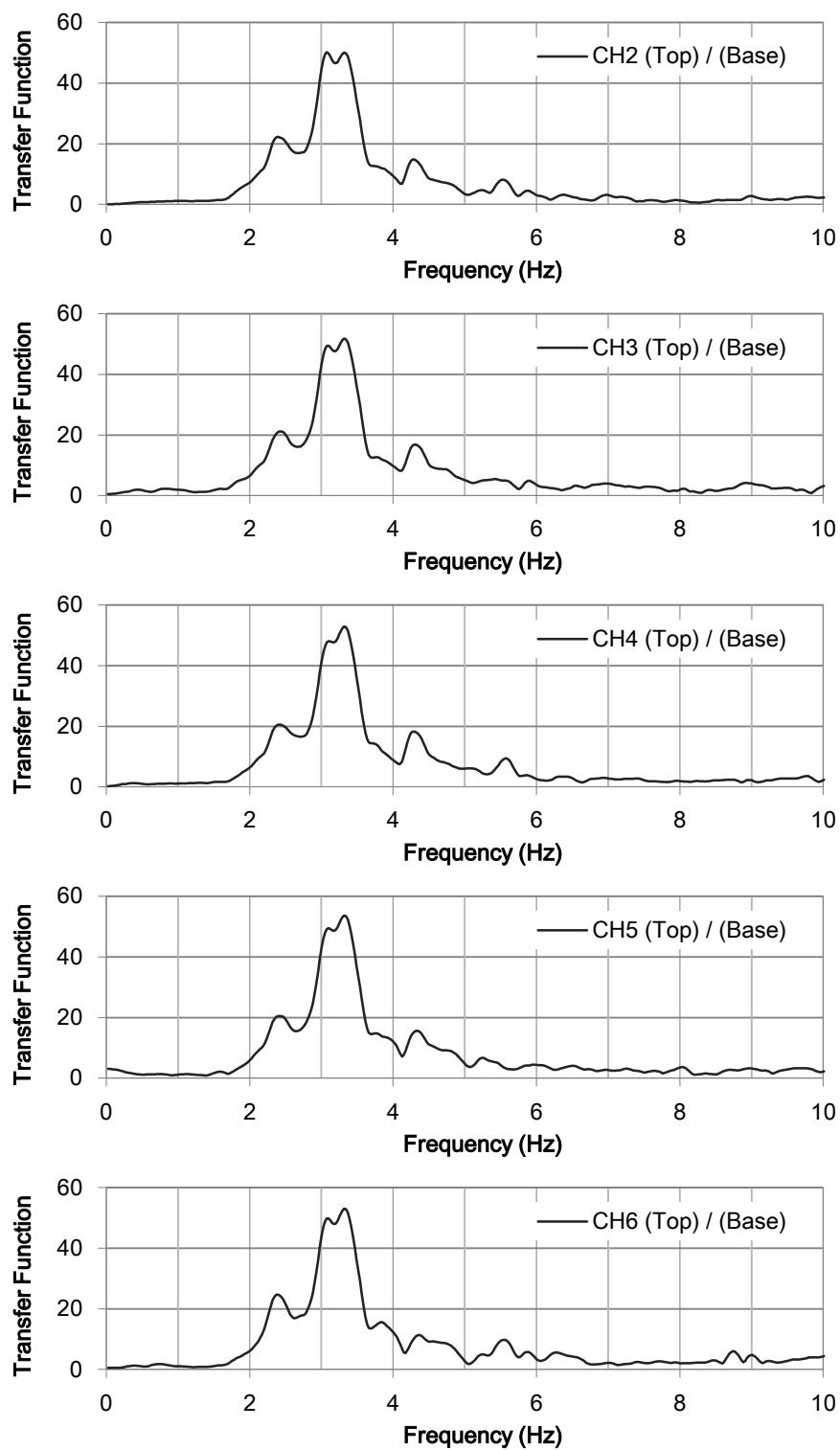


Fig. 2-3 Transfer function of the west colonnade in in-plane direction

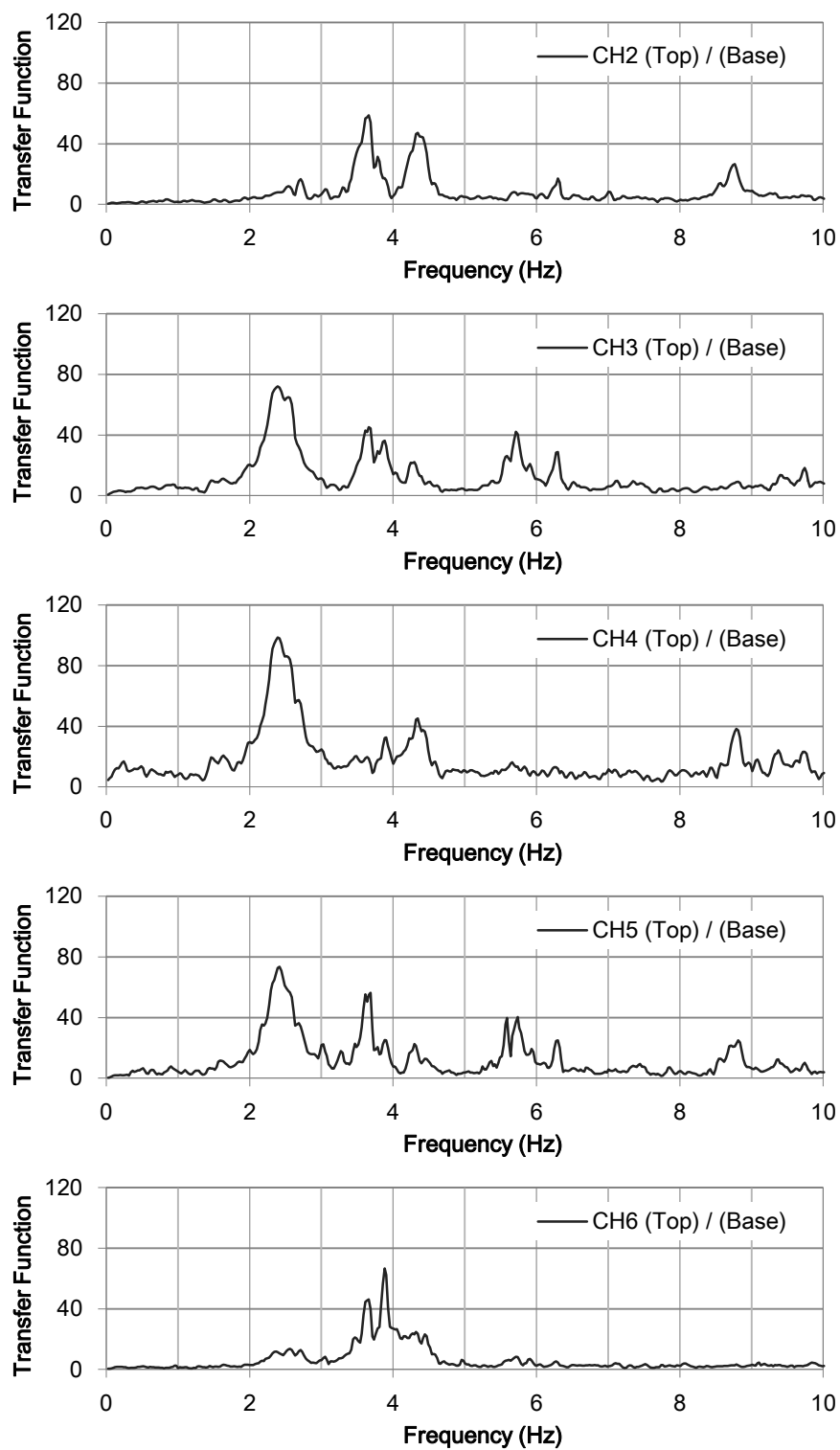


Fig. 2-4 Transfer function of the west colonnade in out-of-plane direction

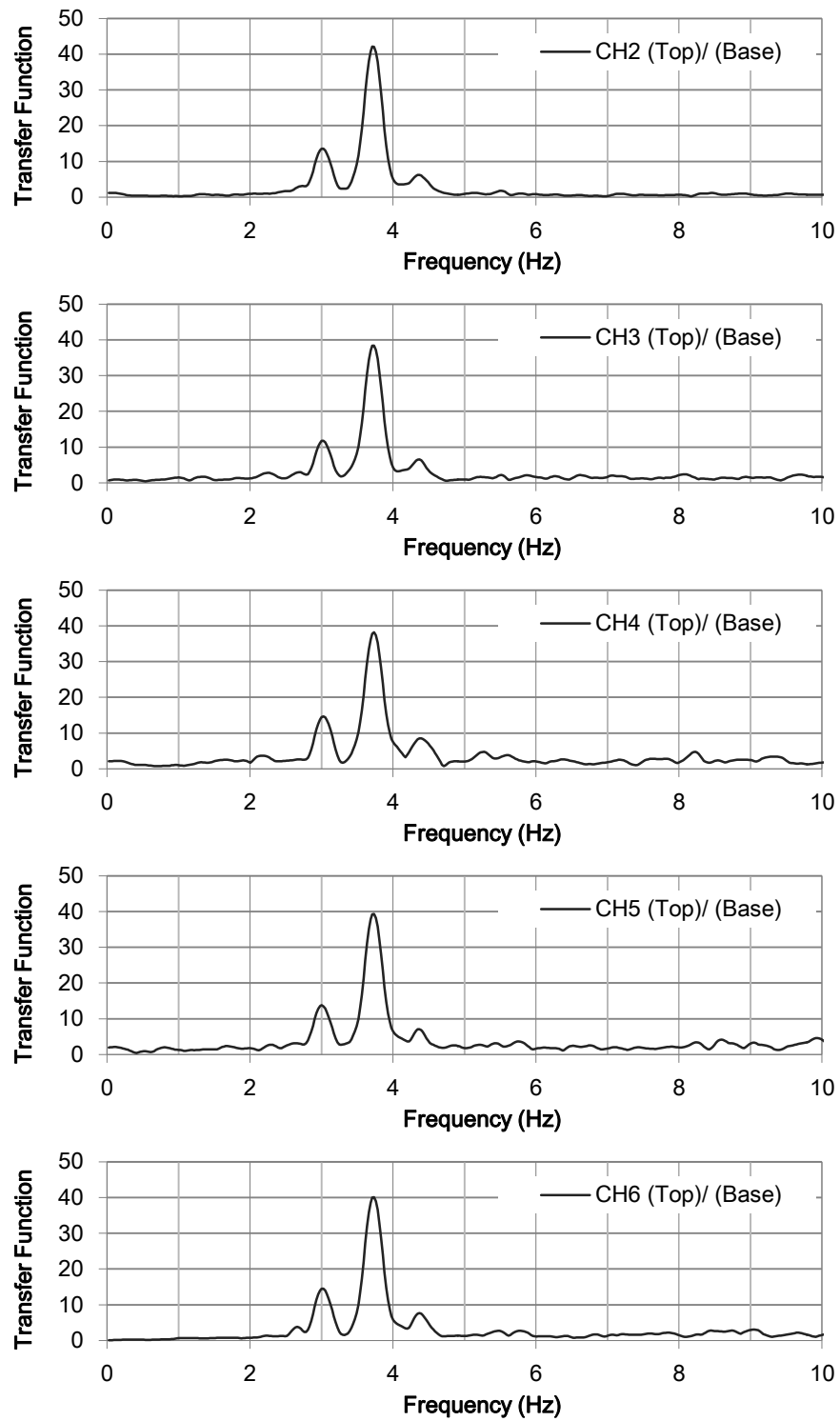


Fig. 2-5 Transfer function of the east colonnade in in-plane direction

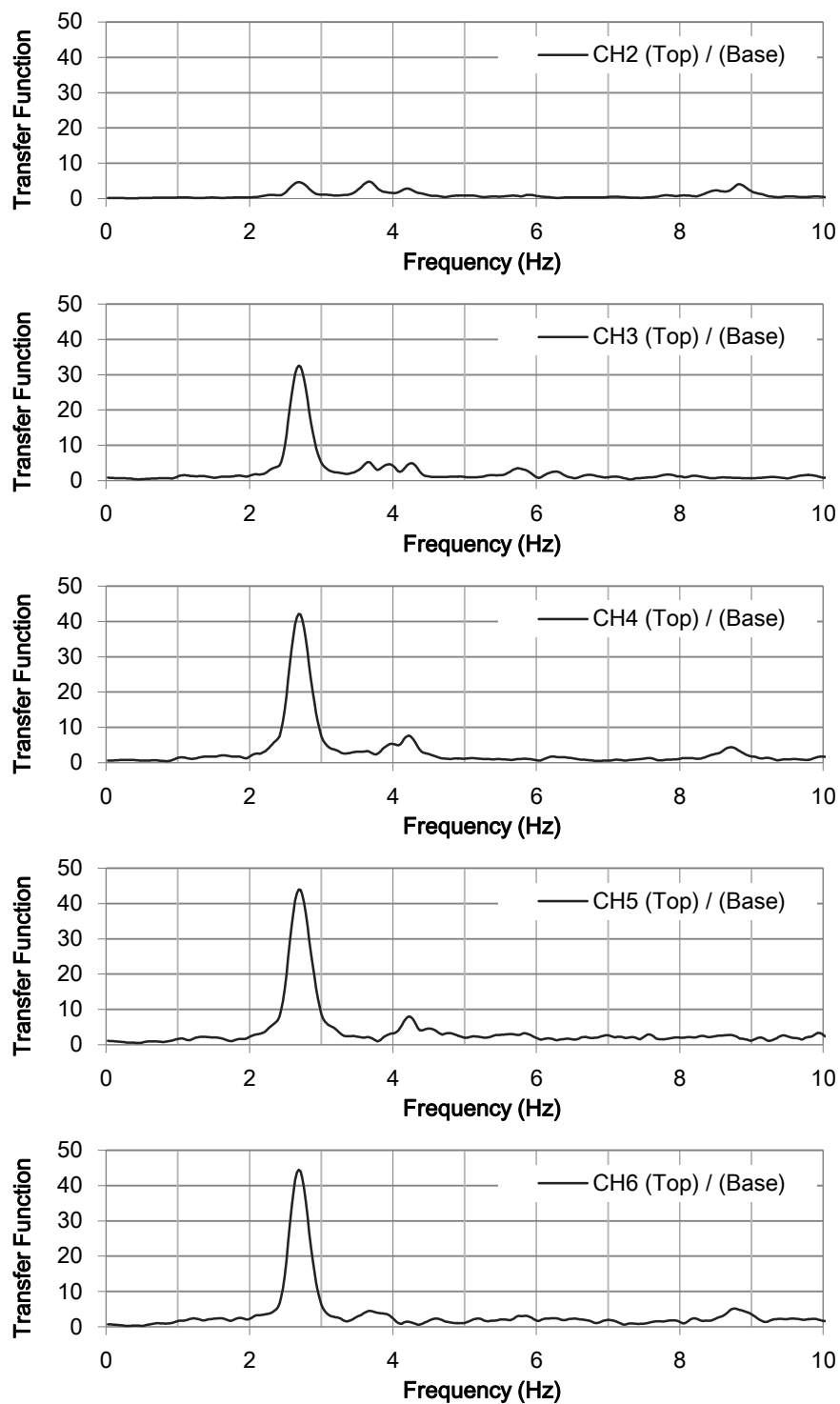


Fig. 2-6 Transfer function of the east column in out-of-plane direction

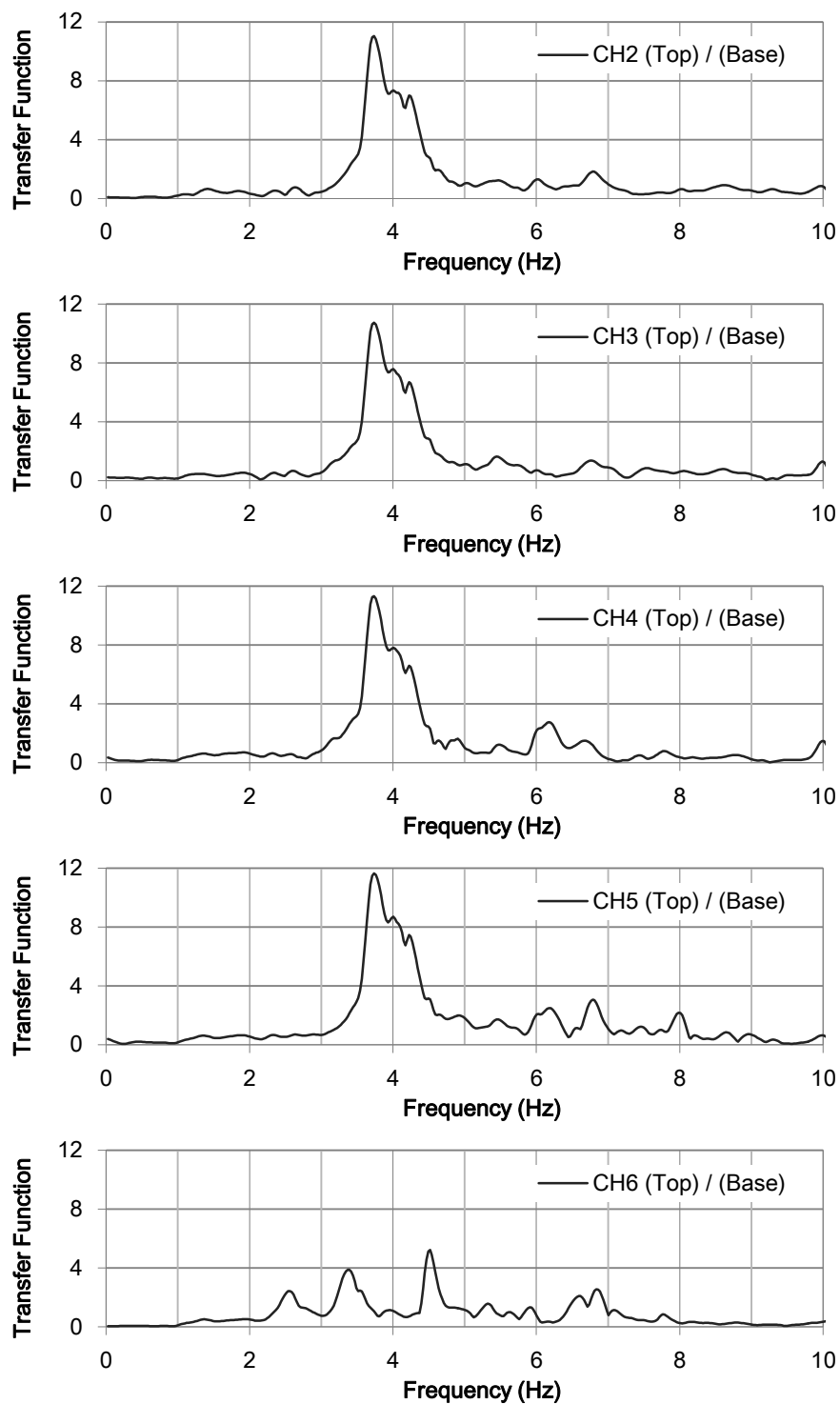


Fig. 2-7 Transfer function of the north colonnade in in-plane direction

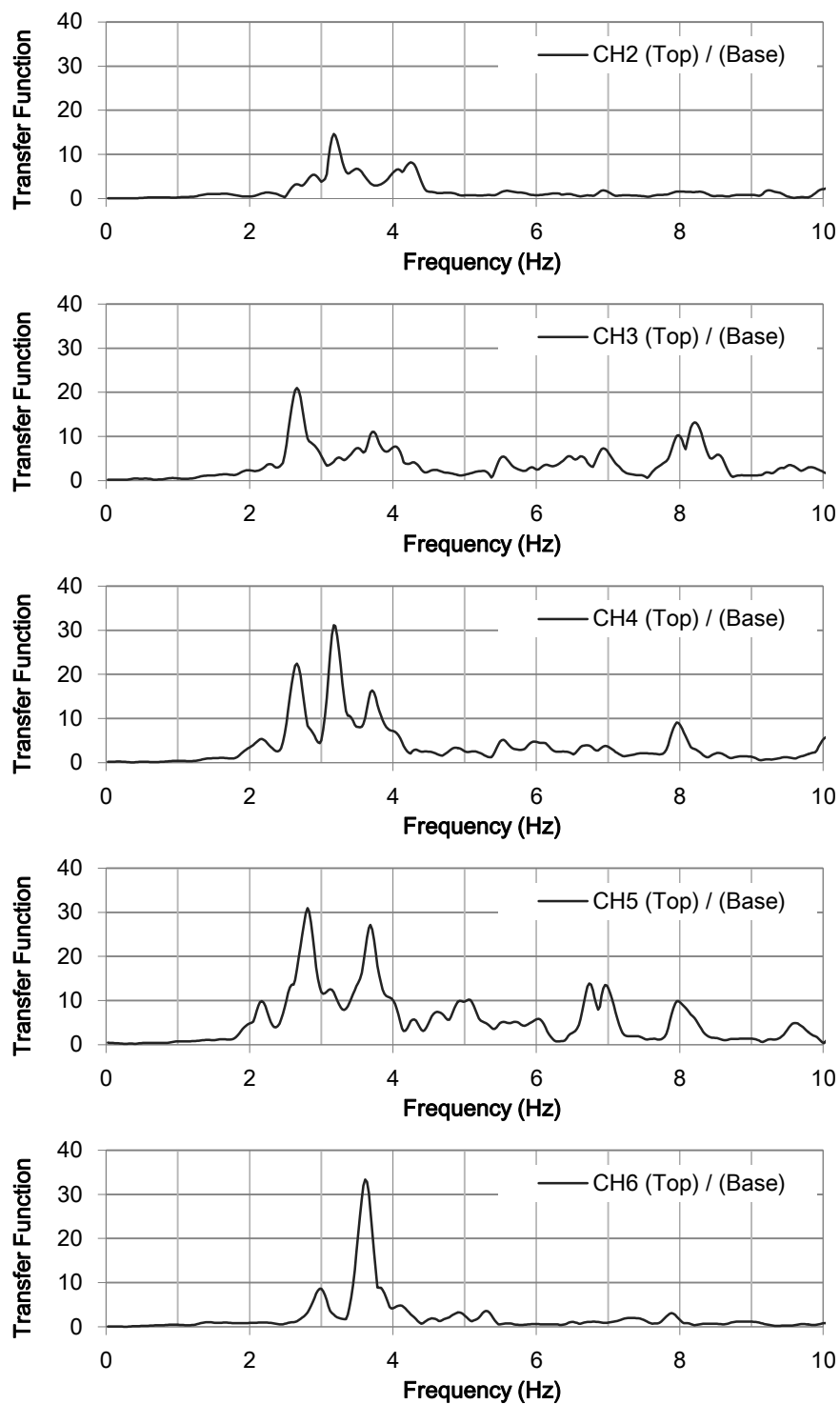


Fig. 2-8 Transfer function of the north colonnade in out-of-plane direction

2.2 Earthquake Monitoring

In September, 2008, two seismograms for earthquake monitoring were installed at the base (master sensor) and at the roof (slave sensor) of the north-east corner, shown in Fig.2-9.

On 2nd of September, 2010, a small earthquake was recorded at the base (see Fig. 2-10). The amplitude of that earthquake record was as small as 0.0007G. The predominant period was found in the response spectra at 0.5s. However, the topographical effect of Acropolis hill on the ground motions still remains as a subject to be studied.

For assessment of the seismic safety of the Parthenon Athens, not only micro-tremor measurements but also such earthquake monitoring is essential from an earthquake engineering point of view. It is expected that, in the near future, earthquake data at appropriate level will be recorded at the Parthenon site.



Fig. 2-9 Servo accelerographs. (A) Master sensor, and (B) Slave sensor

2.3 Concluding Remarks

The microtremor measurements revealed the fundamental natural frequencies at microtremor level as;

- 1) The natural frequencies of the west colonnade were 3.3 Hz and 2.4 Hz in in-plane and out-of plane directions, respectively.
- 2) Those of the east colonnade were 3.7 Hz and 2.7 Hz in in-plane and out-of plane directions, respectively.
- 3) The natural frequency of the north colonnade was 3.7 Hz in in-plane direction.

Those observed natural frequencies were well correlated with the analysis of the past study for the in-plane behaviors. However, there was significant difference between the measurement and the analysis for the out-of plane behaviors. Such difference was caused by the boundary condition of the colonnades at both corners, indicating necessity to take account the effect of the neighboring colonnades in the analysis model.

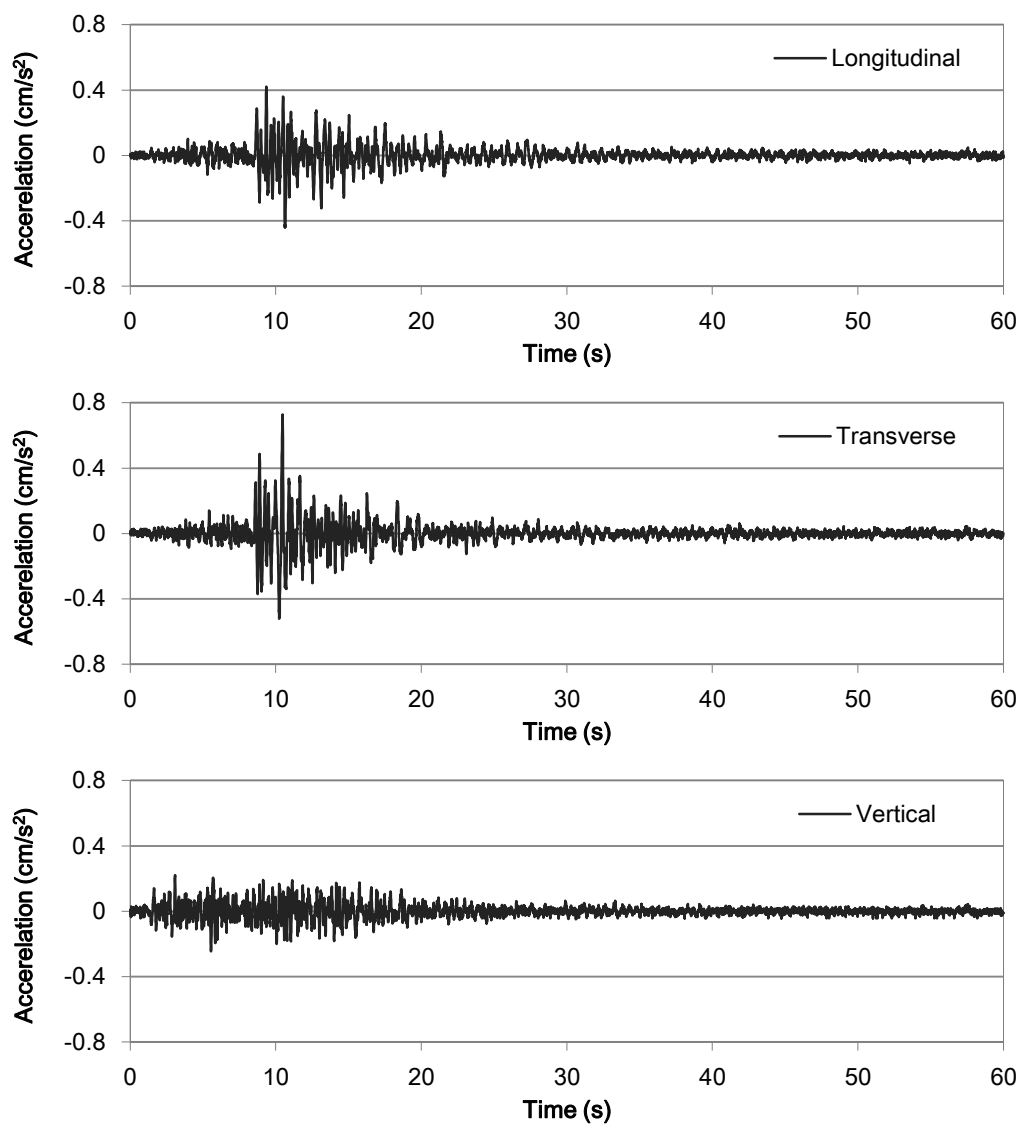


Fig. 2-10 Time histories of ground motions at the base

Chapter 3 Simulation of the Ground Motion at the base of the Acropolis hill

3.1 Introduction

The Parthenon Athens was damaged by the Corinth earthquake in 1981 and these were aggravated by Athens earthquake in 1999. In this chapter, the ground motion at the base of the Acropolis hill was simulated for the two earthquakes. Then, time history of these ground motions were used for shake table test or structural analysis mentioned later in this paper.

The ground motions were simulated with the target acceleration response spectra and phases referred to actual acceleration records obtained at these earthquakes. For generating the earthquake motion, TDAP III (ARK Information Systems) was used.

3.2 Overviews of the Past earthquakes

The epicenters of these earthquakes are shown in fig.3-1 and the basic data of the earthquakes were described in table3-1. Details of the Corinth earthquake and Athens earthquake were mentioned in past studies by the authors [13] or reference [11].

Table 3-1

| | Date | Local time | Distance [km] | Mw |
|--------------------|----------------------------|------------|---------------|-----|
| Athens Earthquake | 7 th Sep. 1999 | 9:56 | 17 | 5.9 |
| Corinth Earthquake | 24 th Feb. 1981 | 20:53 | 64 | 6.7 |
| Aftershock | 25 th Feb. 1981 | - | - | 6.3 |
| Aftershock | 4 th Mar. 1981 | - | - | 6.2 |

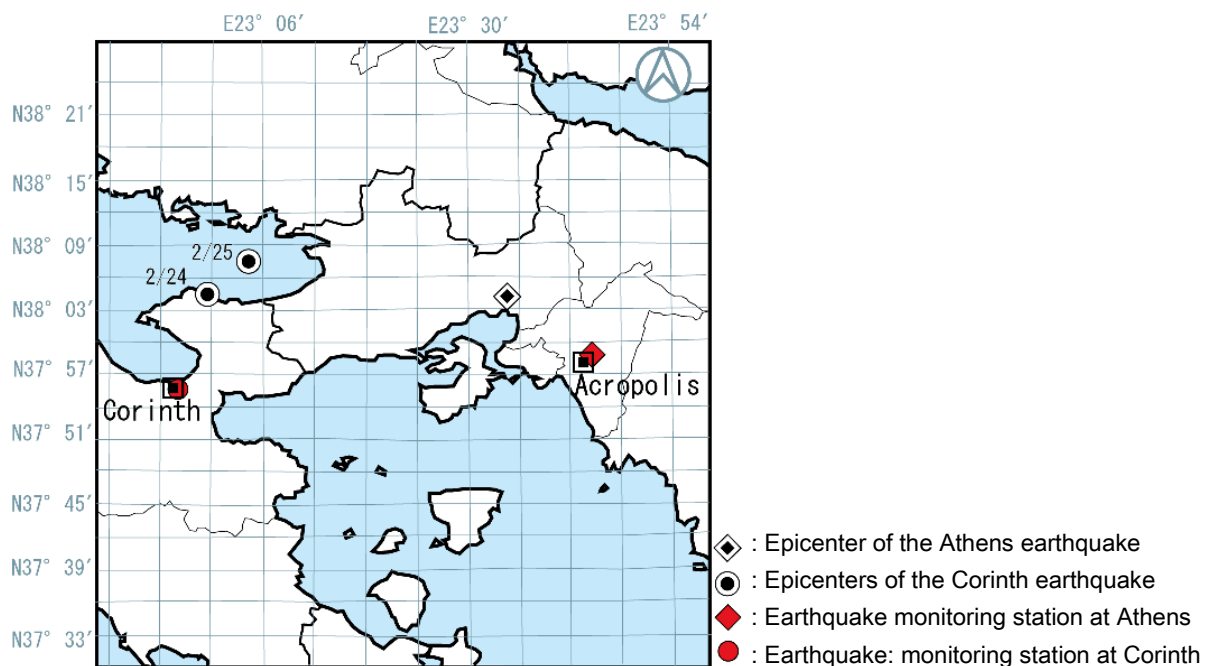


Fig. 3-1 Location of the epicenters and recording points at the past earthquakes

3.3 Target Acceleration Response Spectra and Phases

The target acceleration response spectra for above-mentioned two events were calculated with 5 % damping based on acc. attenuation formula given by N. N Ambraseys et al. [14] as following;

$$\log(y) = C'_1 + C_2M + C_4\log(r) + C_AS_A + C_SS_S + \sigma P \quad (3-1)$$

,where y is the spectral ordinates in g, and M is the surface wave magnitude. S_A takes the value of 1 if the site is classified as rock (R) and 0 otherwise, and S_A and S_S are similarly defined for stiff (A) and Soft (S) soil. In this case, S_A takes the value of 1 and S_S takes 0 since the Acropolis hill is considered stiff. C_1 , C_2 , C_4 , C_A and C_S are defined from table 3-3. The standard deviation of $\log(y)$ is σ which also comes from table 3-3. The constant P takes a value of 0 for mean values and 1 for 84 percentile values of $\log(y)$ and:

$$r = \sqrt{d^2 + h_0^2} \quad (3-2)$$

,where d is the shortest distance from the station to the surface projection of the fault rupture in km, and h_0 is a constant to be determined with C_1 , C_2 , C_3 and C_4 .

This is that acc. response spectra were calculated with M and d. Now, the fault ruptures were obtained in order to define the shortest distance; d from following relationship given by reference [15];

$$M_w = 0.88 \times \frac{\log L + 2.9}{0.6} + 0.54 \quad (3-2)$$

,where M_w is moment magnitude and L is the length of the fault ruptures in km. In this study, d was defined as the value calculated by subtracting L from D which represents epicentral distance from Acropolis hill in km (showed in table3-2). Now, the parameters were derives as following table3-2.

Table 3-2

| | Athens Earthquake | Corinth Earthquake |
|------------------|-------------------|--------------------|
| M_s | 5.4 | 6.7 |
| d (= D - L) [km] | 11.4 | 44.0 |
| L [km] | 5.6 | 20.0 |

Table 3-3 Coefficients of equation (3-1) for spectral ordinates (after Ambraseys [14])

| Period (s) | C ₁ | C ₂ | h ₀ | C ₄ | C _A | C _S | σ |
|------------|----------------|----------------|----------------|----------------|----------------|----------------|------|
| 0.10 | -0.84 | 0.219 | 4.5 | -0.954 | 0.078 | 0.027 | 0.27 |
| 0.11 | -0.86 | 0.221 | 4.5 | -0.945 | 0.098 | 0.036 | 0.27 |
| 0.12 | -0.87 | 0.231 | 4.7 | -0.960 | 0.111 | 0.052 | 0.27 |
| 0.13 | -0.87 | 0.238 | 5.3 | -0.981 | 0.131 | 0.068 | 0.27 |
| 0.14 | -0.94 | 0.244 | 4.9 | -0.955 | 0.136 | 0.077 | 0.27 |
| 0.15 | -0.98 | 0.247 | 4.7 | -0.938 | 0.143 | 0.085 | 0.27 |
| 0.16 | -1.05 | 0.252 | 4.4 | -0.907 | 0.152 | 0.101 | 0.27 |
| 0.17 | -1.08 | 0.258 | 4.3 | -0.896 | 0.140 | 0.102 | 0.27 |
| 0.18 | -1.13 | 0.268 | 4.0 | -0.901 | 0.129 | 0.107 | 0.27 |
| 0.19 | -1.19 | 0.278 | 3.9 | -0.907 | 0.133 | 0.130 | 0.28 |
| 0.20 | -1.21 | 0.284 | 4.2 | -0.922 | 0.135 | 0.142 | 0.27 |
| 0.22 | -1.28 | 0.295 | 4.1 | -0.911 | 0.120 | 0.143 | 0.28 |
| 0.24 | -1.37 | 0.308 | 3.9 | -0.916 | 0.124 | 0.155 | 0.28 |
| 0.26 | -1.40 | 0.318 | 4.3 | -0.942 | 0.134 | 0.163 | 0.28 |
| 0.28 | -1.46 | 0.326 | 4.4 | -0.946 | 0.134 | 0.158 | 0.29 |
| 0.30 | -1.55 | 0.338 | 4.2 | -0.933 | 0.133 | 0.148 | 0.30 |
| 0.32 | -1.63 | 0.349 | 4.2 | -0.932 | 0.125 | 0.161 | 0.31 |
| 0.34 | -1.65 | 0.351 | 4.4 | -0.939 | 0.118 | 0.163 | 0.31 |
| 0.36 | -1.69 | 0.354 | 4.5 | -0.936 | 0.124 | 0.160 | 0.31 |
| 0.38 | -1.82 | 0.364 | 3.9 | -0.900 | 0.132 | 0.164 | 0.31 |
| 0.40 | -1.94 | 0.377 | 3.6 | -0.888 | 0.139 | 0.172 | 0.31 |
| 0.42 | -1.99 | 0.384 | 3.7 | -0.897 | 0.147 | 0.180 | 0.32 |
| 0.44 | -2.05 | 0.393 | 3.9 | -0.908 | 0.153 | 0.187 | 0.32 |
| 0.46 | -2.11 | 0.401 | 3.7 | -0.911 | 0.149 | 0.191 | 0.32 |
| 0.48 | -2.17 | 0.410 | 3.5 | -0.920 | 0.150 | 0.197 | 0.32 |
| 0.50 | -2.25 | 0.420 | 3.3 | -0.913 | 0.147 | 0.201 | 0.32 |
| 0.55 | -2.38 | 0.434 | 3.1 | -0.911 | 0.134 | 0.203 | 0.32 |
| 0.60 | -2.49 | 0.438 | 2.5 | -0.881 | 0.124 | 0.212 | 0.32 |
| 0.65 | -2.58 | 0.451 | 2.8 | -0.901 | 0.122 | 0.215 | 0.32 |
| 0.70 | -2.67 | 0.463 | 3.1 | -0.914 | 0.116 | 0.214 | 0.33 |
| 0.75 | -2.75 | 0.477 | 3.5 | -0.942 | 0.113 | 0.212 | 0.32 |
| 0.80 | -2.86 | 0.485 | 3.7 | -0.925 | 0.127 | 0.218 | 0.32 |
| 0.85 | -2.93 | 0.492 | 3.9 | -0.920 | 0.124 | 0.218 | 0.32 |
| 0.90 | -3.03 | 0.502 | 4.0 | -0.920 | 0.124 | 0.225 | 0.32 |
| 0.95 | -3.10 | 0.503 | 4.0 | -0.892 | 0.121 | 0.217 | 0.32 |
| 1.00 | -3.17 | 0.508 | 4.3 | -0.885 | 0.128 | 0.219 | 0.32 |
| 1.10 | -3.30 | 0.513 | 4.0 | -0.857 | 0.123 | 0.206 | 0.32 |
| 1.20 | -3.38 | 0.513 | 3.6 | -0.851 | 0.128 | 0.214 | 0.31 |
| 1.30 | -3.43 | 0.514 | 3.6 | -0.848 | 0.115 | 0.200 | 0.31 |
| 1.40 | -3.52 | 0.522 | 3.4 | -0.839 | 0.109 | 0.197 | 0.31 |
| 1.50 | -3.61 | 0.524 | 3.0 | -0.817 | 0.109 | 0.204 | 0.31 |
| 1.60 | -3.68 | 0.520 | 2.5 | -0.781 | 0.108 | 0.206 | 0.31 |
| 1.70 | -3.74 | 0.517 | 2.5 | -0.759 | 0.105 | 0.206 | 0.31 |
| 1.80 | -3.79 | 0.514 | 2.4 | -0.730 | 0.104 | 0.204 | 0.32 |
| 1.90 | -3.80 | 0.508 | 2.8 | -0.724 | 0.103 | 0.194 | 0.32 |
| 2.00 | -3.79 | 0.503 | 3.2 | -0.728 | 0.101 | 0.182 | 0.32 |

The fig.3-2 and 3-3 represent target response acceleration spectra for simulation of the ground acceleration for the Athens earthquake and Corinth earthquake respectively.

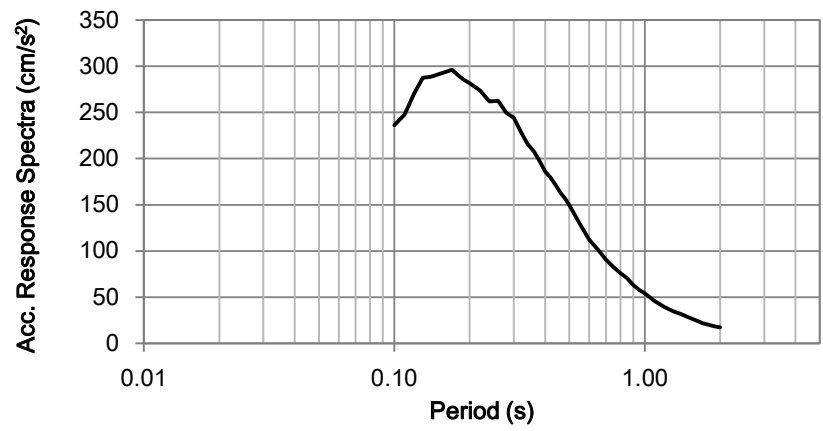


Fig. 3-2 Target acc. response spectra for the foot of the Acropolis hill for the Athens earthquake

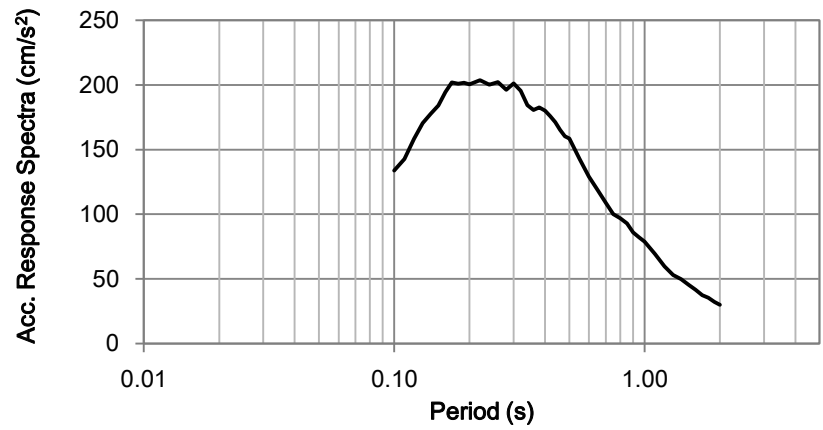


Fig. 3-3 Target acc. response spectra for the foot of the Acropolis hill for the Corinth earthquake

Following figures 3-4 and 3-5 describe the actual acceleration records obtained at Athens earthquake and Corinth earthquake, respectively. Simulated ground motions were generated by referring the phases of these records. While seismic records were obtained from 15 instruments at the Athens earthquake, the record of SYNTAGMA A was used for simulation because the distance to the Acropolis hill was short (about 1 km) and its good quality. For the case of the Corinth earthquake, only one record was caught. Therefore, that record was used for simulation.

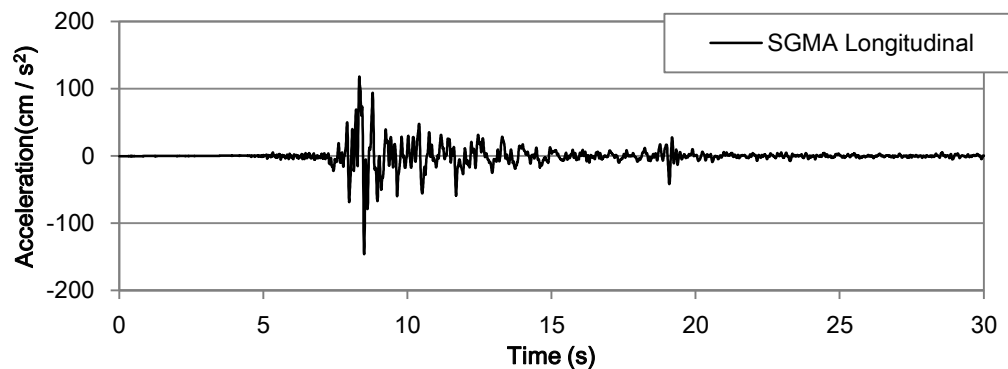


Fig. 3-4 Recorded time history of the acceleration of the Athens earthquake

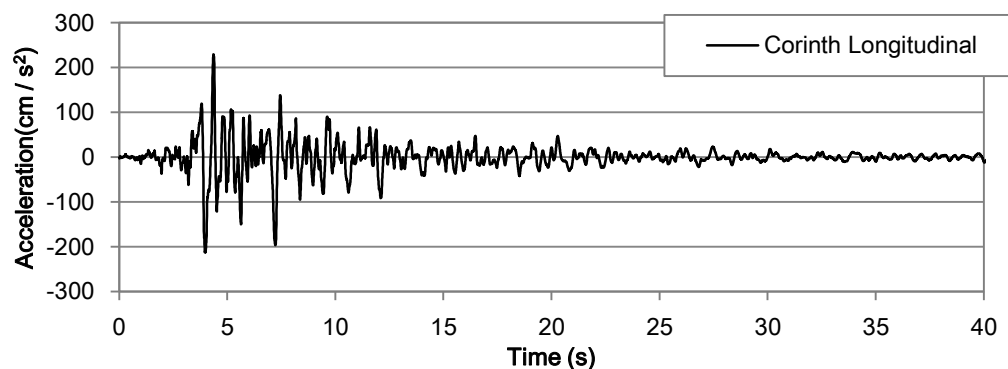


Fig. 3-5 Recorded time history of the acceleration of the Corinth earthquake

3.4 Simulated Earthquake Motions

Figs.3-5 and 3-6 show the simulated motions of the ground acceleration, velocity and displacement at the Athens earthquake and the Corinth earthquake, respectively. Their acceleration response spectra with target spectra are also shown in figs. 3-5 and 3-6 in order to demonstrate the fitting condition. The peak accelerations of these simulated motions are shown in table 3-4. The calculated peak accelerations, which were estimated our previous study [13], are also shown in table 3-4.

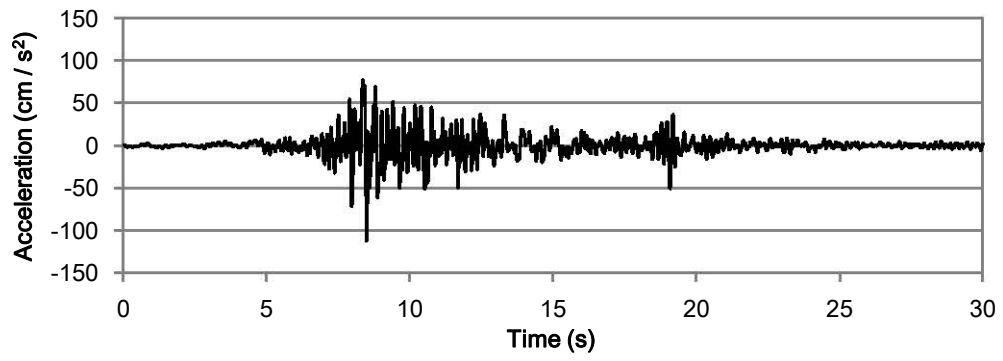
The simulated time history of the displacement at the Corinth earthquake was used for after-mentioned shake table tests as the input motion.

Table 3-4 Maximum acc. of the simulated motions and calculated acc.

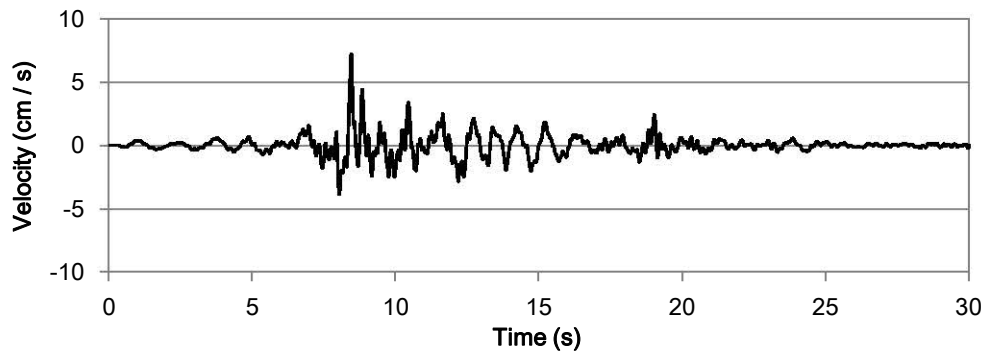
| | Maximum Acceleration [cm/s ²] | Calculated Acceleration [cm/s ²] |
|--------------------|---|--|
| Athens Earthquake | 112.7 | 108.8-122.2 |
| Corinth Earthquake | 90.1 | 48.0-100.2 |

3.5 Concluding Remarks

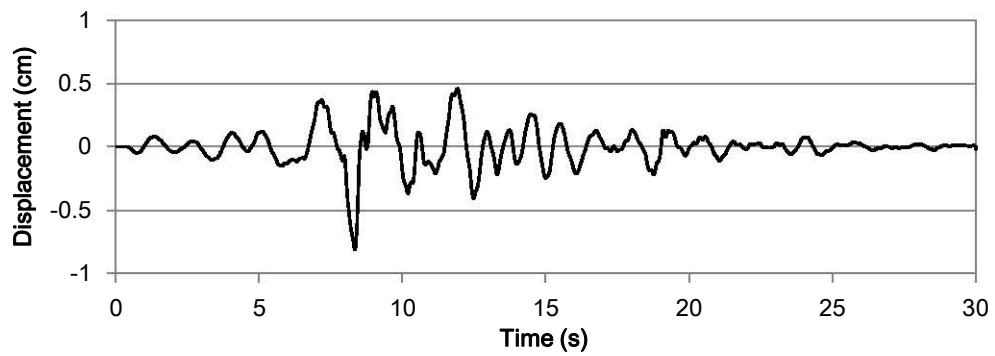
Simulated ground accelerations at the past earthquakes were generated. The peak values of these accelerations were 112.7 cm/s^2 at Athens earthquake and 90.1 cm/s^2 at Corinth earthquake. However, these are the ground motions just at the bottom of the Acropolis hill. Therefore, these motions don't include the topographical effect of the hill. It would be necessary to evaluate the topographical effect in order to estimate the actual seismic response of the Parthenon Athens.



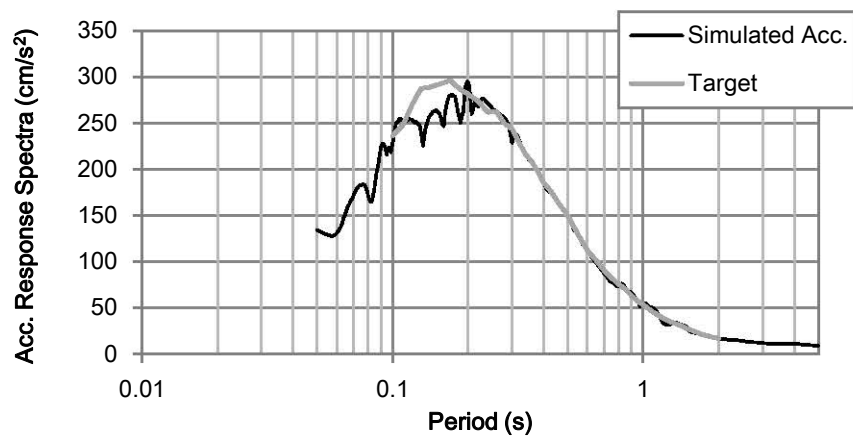
(A)



(B)

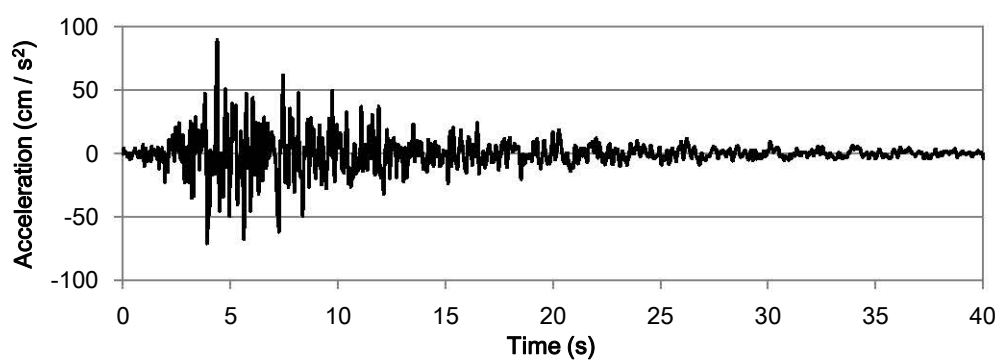


(C)

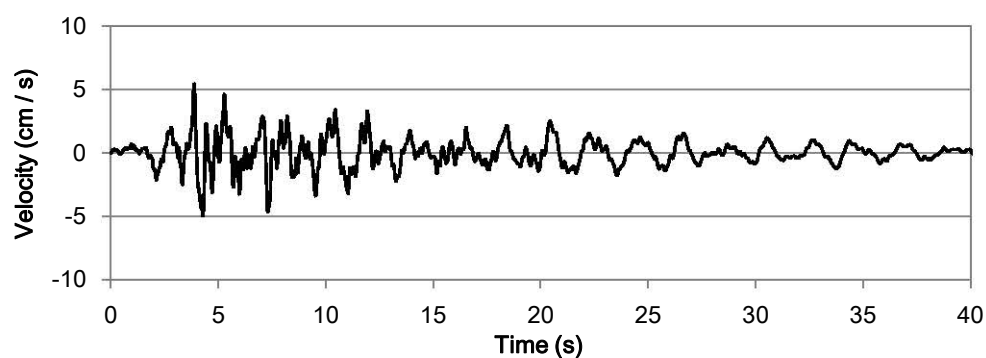


(D)

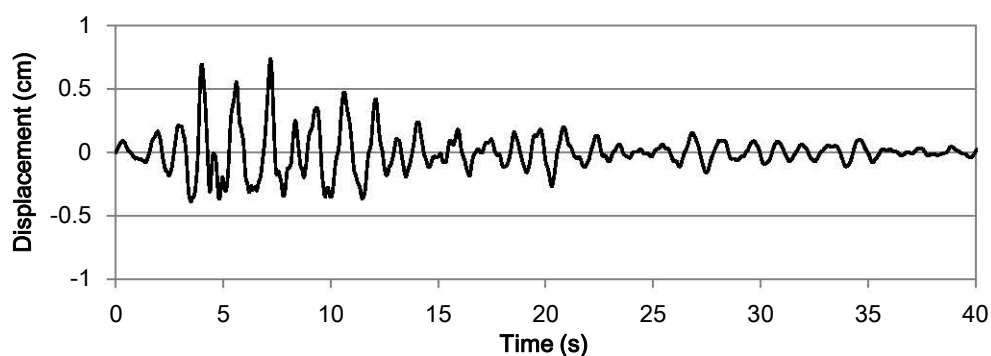
Fig. 3-6 Simulated time history of A) acceleration, B) velocity and C) displacement and D) the response spectra of the simulated acc. at the Athens earthquake



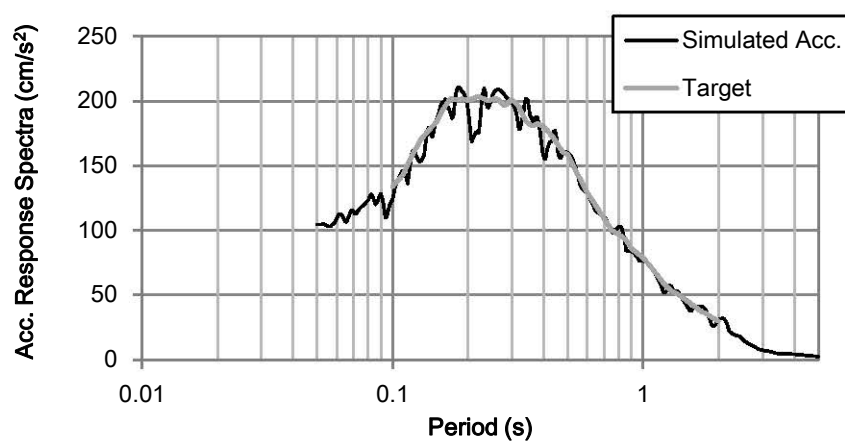
(A)



(B)



(C)



(D)

Fig. 3-7 Simulated time history of A) acceleration, B) velocity and C) displacement and D) the response spectra of the simulated acc. at the Corinth earthquake

Chapter 4 Shake Table Tests on a Simplified Miniature Model of the Parthenon

4.1 Introduction

The shaking table tests were carried out with simplified miniature model of the Parthenon Athens to observe its dynamic behavior of it under the strong ground motions. There were 3 main purposes in this experiment: first was to study the models' responses during excitation. The stone dry-masonry buildings such as the Parthenon must show the high non-linearity response during earthquakes. In the tests, those responses at the safety limit were observed. Second was to clarify the mechanisms of the deformation of the entablatures caused by the Corinth earthquake of 1981. The details of the damage of the entablature were mentioned in chapter 1. Third is to examine the effect of the reinforce technique suggested by the authors. Moreover the specimen was examined on different conditions such as shaking direction, with or without "inner beams" and input motions. Then, its behaviors were also compared.

Of special note is that this is the first experiment with the model of "whole" structure of the colonnades of the monument. In the past study, the shake table tests were conducted with a single multi-drum columns or the model of a part of the monument with classic columns by H. P. Mouzakis *et al.* [8]. However, they did not reproduce the behavior of whole structure of the monument. The specimen used for this test plays the all parts of the colonnades of the monument though the model was quite simplified and reduced from the actual monument.

The experiments were consisted of 2 phases: in phase1, measurements using the accelerometers were conducted. On the other hand, in phase 2, 3 dimensional displacement measuring system was employed. The residual displacement of the model such as rotations or translations of the drums of the columns were recorded throughout the tests.

4.2 Phase 1

4.2.1 Model Description

The specimen was about 1/60 scaled model of the Parthenon Athens shown in figs. 4-1 through 4-4. The model drums and beams were made of cement. The number of members, entasis of the columns, the proportions etc. were simplified. It was rested on the cement base fixed on the shaking table. The model column was composed of 4 drums and a capital. The entablature: architraves, friezes and cornices were on the capitals. The diameter of drums was 50 mm. A special form was given to the contact surface between neighboring drums shown in fig. 4-5 in order to ease to fit drums, but not all drums had such contact surface. Wooden (balsa) dowels were between the drums of the columns and between the cement base and drum (see fig. 4-5). In addition, horizontal clamps made of brass were between beams (see fig.4-6). The beams were not connected vertically.

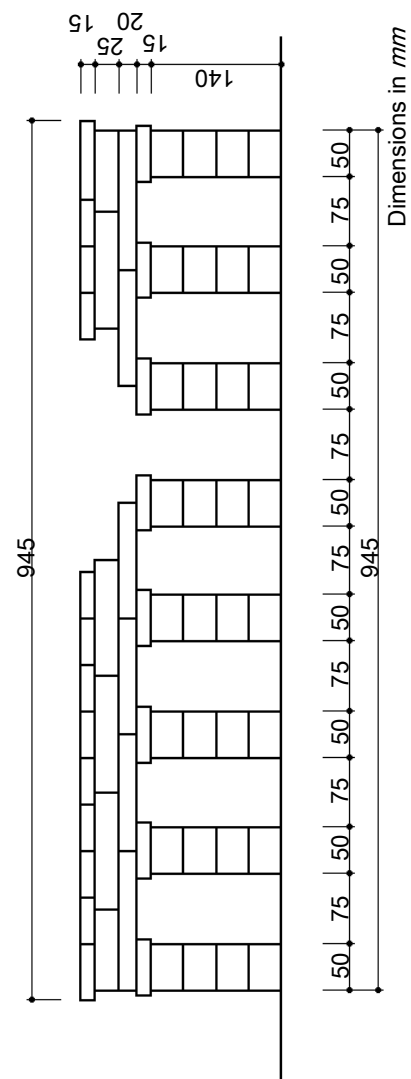
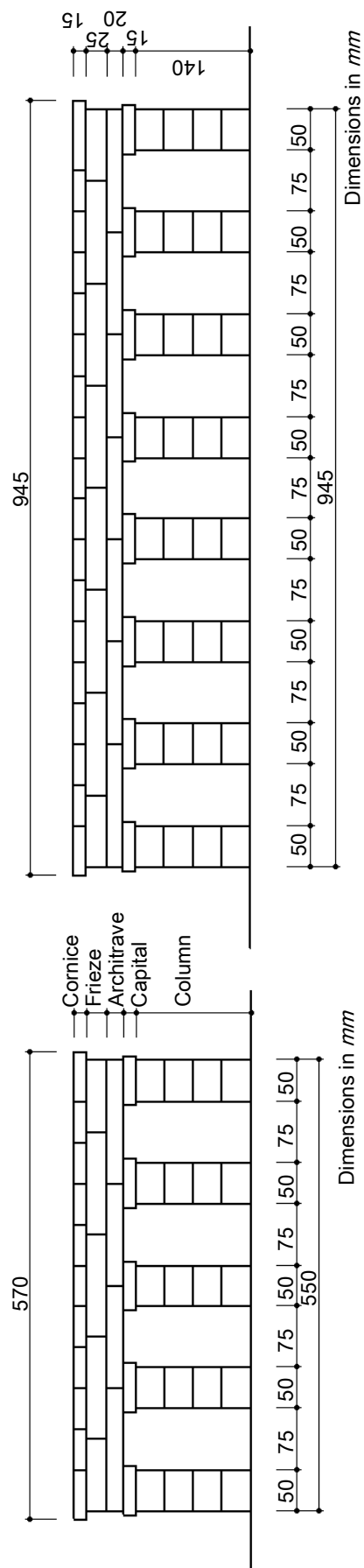


Fig. 4-1 Elevation of the north colonnade

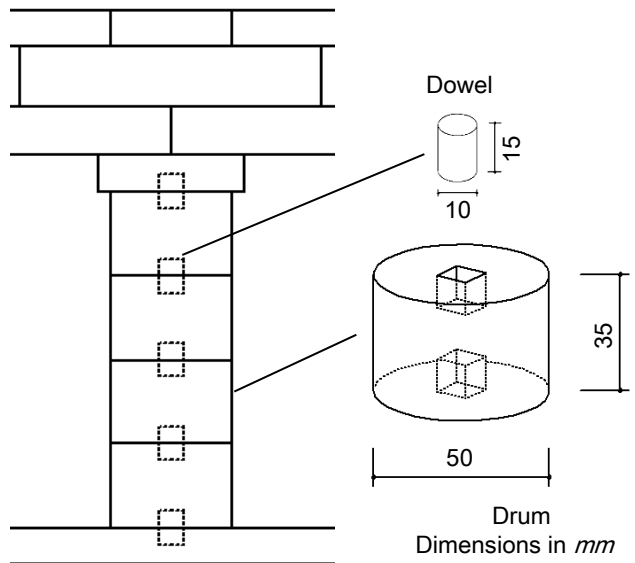
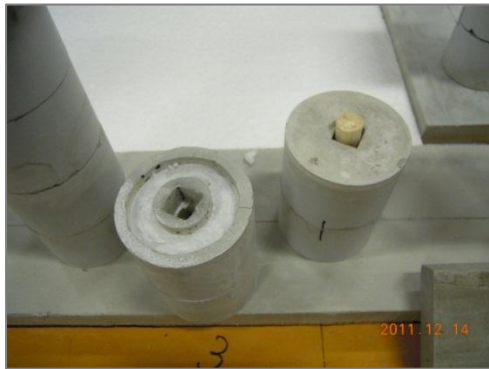


Fig. 4-5 Drums of the columns and wooden dowels

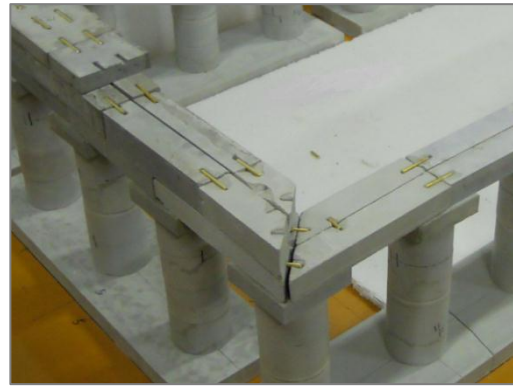


Fig. 4-6 Horizontal clamps between beams

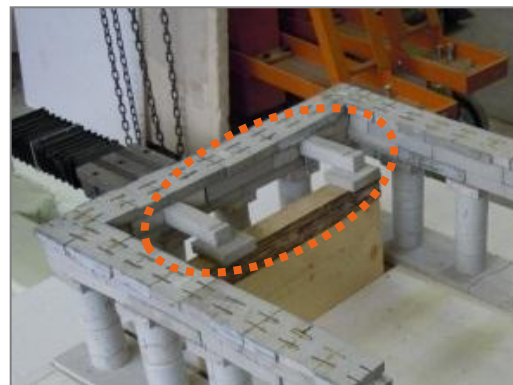
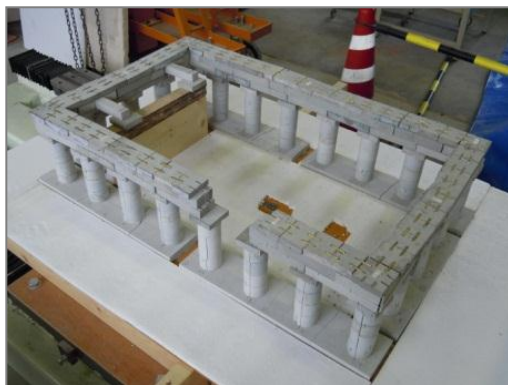


Fig. 4-7 Inner beams

In some tests, “inner beams” were added in the model (see fig. 4-7). The inner beams represented the horizontal beam between the west colonnade and the inner colonnade of the west. Those members in the actual monument were removed after the Corinth earthquake of 1981 in order to exchange the friezes of the inner colonnade to the copies.

The friction coefficients of members were measured to be around 0.5. This value was average of the 2 kinds of measurement; between the capital and the architrave and between the frieze and the cornice. The measurements were conducted with the force gauge AD-4932-50N (A&D Company Limited) (fig. 4-8). Fig. 4-9 shows the measurement between the frieze and the cornice. In the figure, there is no weight on the member, but the multiple measurements were carried out with several weights. In past study, the friction coefficients of marble drums were measured and the values were in the range of 0.36 to 0.80 [6].



Fig. 4-8 Force gauge



Fig. 4-9 Friction coefficient test

4.2.2 Experimental Setup

All the experiments were carried out on the shaking table facility of the laboratory for Department of the Architecture of Mie University. The table has dimensions $1.0\text{ m} \times 1.0\text{ m}$ and it can move just one degree of freedom. Details of the shaking table were shown in table 4-1.

The accelerations of the specimen were measured by 7 accelerometers ARF-100A (Tokyo Sokki Kenkyujo Co., Ltd.) The experiments were conducted with 0° , 90° or 45° input base motion angle and the differences of model responses were compared. Moreover, the residual deformations of the model were observed after each test except the case in which the displacement was extremely tiny. All the experiments were video recorded by two cameras. Set up of the model and instruments were shown in fig. 4-12.

After each tests, the model was placed back in their initial position using the marks drawn on the surface of the members. In some test, the permanent displacements were so small that the model was not repositioned. In such case, the residual deformation of the model was not recorded as above-mentioned.

4.2.3 Exciting Input Motions

Two input motions were used for the tests:

1. The accelerogram recorded at the base of the Parthenon Athens, which was installed by the authors, in 2nd September 2010. As previously indicated in chapter 2, the PGA was 0.7 cm/s^2 and it was too small to use for the test. Therefore, the input motion amplified by multiplying factor of 500 was utilized to perform the shaking table tests. The peak acc. of the input motion for the tests was 364.4 cm/s^2 .
2. The simulated ground motion at the Corinth earthquake in 1981 mentioned in chapter 3. Double displacement time history was used for the tests because it didn't have enough magnitude for experiment

Each motion was used for different levels shown in table 4-2. Figs. 4-10 and 4-11 show the input motions in 100 % scale.

Table 4-1 Specifications of the shaking table

| | |
|------------------------|--------------------------|
| Production | MTS (U. S. A.) |
| Degree of freedom | 1-axial excitation |
| Exciting equipment | Hydraulic power actuator |
| Maximum exciting force | 50 [kN] |
| Maximum stroke | 125 [mm] |
| Table size | 1 [m] × 1 [m] |
| Control method | Displacement control |
| Control software | Multi Purpose Test Ware |
| Operating frequency | 0.1 – 50 [Hz] |

Table 4-2 Input base motion of the test

| Phase | Scale | Maximum Disp. [mm] | Maximum Acc. [cm/s^2] |
|-----------|-------|--------------------|----------------------------------|
| Sep. 2010 | 100% | 16.4 | 364.4 |
| | 75% | 12.3 | 273.3 |
| | 50% | 8.2 | 182.2 |
| | 25% | 4.1 | 91.1 |
| Corinth | 100% | 14.7 | 180.1 |
| | 75% | 11.0 | 135.1 |
| | 50% | 7.4 | 90.1 |
| | 25% | 3.7 | 45.0 |

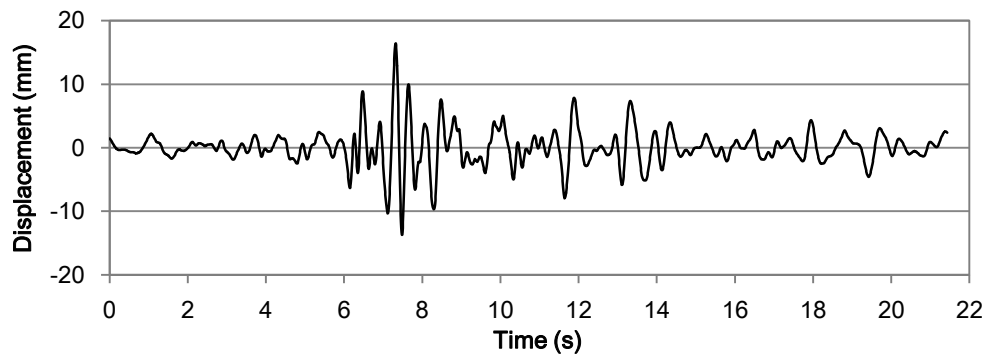


Fig. 4-10 Input base motion of 2th Sep. 2010 phase

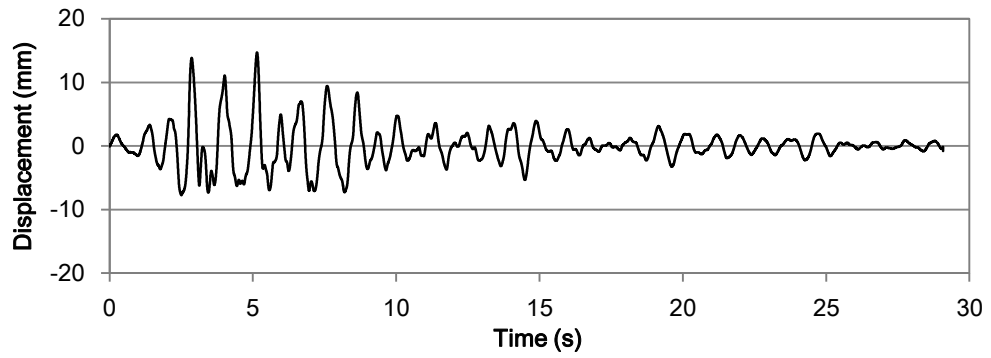


Fig. 4-11 Input base motion of Corinth earthquake phase

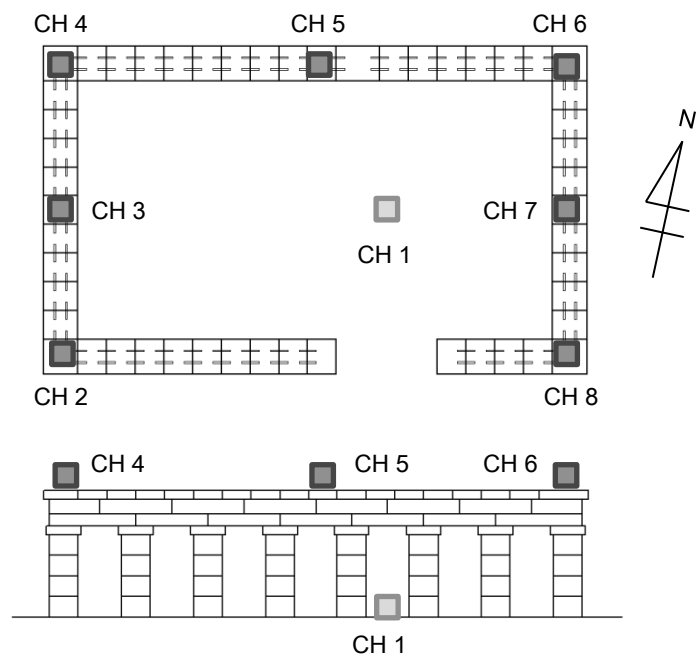
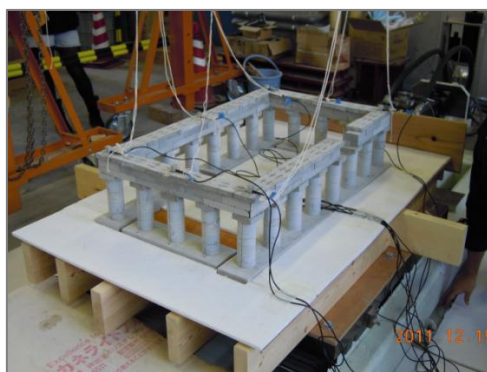


Fig. 4-12 Arrangement of the accelerometers

4.2.4 Results

The test series were shown in table 4-3. Figs. 4-13 through 4-22 show the examples of destructed model. The arrows indicated the shaking direction. The larger arrow means the direction of the peak displacement of the shaking table.

Table 4-3 Test series

| Phase | Scale | Without Inner Beam | | | With Inner Beam | | |
|-----------|-------|--------------------|------|------|-----------------|------|------|
| | | 0° | 90° | 45° | 0° | 90° | 45° |
| Corinth | 25% | (2) | (14) | (20) | - | (8) | (17) |
| | 50% | 3 | 15 | 22 | - | 10 | 19 |
| | 75% | 4 | 43 | 26 | 6 | 11 | 23 |
| | 100% | 47 | 44 | 27 | 52 | 38** | 24 |
| | -75% | 45 | 35 | - | - | - | - |
| | -100% | 46 | 37 | 31 | - | 39 | 29 |
| Sep. 2010 | 25% | (1) | (13) | (21) | - | (9) | (18) |
| | 50% | 5 | 33 | 28** | 7 | 12 | 25** |
| | 75% | 50** | 34** | - | 51** | 40** | - |
| | -50% | 48 | - | 32 | - | 41 | 30 |
| | -75% | 49 | 36** | - | - | 42** | - |

() Non observation

**Destructed

The test results were summarized as follows:

1. These tests verified that south colonnade was vulnerable part in the model. There were 9 cases in which the model collapsed and the south colonnade was destructed in 7 cases of them. Moreover, in some case in which the specimen was not destructed, the south colonnade become deformed seriously. Some of the beams were lost in the south colonnade as shown in fig.4-2. Therefore, the south colonnade has gap. It was supposed that this part caused the structure vulnerable.
2. The residual deformations of the west colonnade of the actual monument were successfully reproduced as shown in fig. 4-22. This deformation mode was observed in both plus and minus direction of the phase. However, the definite correlation between the degree of the displacement and magnitude of the base motion was not observed. Moreover, in the 45° input motion, the deformations of the entablatures were less than that in the 0° or 90° input motion.

As results of observation during and after excitation, it was supposed that the deformations of the entablature were produced by accumulation of the displacement of the beams. That is, one beam was moved during excitation (fig 4-23 (B)) then, it moved another beam. Finally, at the corner, the entablatures were expanded outside (fig 4-23 (C)). It could be said that such behavior was high non-linear response of the dry masonry.

3. The rotational displacements of the drums of the columns were observed in such small model but it was difficult to study the tendency of the drums behavior in basis of characteristics of input base motion or its magnitude.
4. It was difficult to examine the effect of the inner beams or difference of the response between two input motions from the records of the acceleration.

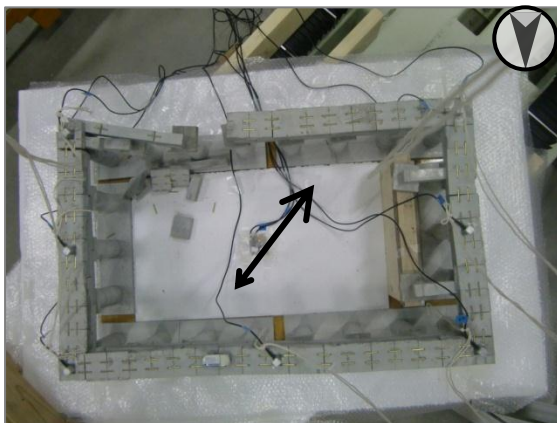


Fig. 4-13 Case 25

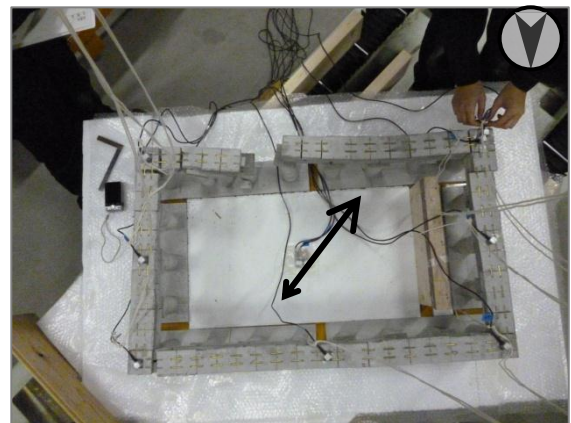


Fig. 4-14 Case 28

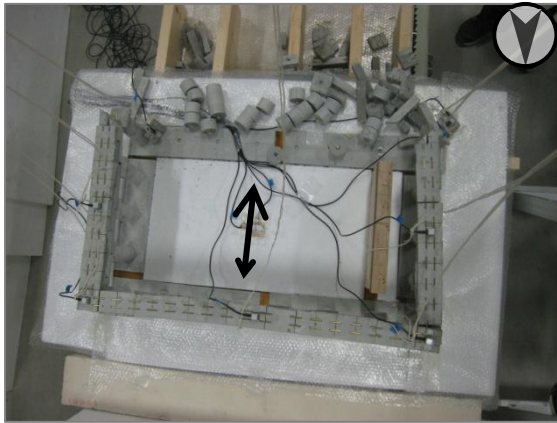


Fig. 4-15 Case 34

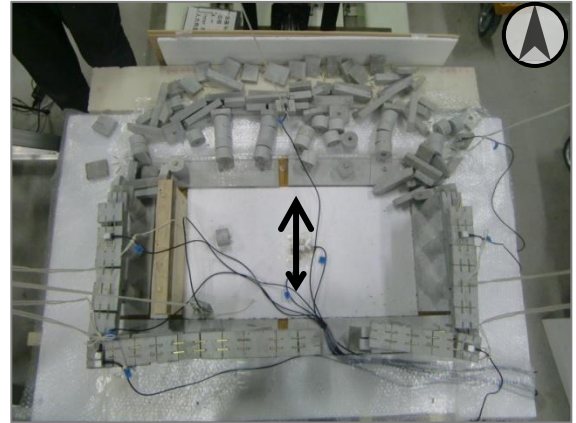


Fig. 4-16 Case36

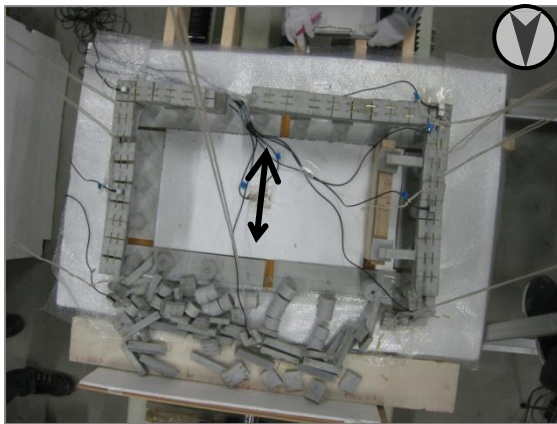


Fig. 4-17 Case 38

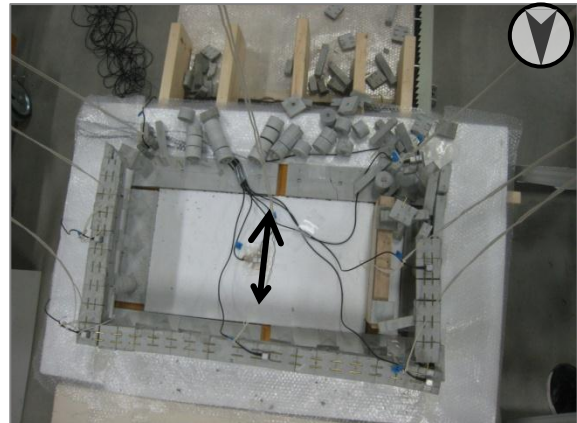


Fig. 4-18 Case 40

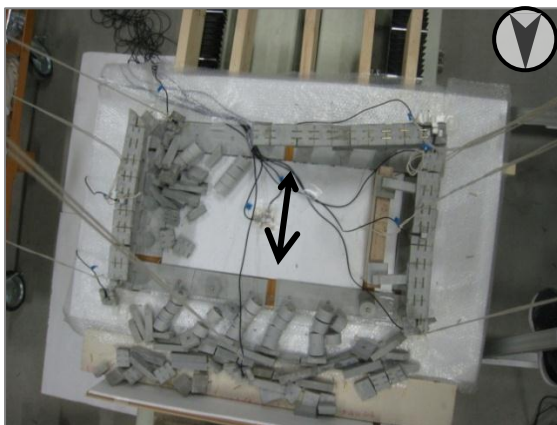


Fig. 4-19 Case 42

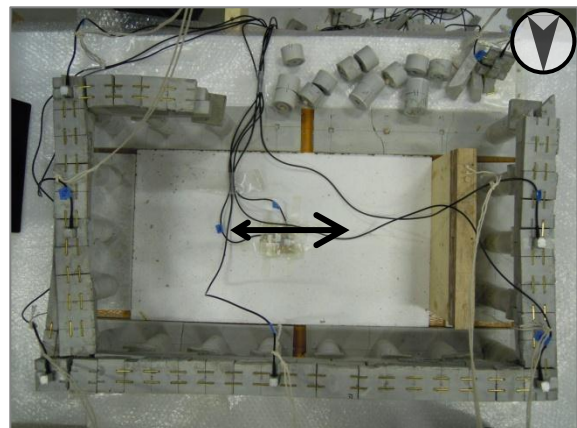


Fig. 4-20 Case 50

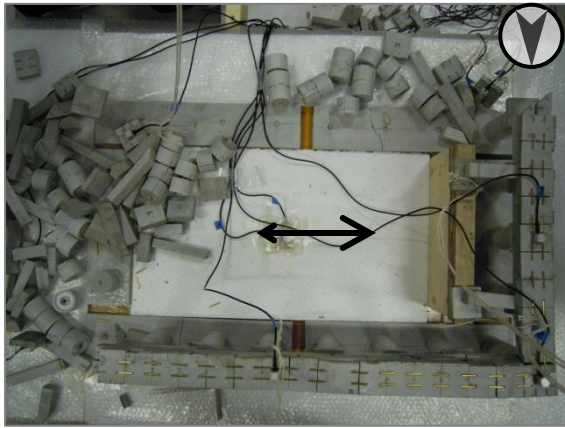


Fig. 4-21 Case 51

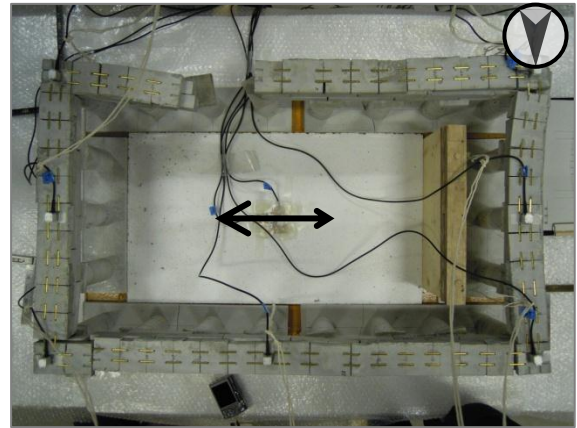


Fig. 4-22 Case 4

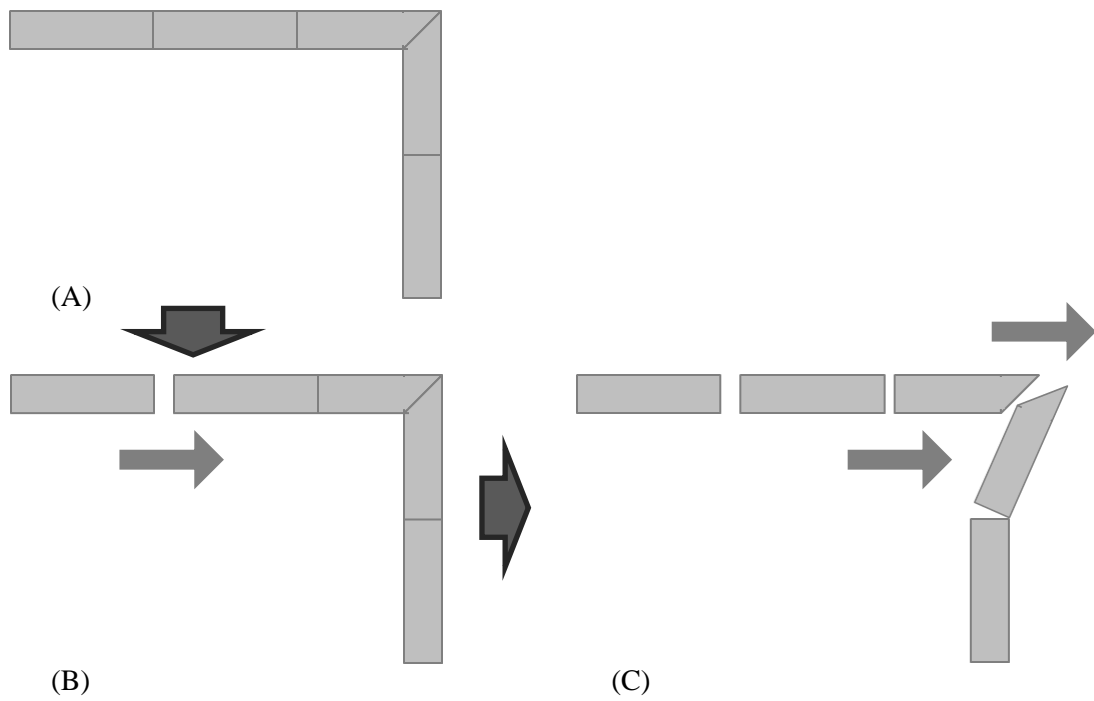


Fig. 4-23 Mechanism of the deformation of the entablature

4.3 Phase 2

In phase 2, displacements of several points of the model were recorded in 3D. Moreover, the effect of the reinforcement was examined.

4.3.1 Suggestions of Reinforcement

On receiving the results of phase 1, 2 methods of reinforcement were suggested.

Method 1: Additional beam members were installed in the south colonnade to solve the structural problem that a part of the south colonnade has been missing by the explosion in 17th century, which might indicate imperfect structure against earthquakes.

Method 2: Connection between stone beams members was ensured by use of metal tie-bands or tie-rods for reinforcement, which must be effective in improvement of seismic performance. Residual displacement caused by the past earthquake would be prevented during future earthquake by employing such technique.

In the experiments, effects of above reinforcements were also examined.

4.3.2 Model Description

Basically, the model used for tests was same as phase 1. In phase 2, however, the model was reinforced in some cases. 2 methods of reinforcement: method 1 and method 2 were applied to the model. Method 1 is to add the beams to the south colonnade (see fig. 4-24). Method 2 shown in fig. 4-25, is to connect beams in same height levels horizontally with adhesive tape or PP-Band instead of metal tie-bands or tie-rods. There is no vertical connection between horizontal members in both methods.

4.3.3 Experimental Setup

In this section, the displacements of the several points of the model were recorded by the 3 dimensional measurement systems (Netplus Co., Ltd.). This system is to record the markers by highly sensitive cameras and measure the displacement of them in 3 dimensions accurately. Both absolute and relative displacements were measured with the system. In this experiment, 2 cameras and 19 LED markers were used for this measurement. 15 markers were for the specimen, and 4 markers were placed on the shaking table. Fig. 4-26 and 4-27 shows the arrangement of cameras and the markers, respectively.

4.3.4 Seismic Input Motions

The input base motion in phase 2 was the wave of Sep. 2010 in 75 % scale. This motion was elected on the basis of the results of the experiment of phase 1.

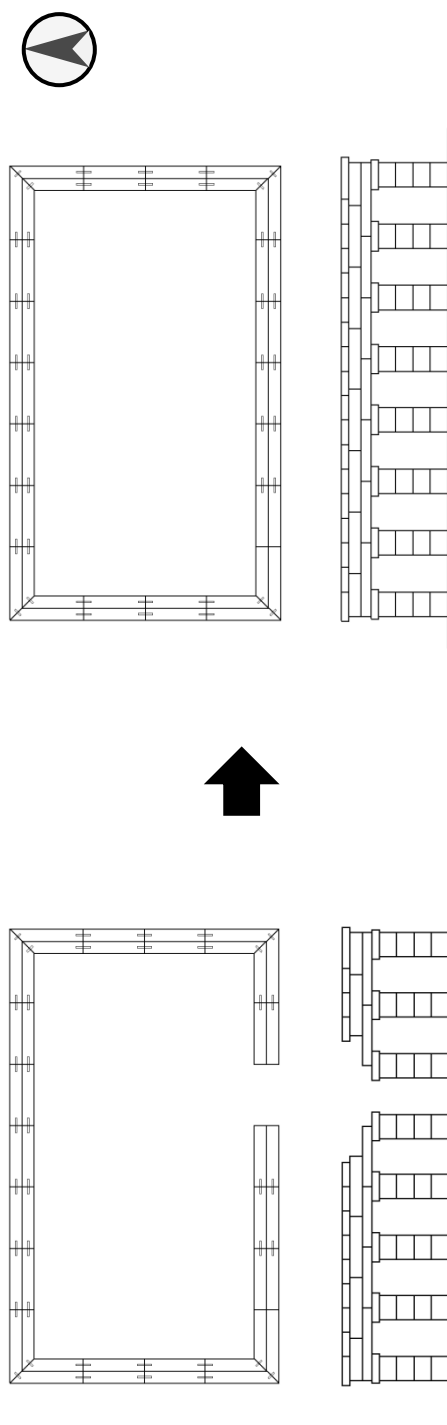


Fig. 4-24 Reinforcement method 1

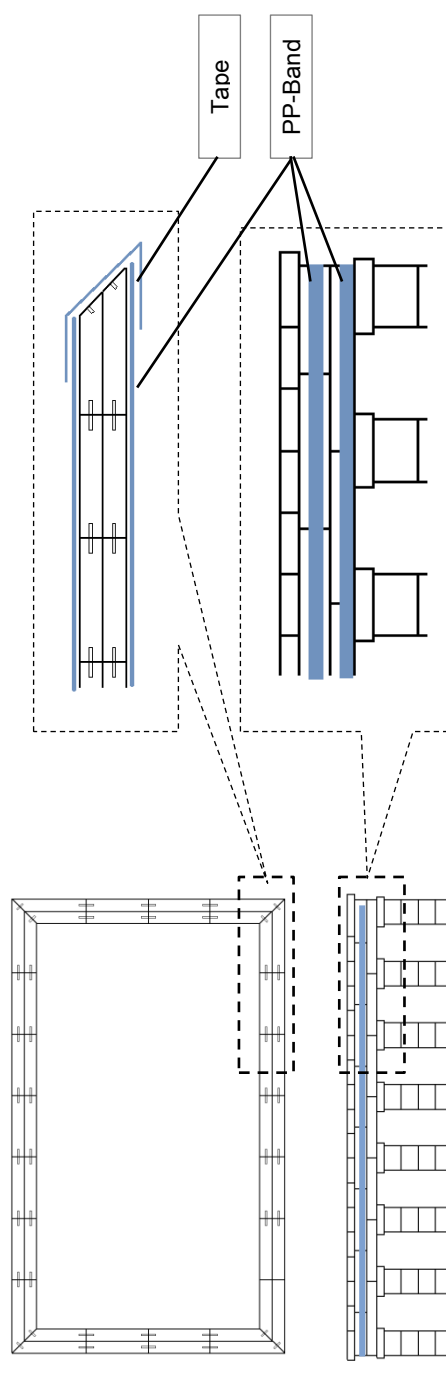


Fig. 4-25 Reinforcement method 2

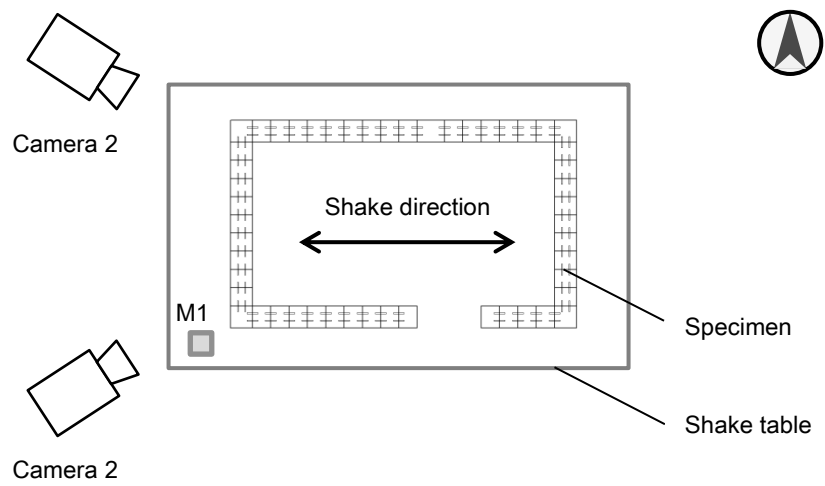


Fig. 4-26 Arrangement of the cameras for 3D measurements

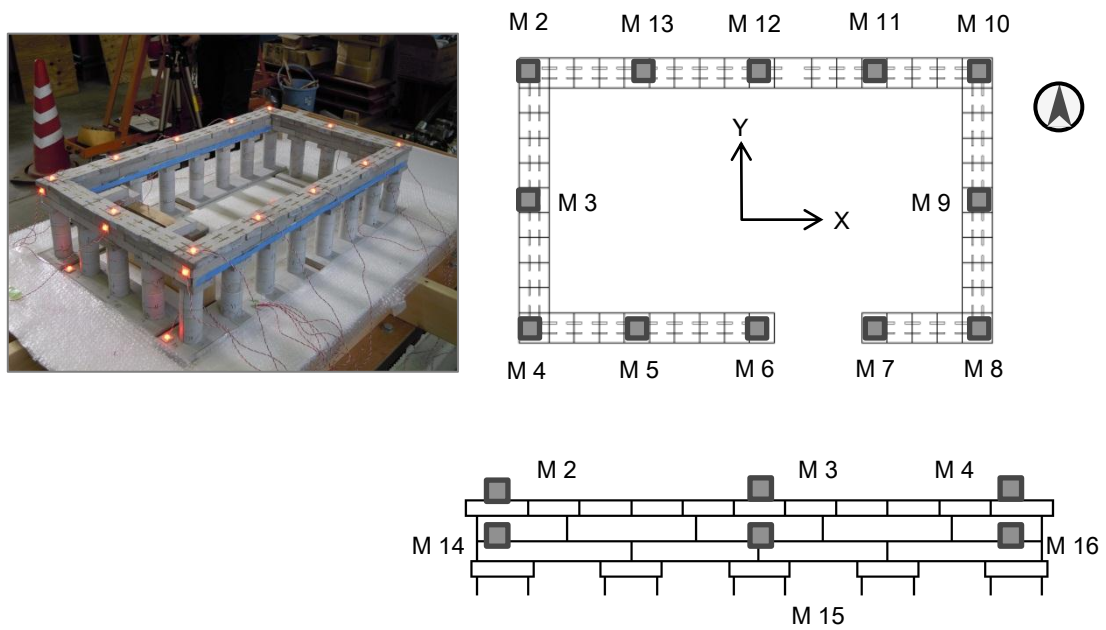


Fig. 4-27 Arrangement of the markers

4.3.5 Results

The results of the experiments were shown in table 4-4. The results of case50 and 51 conducted at phase 1 were also shown in table 4-4. Case 50 was conducted under the same conditions as case 57 and case 51 was carried out under the same conditions as case 58.

Although under the same condition, the result of case 58 and case 51 were different. In addition, the rupture pattern of case 57 was not the same as that of case 50. These were attributed to the high sensitivity of the phenomenon to very small irregularities of the initial arrangement or input motion characteristics.

Table 4-4 Result of experiments

| Input Motion | Reinforced method 2 | | Reinforced method 1 | | Unreinforced | |
|-----------------|---------------------|-----------------|---------------------|-----------------|--------------------|-----------------|
| | Without inner beam | With inner beam | Without inner beam | With inner beam | Without inner beam | With inner beam |
| Sep. 2010 (75%) | 54 | 53 | 56** | 55** | 57** (50**) | 58 (51**) |

**....Destroyed

The time histories of displacements of the markers on the west colonnade were shown in figs. 4-28 to 4-33. These dynamic displacements describe relative displacement to the shaking table.

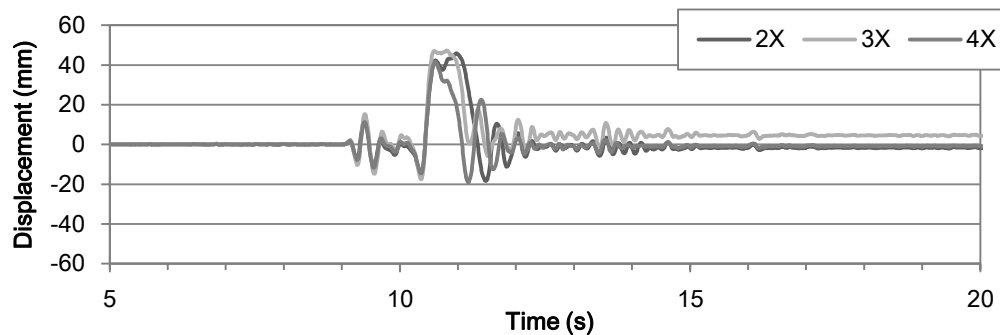


Fig. 4-28 Displacement of markers on the west colonnade on Case53 (With beam)

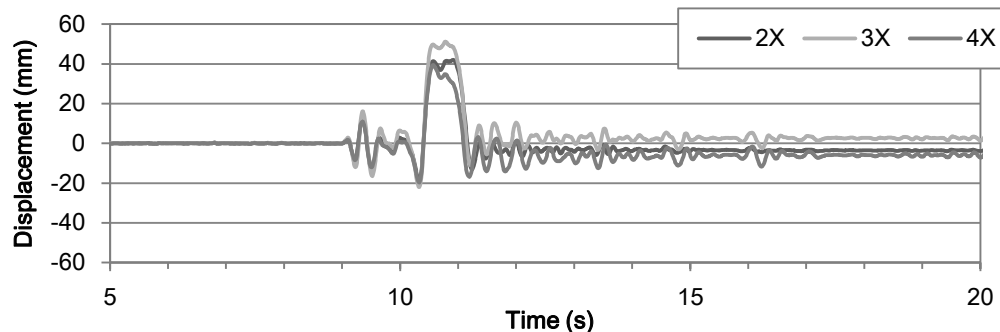


Fig. 4-29 Displacement of markers on the west colonnade on Case54 (Without beam)

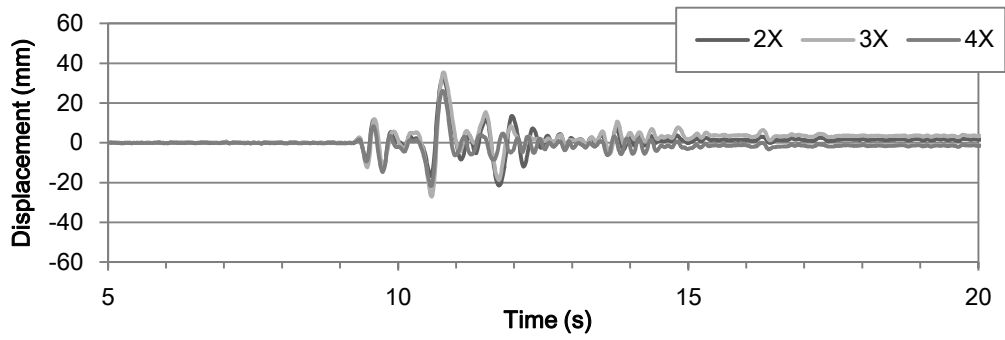


Fig. 4-30 Displacement of markers on the west colonnade on Case55 (With beam)

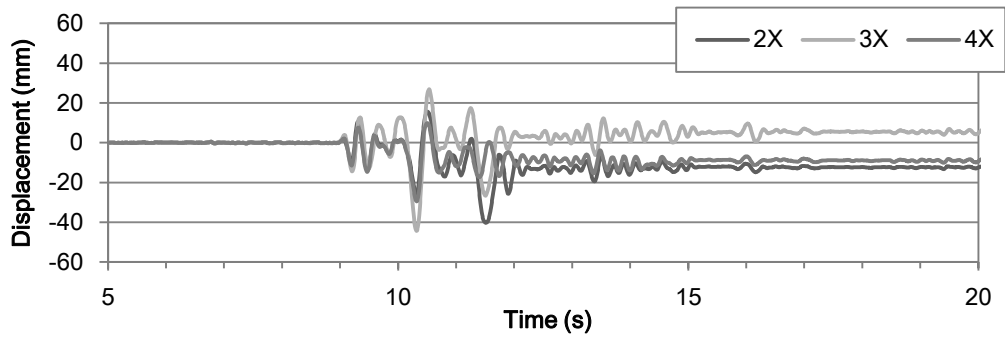


Fig. 4-31 Displacement of markers on the west colonnade on Case56 (Without beam)

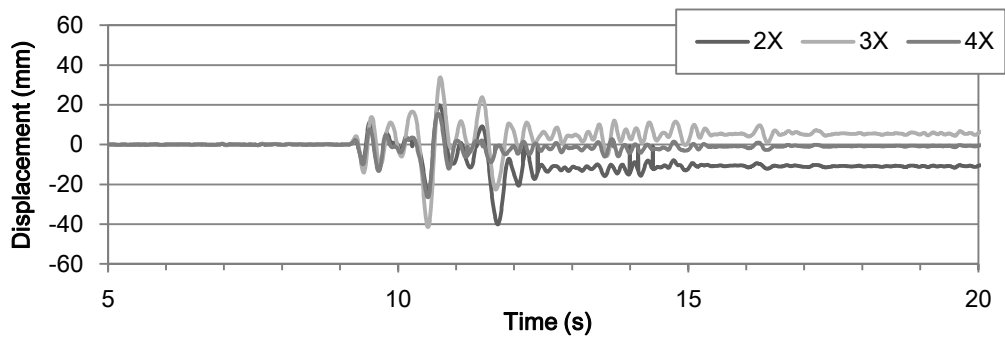


Fig. 4-32 Displacement of markers on the west colonnade on Case57 (Without beam)

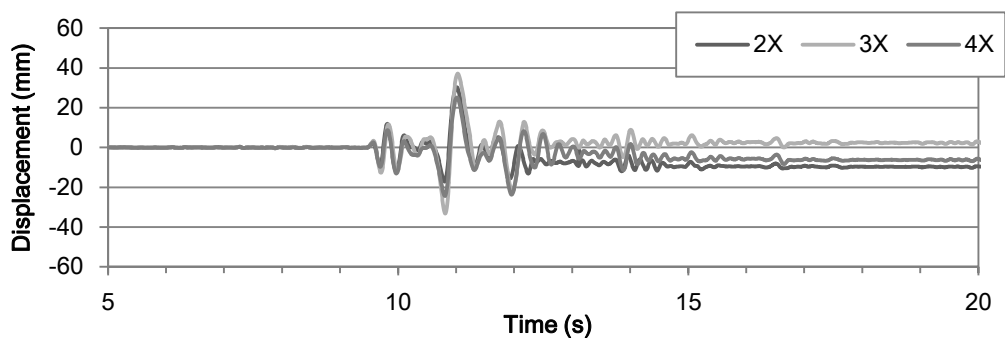


Fig. 4-33 Displacement of markers on the west colonnade on Case58 (With beam)

Compared time histories of case 55 with case 56 and case 58 with case 57, the time histories showed significant difference. On the other hand, compared case 55 with case 58, the time histories of displacement seem to have same characteristics. These difference or similarity might be caused by the “inner beam.” It could be said that the inner beams were effective to control the displacement of the west colonnade in out-of-plane direction. In particular, the inner beams reduced the deformation of the colonnade toward outside of the structure.

Table 4-5 Response displacements of the model in case 53

| | Max. disp. [mm] | Min. disp. [mm] | Abs. max. disp. [mm] | Residual disp. [mm] | Max. story drift |
|-----|--------------------|--------------------|-------------------------|------------------------|---------------------|
| M2 | 45.9 | -18.3 | 45.9 | -1.6 | 1/5 |
| M3 | 47.4 | -17.5 | 47.4 | 4.6 | 1/5 |
| M4 | 41.6 | -19.0 | 41.6 | -0.7 | 1/5 |
| M5 | 42.9 | -15.7 | 42.9 | 0.2 | 1/5 |
| M6 | 42.8 | -15.9 | 42.8 | 0.2 | 1/5 |
| M7 | 42.3 | -15.5 | 42.3 | 0.1 | 1/5 |
| M8 | 52.1 | -11.8 | 52.1 | 2.8 | 1/4 |
| M9 | 60.1 | -21.3 | 60.1 | -1.8 | 1/4 |
| M10 | 52.5 | -13.4 | 52.5 | 2.6 | 1/4 |
| M11 | 46.7 | -13.6 | 46.7 | -0.2 | 1/5 |
| M12 | 46.3 | -15.0 | 46.3 | -0.4 | 1/5 |
| M13 | 46.3 | -16.0 | 46.3 | -1.0 | 1/5 |

Table 4-6 Response displacements of the model in case 54

| | Max. disp. [mm] | Min. disp. [mm] | Abs. max. disp. [mm] | Residual disp. [mm] | Max. story drift |
|-----|--------------------|--------------------|-------------------------|------------------------|---------------------|
| M2 | 42.1 | -18.6 | 42.1 | -3.5 | 1/5 |
| M3 | 51.2 | -22.0 | 51.2 | 2.8 | 1/5 |
| M4 | 39.5 | -19.7 | 39.5 | -5.7 | 1/5 |
| M5 | 41.6 | -15.5 | 41.6 | -4.8 | 1/5 |
| M6 | 41.3 | -15.8 | 41.3 | -5.6 | 1/5 |
| M7 | 40.7 | -15.8 | 40.7 | -4.3 | 1/5 |
| M8 | 48.8 | -14.4 | 48.8 | -4.2 | 1/5 |
| M9 | 59.8 | -24.2 | 59.8 | -1.5 | 1/4 |
| M10 | 50.1 | -13.4 | 50.1 | 1.1 | 1/4 |
| M11 | 42.9 | -14.6 | 42.9 | 0.6 | 1/5 |
| M12 | 43.0 | -14.8 | 43.0 | 0.6 | 1/5 |
| M13 | 42.9 | -14.8 | 42.9 | 0.1 | 1/5 |

Table 4-7 Response displacements of the model in case 55

| | Max. disp. [mm] | Min. disp. [mm] | Abs. max. disp. [mm] | Residual disp. [mm] | Max. story drift |
|-----|--------------------|--------------------|-------------------------|------------------------|---------------------|
| M2 | 32.8 | -21.5 | 32.8 | 1.2 | 1/6 |
| M3 | 35.4 | -27.1 | 35.4 | 3.1 | 1/6 |
| M4 | 26.2 | -21.9 | 26.2 | -1.7 | 1/8 |
| M5 | 27.7 | -17.8 | 27.7 | -0.9 | 1/8 |
| M6 | 30.9 | -17.7 | 30.9 | -0.5 | 1/7 |
| M7 | 31.3 | -17.3 | 31.3 | 1.1 | 1/7 |
| M8 | - | -16.7 | - | - | - |
| M9 | - | -32.5 | - | - | - |
| M10 | - | -15.3 | - | - | - |
| M11 | 33.7 | -18.2 | 33.7 | 2.2 | 1/5 |
| M12 | 33.4 | -19.9 | 33.4 | 2.2 | 1/5 |
| M13 | 32.9 | -20.3 | 32.9 | 1.5 | 1/5 |

Table 4-8 Response displacements of the model in case 56

| | Max. disp. [mm] | Min. disp. [mm] | Abs. max. disp. [mm] | Residual disp. [mm] | Max. story drift |
|-----|--------------------|--------------------|-------------------------|------------------------|---------------------|
| M2 | 15.7 | -40.3 | 40.3 | -12.3 | 1/6 |
| M3 | 26.9 | -44.4 | 44.4 | 5.4 | 1/4 |
| M4 | 9.9 | -29.5 | 29.5 | -9.2 | 1/8 |
| M5 | 11.4 | -23.8 | 23.8 | -8.6 | 1/9 |
| M6 | 28.2 | -17.4 | 28.2 | -0.4 | 1/8 |
| M7 | 28.5 | -17.7 | 28.5 | 0.5 | 1/8 |
| M8 | - | -17.3 | - | - | - |
| M9 | - | -26.3 | - | - | - |
| M10 | 33.8 | -12.6 | 33.8 | 3.5 | 1/8 |
| M11 | 32.5 | -18.8 | 32.5 | 1.0 | 1/8 |
| M12 | 32.0 | -20.3 | 32.0 | 0.1 | 1/8 |
| M13 | 29.6 | -19.6 | 29.6 | 0.2 | 1/7 |

Tables 4-5 to 4-10 show the response displacement of the markers on the model in each case. The positions of the markers were shown in fig. 4-27.

It was clarified that the reinforcement method 2 could not control the displacement of the model during excitation. Of course, the reinforcement produced its effect to keep the confinement of the structure and reduced the residual displacement of the entablature. However, the maximum displacement and maximum story drift of the model with reinforcement method 2 during excitation became larger than ones of non-reinforced model.

Table 4-9 Response displacements of the model in case 57

| | Max. disp. [mm] | Min. disp. [mm] | Abs. max. disp. [mm] | Residual disp. [mm] | Max. story drift |
|-----|--------------------|--------------------|-------------------------|------------------------|---------------------|
| M2 | 19.8 | -40.1 | 40.1 | -10.8 | 1/5 |
| M3 | 33.9 | -41.5 | 41.5 | 5.6 | 1/5 |
| M4 | 15.6 | -26.6 | 26.6 | -0.7 | 1/8 |
| M5 | 17.1 | -23.0 | 23.0 | -0.4 | 1/10 |
| M6 | 21.0 | -18.9 | 21.0 | 1.0 | 1/10 |
| M7 | 5.9 | -49.7 | 49.7 | -6.3 | 1/5 |
| M8 | - | -46.6 | - | - | - |
| M9 | - | -46.0 | - | - | - |
| M10 | - | -50.7 | - | - | - |
| M11 | 28.5 | -15.6 | 28.5 | 3.5 | 1/7 |
| M12 | 27.8 | -17.0 | 27.8 | 1.1 | 1/7 |
| M13 | 26.8 | -15.8 | 26.8 | 1.0 | 1/8 |

Table 4-10 Response displacements of the model in case 58

| | Max. disp. [mm] | Min. disp. [mm] | Abs. max. disp. [mm] | Residual disp. [mm] | Max. story drift |
|-----|--------------------|--------------------|-------------------------|------------------------|---------------------|
| M2 | 30.3 | -17.2 | 30.3 | -9.6 | 1/7 |
| M3 | 37.2 | -33.3 | 37.2 | 2.6 | 1/5 |
| M4 | 25.2 | -24.4 | 25.2 | -6.1 | 1/9 |
| M5 | 27.7 | -19.3 | 27.7 | -1.9 | 1/10 |
| M6 | 32.4 | -16.2 | 32.4 | 2.0 | 1/6 |
| M7 | 6.3 | -42.1 | 42.1 | -9.7 | 1/5 |
| M8 | 12.9 | -37.7 | 37.7 | -4.0 | 1/7 |
| M9 | 24.8 | -42.8 | 42.8 | 1.7 | 1/5 |
| M10 | 31.5 | -16.0 | 31.5 | 7.8 | 1/7 |
| M11 | 30.1 | -16.0 | 30.1 | -2.2 | 1/7 |
| M12 | 31.6 | -14.7 | 31.6 | -0.8 | 1/7 |
| M13 | 29.4 | -14.3 | 29.4 | -0.8 | 1/7 |

Moreover, the displacement of the tops of the model seemed to be caused by not only inclination of the columns but also by slip of the horizontal members; therefore, the actual story drift of the non-reinforced model must be less than the those presented in tables 4-7 through 4-10.

The reinforcement method 2 is capable of increasing the dynamic response, but this technique would be very effective as far as the input motion level was low. In the past study, it was estimated the Parthenon may not have been suffered by large earthquake as PGA of 200 cm/s^2 at the site during 25 centuries. The method 2 was expected to protect the monument against the deformation in case of such earthquake as PGA of 200 cm/s^2

The response deformation in the horizontal in-plane at the roof level is drawn in Figs. 4-35, 4-37, 4-39, 4-41, 4-43 and 4-45. These figures show the simultaneous displacements at the time when the measuring points reached the peak displacement which was the largest of all the points during the excitation. Figs 4-36, 4-38, 4-40, 4-42, 4-44 and 4-46 show the residual displacement after each test.

In all measurement points of the top of the model, marker3 or marker 9 located at the middle of the colonnade tended to show the largest response through case 53 to case 58. This might be affected by shaking direction. The residual displacements of them, however, were not always the largest. The phenomenon that the maximum dynamic response did not always coincide with the maximum residual displacement was exceptionally-interesting from an engineering point of view.

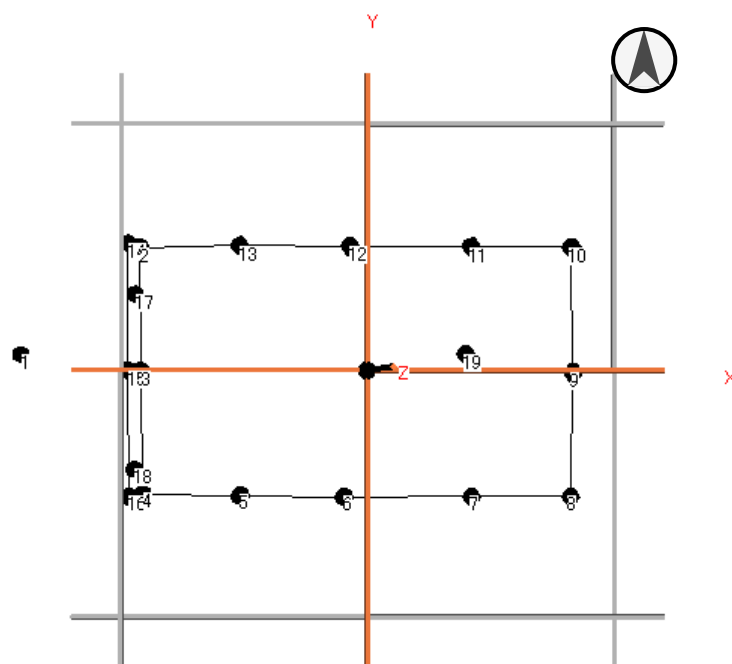


Fig. 4-34 Initial Position of the markers on the model

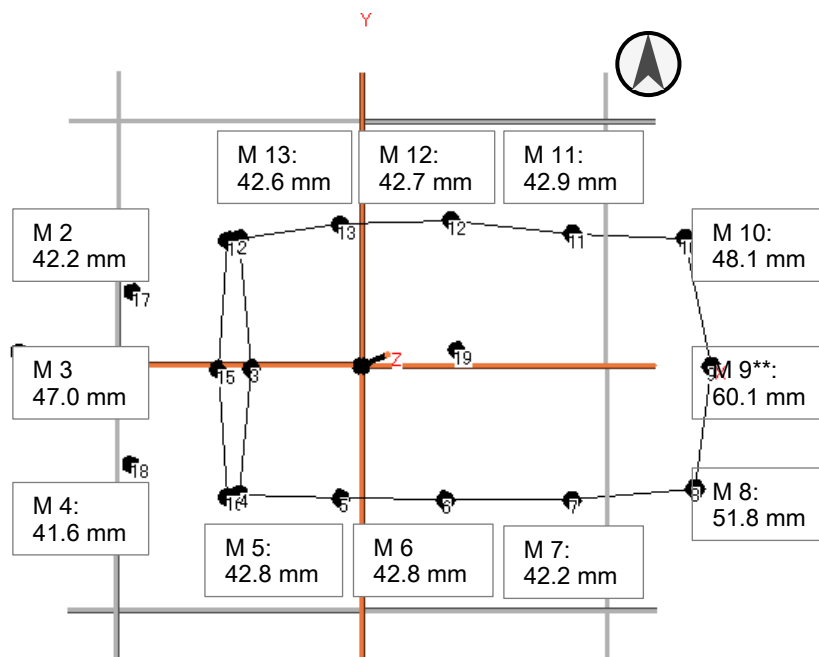


Fig. 4-35 Deformation when M 9 reached its maximum displacement at case 53

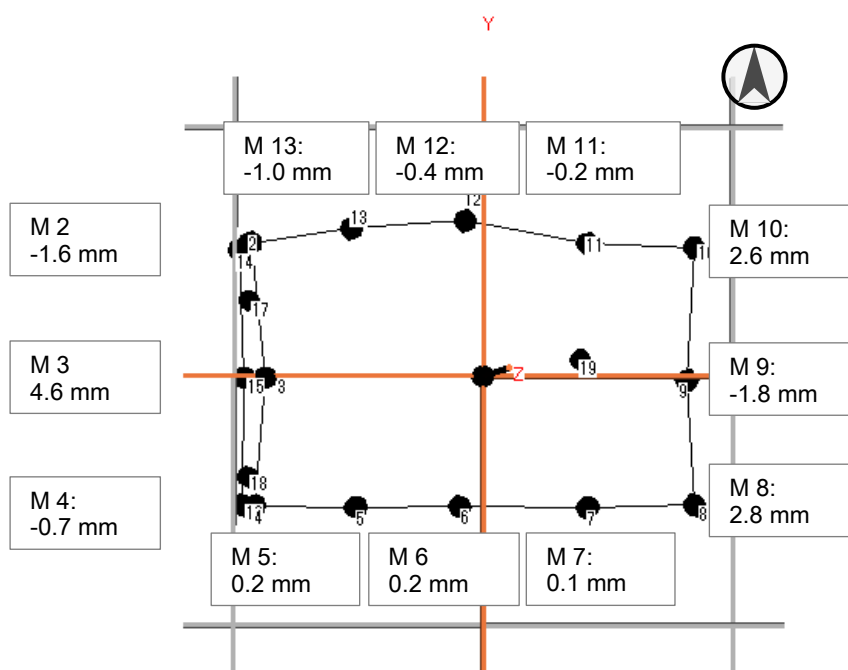


Fig. 4-36 Deformation after case 53

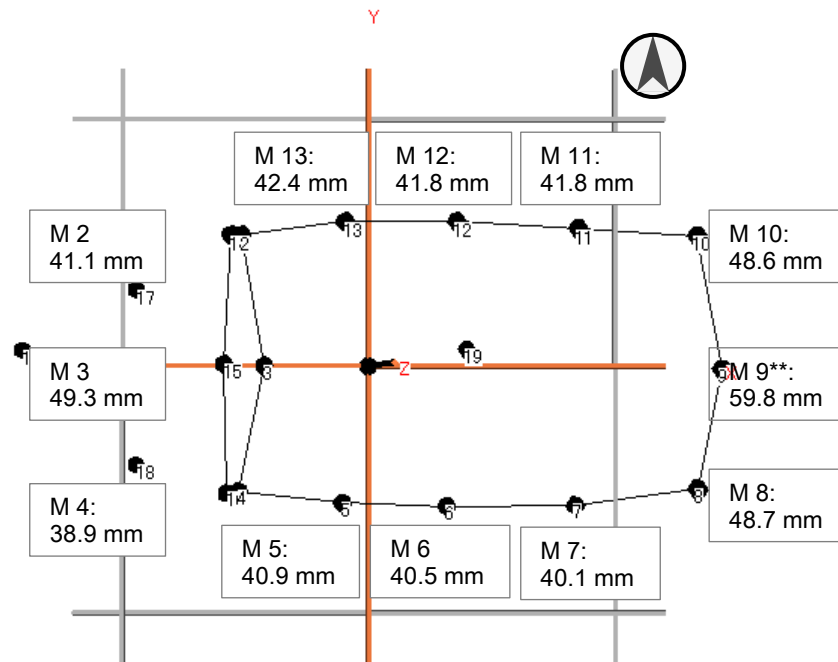


Fig. 4-37 Deformation when M 9 reached its maximum displacement at case 54

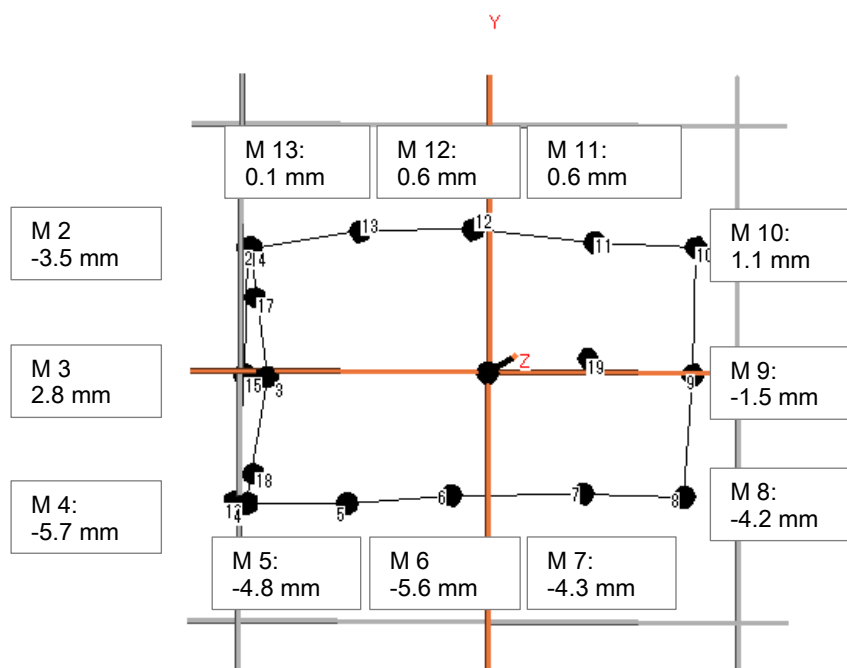


Fig. 4-38 Deformation after case 54

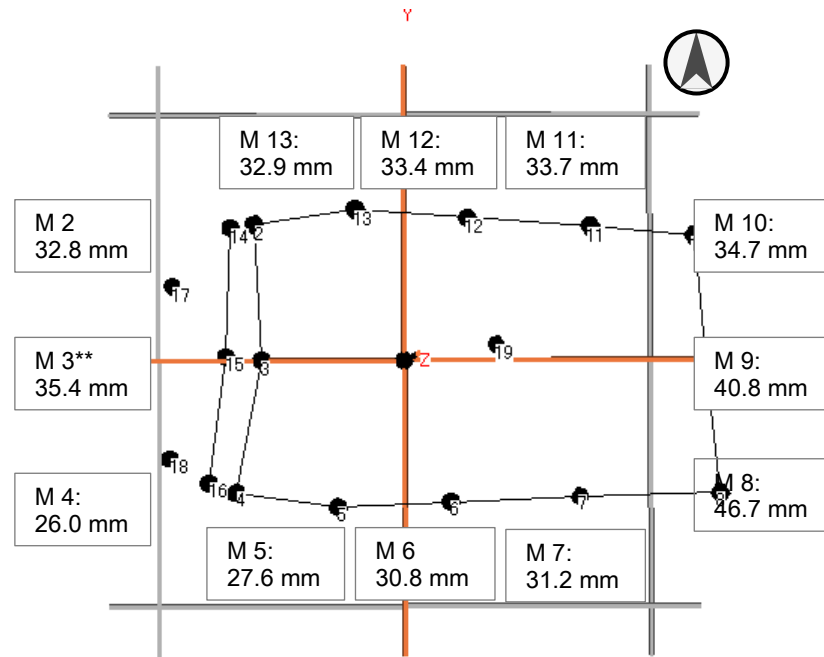


Fig. 4-39 Deformation when M 3 reached its maximum displacement at case 55

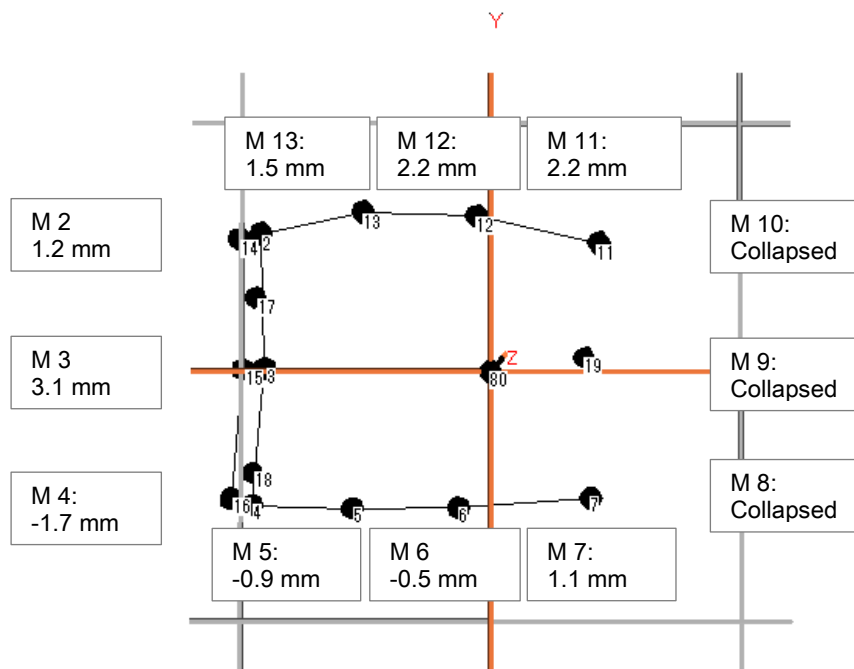


Fig. 4-40 Deformation after case 55

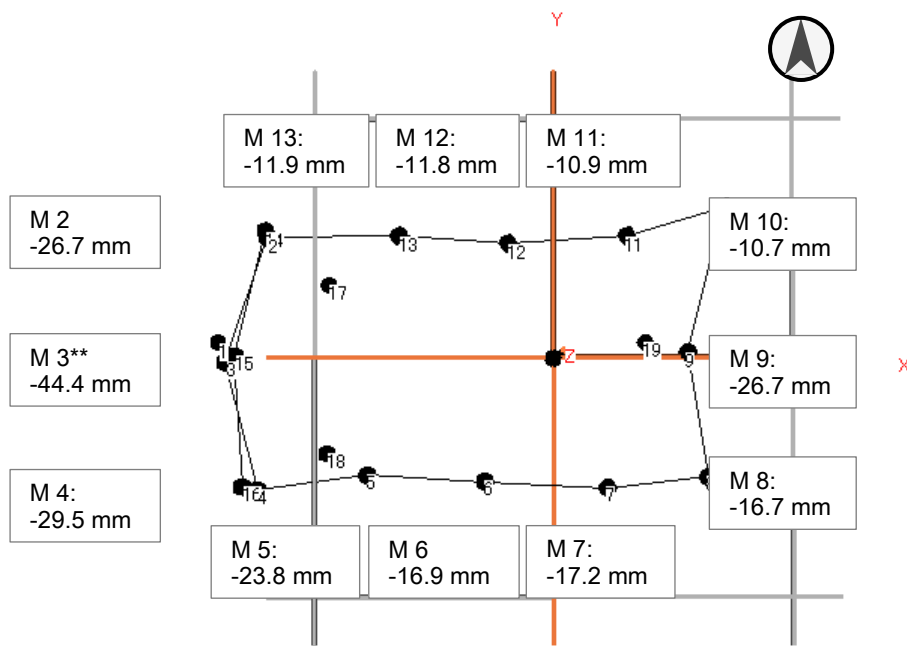


Fig. 4-41 Deformation when M 3 reached its maximum displacement at case 56

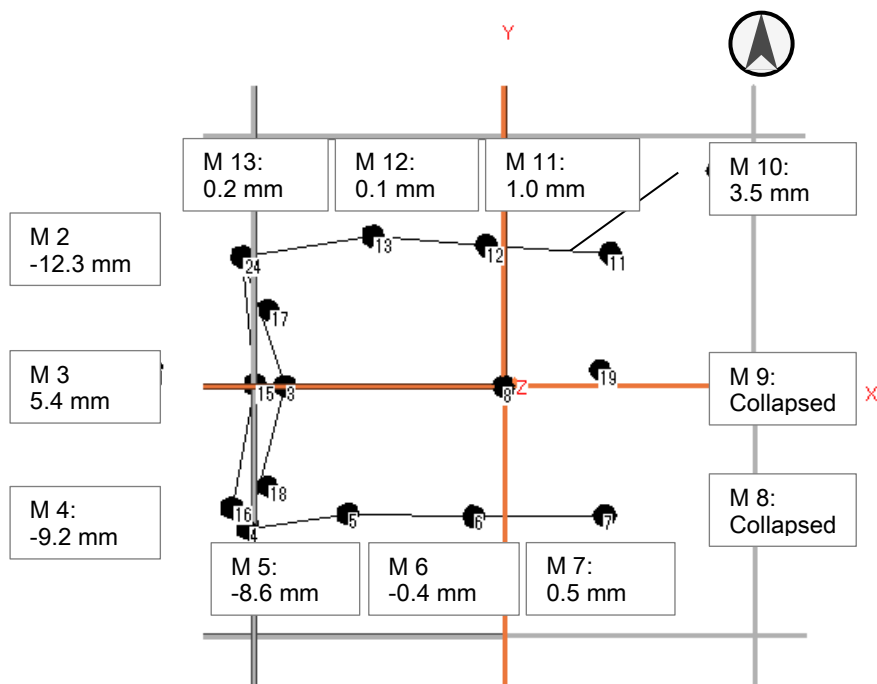


Fig. 4-42 Deformation after case 56

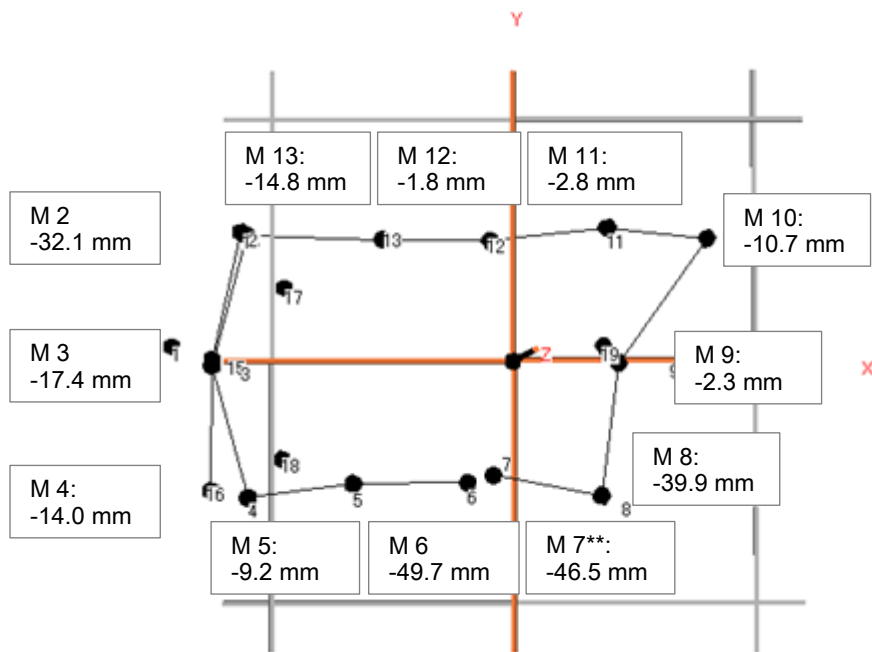


Fig. 4-43 Deformation when M 7 reached its maximum displacement at case 57

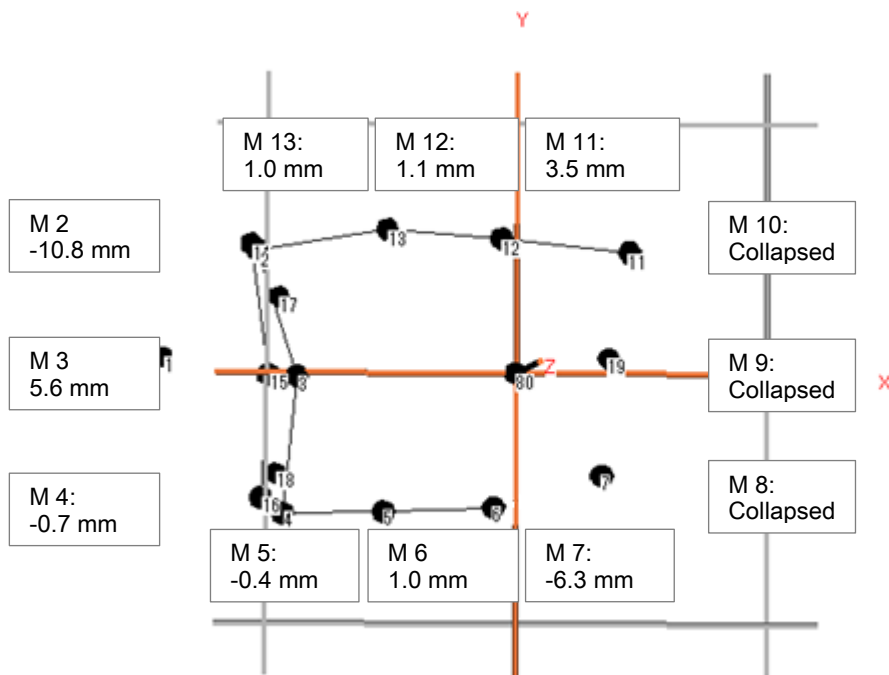


Fig. 4-44 Deformation after case 57

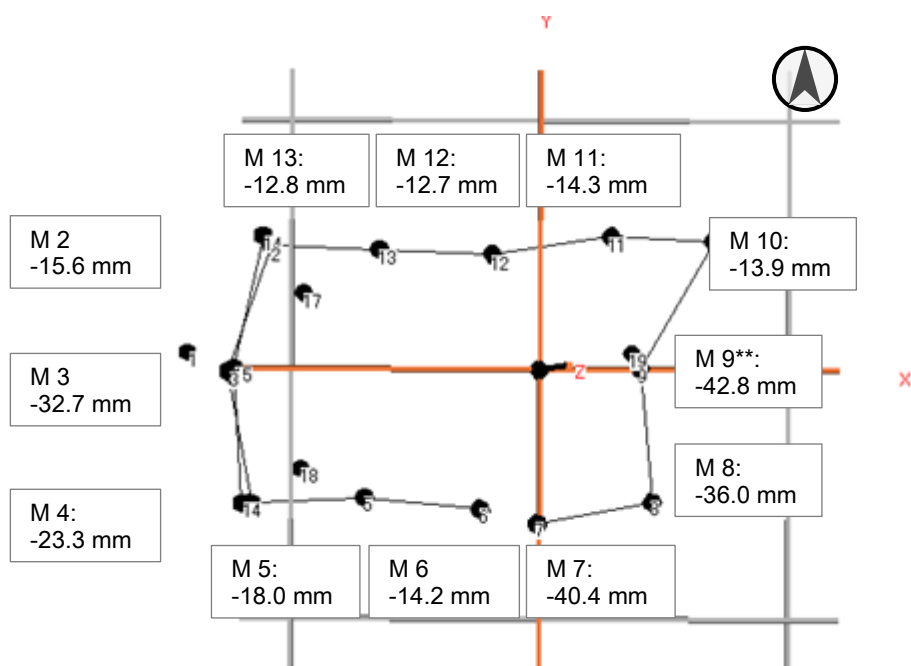


Fig. 4-45 Deformation when M 9 reached its maximum displacement at case 58

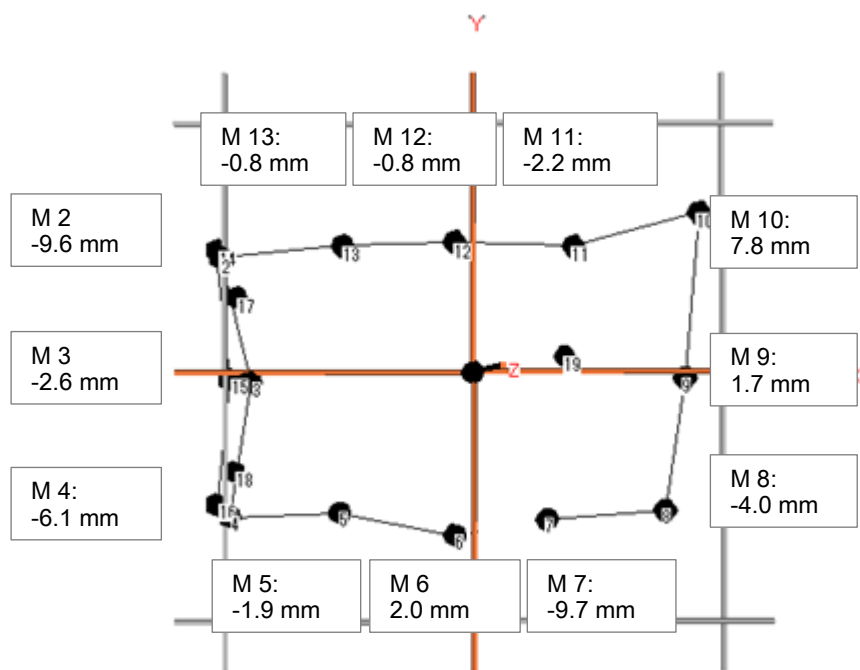


Fig. 4-46 Deformation after case 58

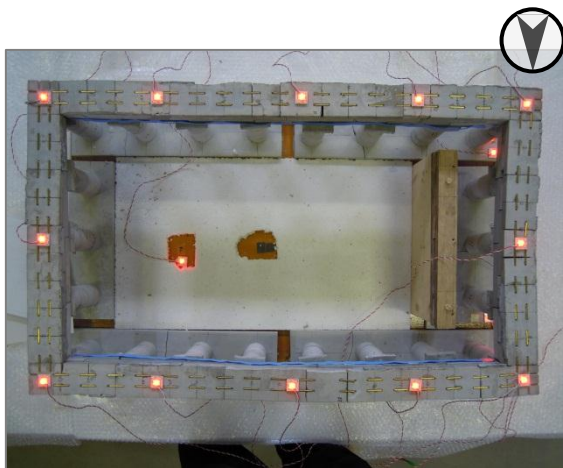


Fig. 4-47 Case 54

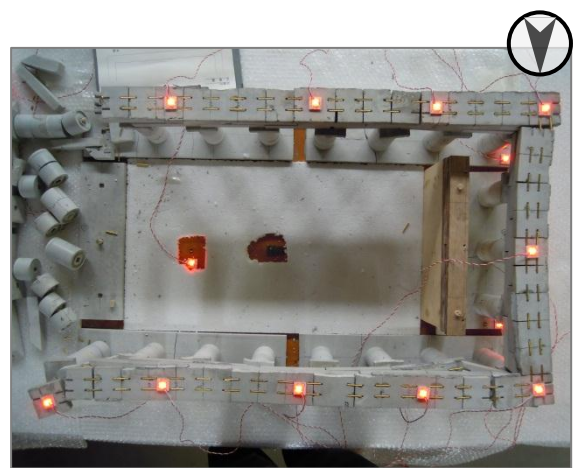


Fig. 4-48 Case 56

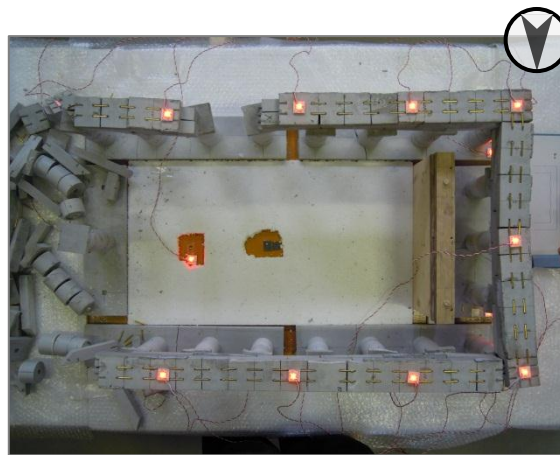


Fig. 4-49 Case 57

The following photos (figs. 4-47 through 4-49) show the deformation and partial failure of the model after each test. The reinforce method 2 protected the model against collapse and reduced the deformations of the entablatures (fig.4-47).

The remarks of this experiment were summarized as follows:

1. The reinforcement method 2 suggested by the authors were effective to prevent the collapse of the model and contribute to confinement of the structure. However, it could not be said that reinforcement reduces the displacement during the base motions. The dynamic displacement of some markers became the largest at the case in which the model was reinforced with the method 2.
2. The “inner beams,” carried their binding force to cause the out-of-plane behavior of the west colonnade; in particular, to the behavior in outside direction. For example, compared case 57 with case 58, the displacement of the middle of the west colonnade toward outside the structure was reduced by 20% for the case in which the model had inner beams.
3. The deformations during excitation were occurred in perpendicular to shaking direction as well. However, the residual displacement didn't always coincide with the dynamic response during excitations.

4.4 Concluding remarks

Through the experiments phase 1 and phase 2, the residual displacement of the west colonnade of the actual monument caused by the earthquake of 1981 could be reproduced quite well. Moreover, it was supposed that the deformations of the entablature depended on high non-linear response of the dry stone masonry. The behavior of the monument was figured out qualitatively, but it was not enough because the specimen could not recreate the behavior of the monument exactly. These tests results were fruitful but more accurate model is necessary to study the seismic performance of the monument.

The model showed different response characteristics among same input motions. The differences observed were the pattern of destruction. These were attributed to the sensitivity of the phenomenon to even small irregularities as H. P. Mouzakis *et al.* indicated [8].

Chapter 5 Structural Analysis

5.1 Introduction

The structural analysis is very useful to study the dynamic behaviors of the monument under the strong motions. In this chapter, equivalent linear analysis was conducted and the attempts were made to clarify the mechanisms the damage of the monument caused by the Corinth earthquake in 1981.

At first, the structural model introduced by Hanazato *et al.* [2] was revised and verified by the micro tremor measurements. Then, seismic simulation analyses were carried out with seismic input motion of record at the Acropolis hill and simulated wave synthesized in chapter 3. The analysis was conducted with the software TDAP III (ARK Information Systems).

5.2 Analysis Model

The model used for simulation was equivalent linear model based on the model proposed in the past study of which model was represented by a single column. In previous study, the models were composed of those columns and horizontal beams, and representing the whole peripteral structures of the monument.

The masses were substituted for the drums of columns. Each mass was connected with vertical beam element which has appropriate young modulus and shear modulus of rigidity for rotation and translation of each drum. Mass 14 and mass13 which represent cornice & frieze and architrave respectively was connected with translational spring. Moreover, horizontal beam element connected the columns at each level of cornice & frieze and architrave. This model is called the model 1 in the following sections of this thesis. Fig. 5-1 shows the model and table 5-1 says their parameters of the model.

Table 5-1 Parameters used for columns of analysis model

| Mass | Weight [tf] | Height [m] | Vertical element | Young's modulus [tf / m ²] | Shear modulus of rigidity [tf / m ²] |
|------|----------------|---------------|---------------------|---|---|
| M 14 | 363.48 | 12.779 | k 14 | 77000000 | - |
| M 13 | 232.06 | 11.204 | L 13 | 1351198 | 3010000 |
| M 12 | 64.97 | 10.080 | L 12 | 363740 | 1646670 |
| M 11 | 42.73 | 9.135 | L 11 | 1113884 | 3102251 |
| M 10 | 44.88 | 8.265 | L 10 | 1123115 | 3100930 |
| M 9 | 47.04 | 7.395 | L 9 | 1131999 | 3106048 |
| M 8 | 49.20 | 6.525 | L 8 | 1137962 | 3098563 |
| M 7 | 51.55 | 5.655 | L 7 | 1144850 | 3097182 |
| M 6 | 53.61 | 4.785 | L 6 | 1155627 | 3111361 |
| M 5 | 56.15 | 3.915 | L 5 | 1159457 | 3093117 |
| M 4 | 58.51 | 3.045 | L 4 | 1173899 | 3090823 |
| M 3 | 60.96 | 2.175 | L 3 | 1174212 | 3089491 |
| M 2 | 63.41 | 1.305 | L 2 | 1187057 | 3092325 |
| M 1 | 66.15 | 0.435 | L 1 | 1192193 | 3080128 |

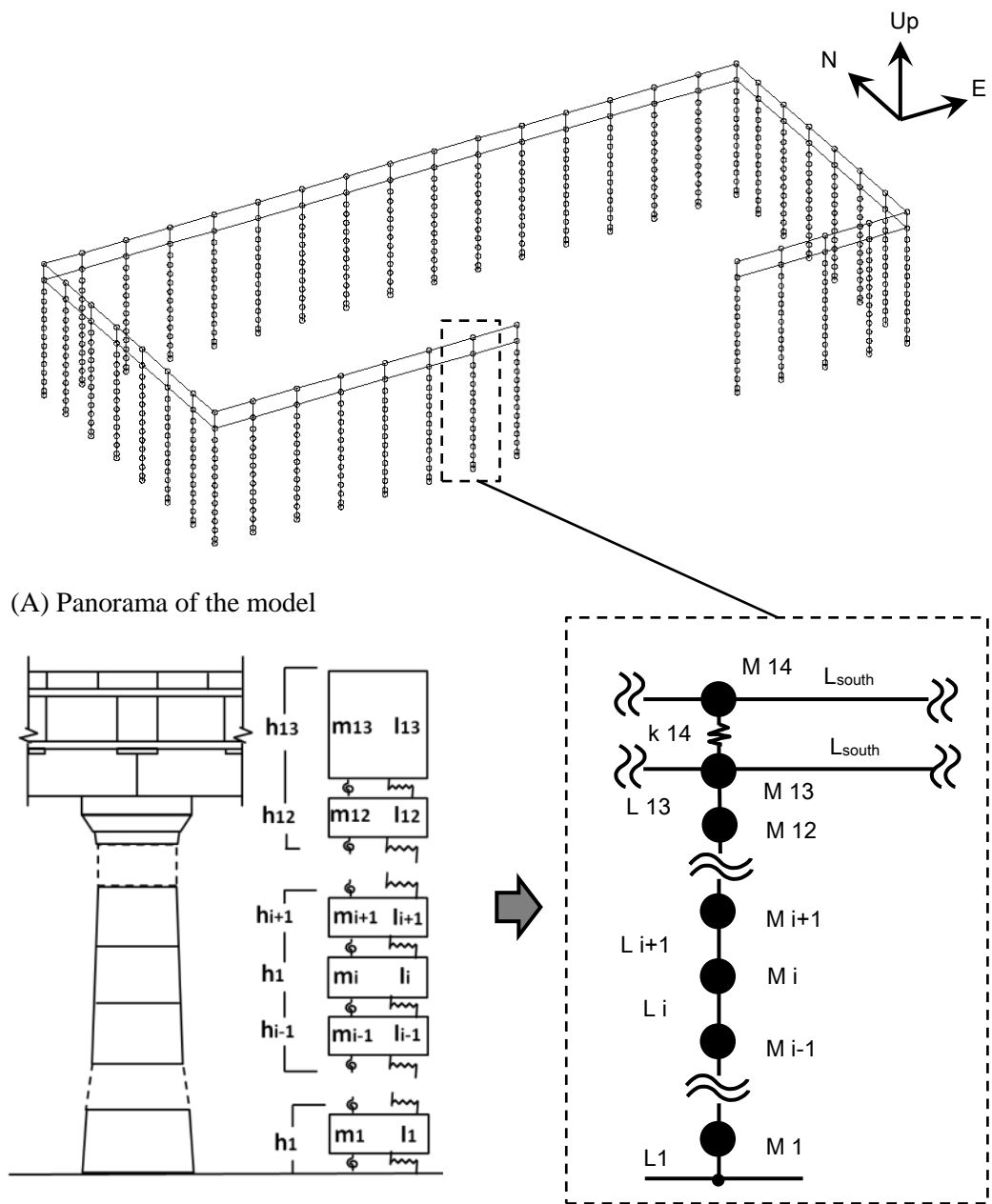


Fig. 5-1 Analysis model 1

5.3 Identification of the Model Parameters

The analysis model was identified by use of the results of microtremor measurements. As results, the stiffness of the horizontal beams and the natural frequencies of the colonnades of the model were successfully determined as shown in table 5-2 and table 5-3, respectively.

Table 5-2 Parameters used for horizontal beams of model 1

| | Young's modulus [tf / m ²] | Shear modulus of rigidity [tf / m ²] | Reduction factor* |
|-----------------|---|---|----------------------|
| West colonnade | 616000 | 269600 | 2 / 25 |
| East colonnade | 462000 | 202200 | 3 / 50 |
| North colonnade | 4235000 | 1853500 | 11 / 20 |
| South colonnade | 4235000 | 1853500 | 11 / 20 |

* Reduction factor denotes the ration of the stiffness of the model to that of the marble material

Table 5-3 Natural frequencies of the model 1 and result of measurements

| | In-plane | | out-of-plane | |
|-----------------|----------|-------------|--------------|-------------|
| | Analysis | Measurement | Analysis | Measurement |
| West colonnade | 3.94 Hz | 3.3 Hz | 2.49 Hz | 2.4 Hz |
| East colonnade | 3.29 Hz | 3.7 Hz | 2.74 Hz | 2.7 Hz |
| North colonnade | 3.64 Hz | 3.7 Hz | 2.67 Hz | 2.7 Hz |
| South colonnade | 3.64 Hz | - | 2.67 Hz | - |

In general, such parameters of elements in the model were expected to take the same values in each colonnade because it was assumed that the horizontal beam element was made by the same material and had same length, cross-section shape for each colonnade. The differences between the stiffness of the beam elements shown in table 5-2 were too big even after considering the weight of the pediment which is on the west and east colonnades. In order to explain this phenomenon, another model: model 2 was assumed. The model 2 was almost the same as the model 1, but the model 2 has the weak rotational spring acting in horizontal plane at joint of horizontal beams (see fig. 5-2). Moreover, the horizontal beam elements have different properties affected by the position of the colonnade for the model 1. However, those of the model 2 have just the same properties at any colonnade.

The parameters of the rotational spring and horizontal beams and natural frequencies of the model 2 were shown in table 5-4 and table 5-5, respectively.

According to the micro tremor measurement, the natural frequency of the colonnade did not depend on the length of the colonnade. It suggested that the colonnade would be composed of structural unit of the 2 columns and 1 horizontal beam. It was the same condition that the horizontal beams were connected with weak rotational spring in the model 2. In the model 1, however, horizontal beams were jointed each other rigidly. Therefore, such unit condition was lost and a number of beams behaved as one long beam. In this case, the natural frequency of the colonnade

depends on the length of the colonnade. So, the natural frequency of the shorter colonnade (west and east colonnade) became higher than that of longer colonnade (north colonnade). In addition, the west and east colonnade have the weight of the pediment which make the natural frequency lower. Hence, it was necessary to reduce the rigidity of the horizontal beams of the west and east colonnade in the model 1 to identify with the results of measurements.

Table 5-4 Parameters of the horizontal elements for model 2

| | Young's modulus [tf / m ²] | Shear modulus of rigidity [tf / m ²] | Spring constant [tf * m] |
|----------------|---|---|-----------------------------|
| L _H | 7700000 | 3370000 | - |
| k _R | - | - | 1000 |

Table 5-5 Natural frequencies of the model 1 and model 2

| | In-plane | | out-of-plane | |
|-----------------|----------|---------|--------------|---------|
| | Model 2 | Model 1 | Model 2 | Model 1 |
| West colonnade | 3.52 Hz | 3.94 Hz | 2.45 Hz | 2.49 Hz |
| East colonnade | 3.83 Hz | 3.29 Hz | 2.93 Hz | 2.74 Hz |
| North colonnade | 3.90 Hz | 3.64 Hz | 2.27 Hz | 2.67 Hz |
| South colonnade | 3.88 Hz | 3.64 Hz | 2.30 Hz | 2.67 Hz |

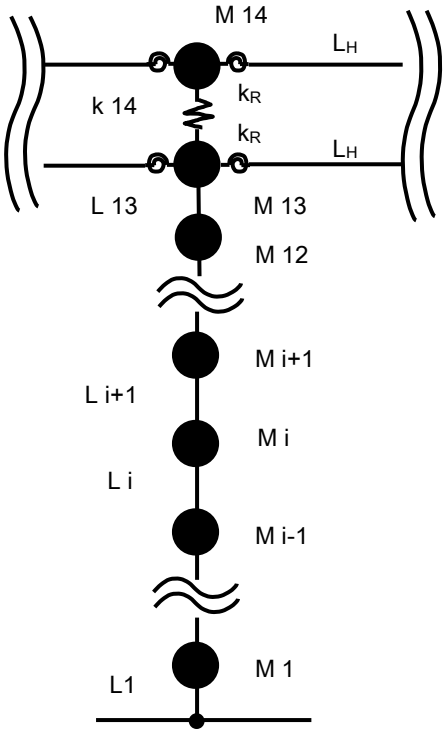


Fig. 5-2 Analysis model 2

5.4 Seismic Input Ground Motion

There were 2 input ground motions for the dynamic response analysis as follows:

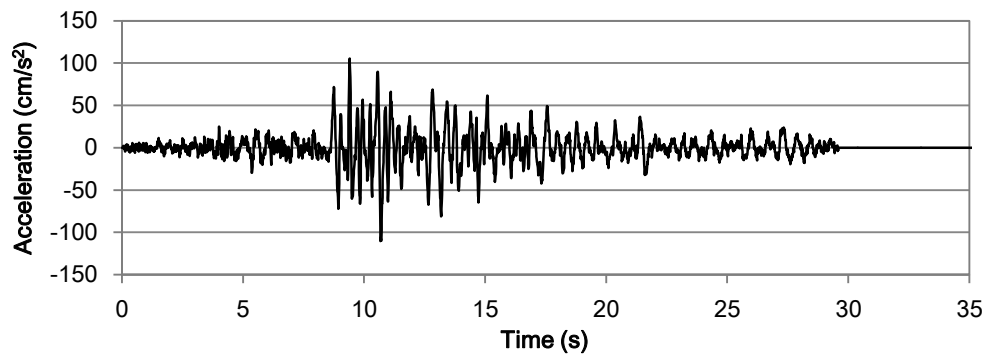
1. Accelerogram obtained at the base of the Parthenon Athens in Sep. 2010. It was, however, very small as mentioned in chapter 2, so the time history of acceleration with 250 % of the record was used. It was called “Sep.2010 motion” in the following sections of this chapter. Table 5-6 shows the detail of the input motion and figs 5-3 and 5-4 show the time histories of input motion.
2. The simulated ground motion at the base of the Acropolis hill when the Corinth earthquake in 1981 synthesized in chapter 3 but the magnitude was doubled in order to set the acceleration level with Sep. 2010 motion. It was called “Corinth motion” in the below of this chapter. Table 5-7 shows the detail of this motion and figs 5-5 and 5-6 show the time histories of this motion.

The acceleration level of the input ground motion was decided in dependence upon the calculated acceleration in the past study by the authors [13]. It was calculated that maximum ground acceleration that the Parthenon Athens has experienced for 2500 years was around 200 cm/s^2 .

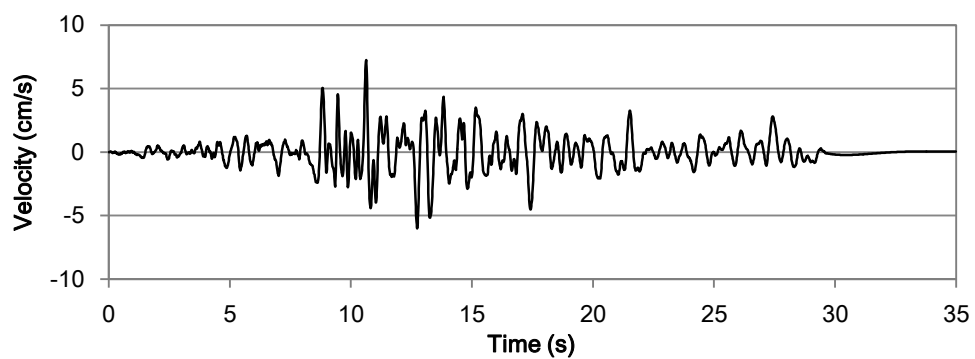
The differences of these two motions were that Corinth motion involved long-period seismic wave.

Table 5-6 Detail of the Sep. 2010 motion

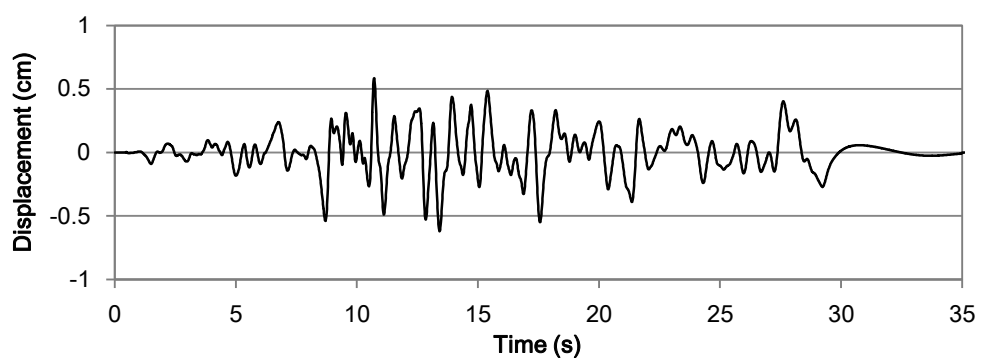
| Direction | | Acceleration [cm/s ²] | Velocity [cm/s] | Displacement [cm] |
|-----------|------|-----------------------------------|-----------------|-------------------|
| N-S | Max. | 105.3 | 7.1 | 0.59 |
| | Min. | -110.4 | -6.0 | -0.61 |
| E-W | Max. | 182.2 | 7.7 | 0.66 |
| | Min. | -130.2 | -10.6 | -0.55 |



(A)

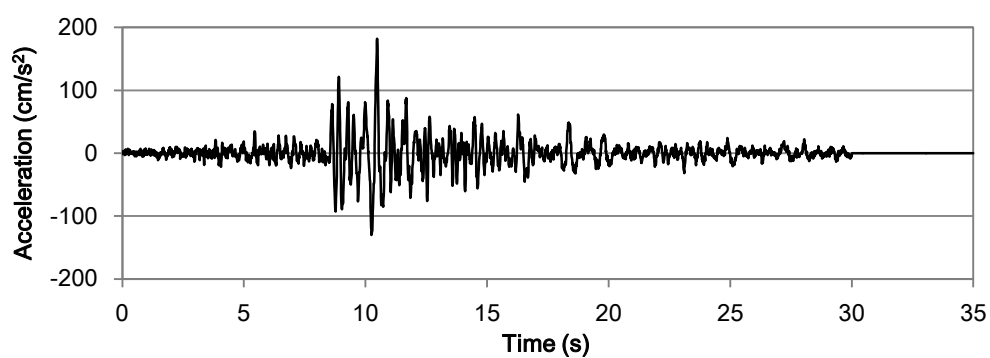


(B)

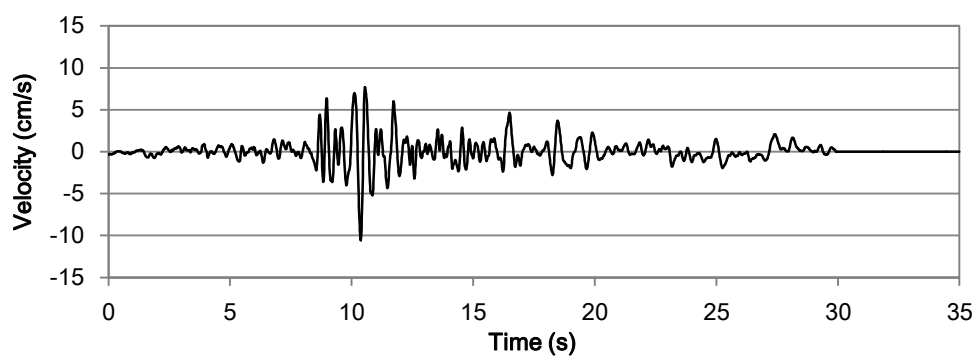


(C)

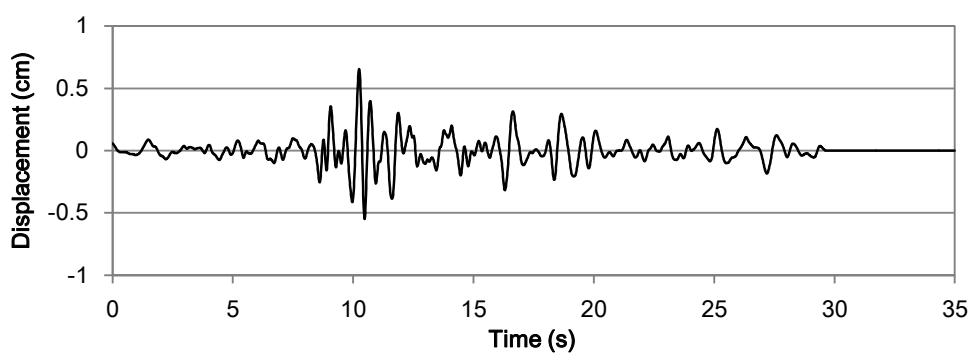
Fig. 5-3 Time histories of A) acceleration, B) velocity and C) displacement of Sep. 2010 motion in N-S direction



(A)



(B)



(C)

Fig. 5-4 Time histories of A) acceleration, B) velocity and C) displacement of Sep. 2010 motion in E-W direction

Table 5-7 Detail of the Corinth motion

| Direction | | Acceleration [cm/s ²] | Velocity [cm/s] | Displacement [cm] |
|-----------|------|-----------------------------------|-----------------|-------------------|
| N-S | Max. | 180.1 | 10.9 | 1.47 |
| | Min. | -142.1 | -10.0 | -0.77 |
| E-W | Max. | 180.5 | 9.9 | 1.34 |
| | Min. | -160.8 | -9.9 | -1.68 |

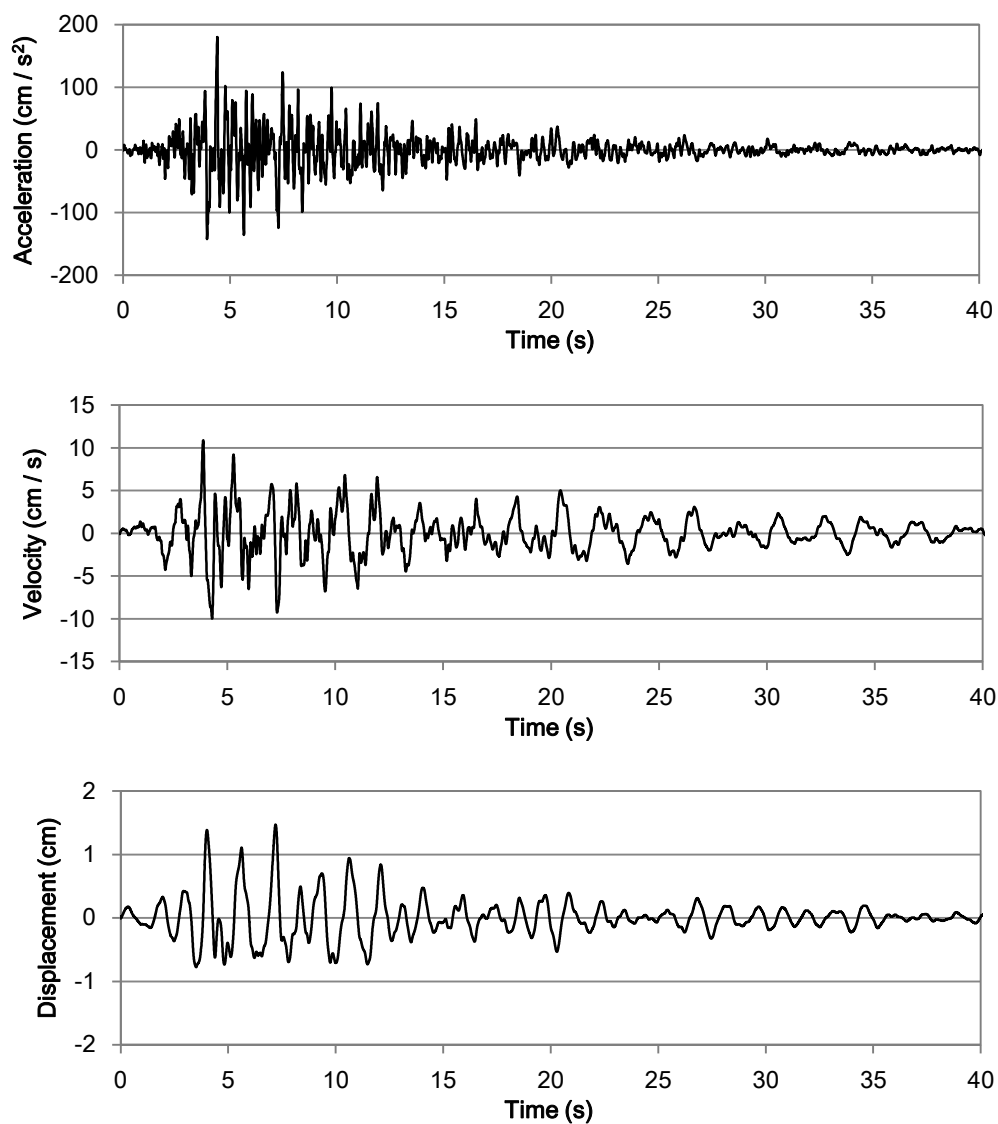


Fig. 5-5 Time histories of A) acceleration, B) velocity and C) displacement of Corinth motion in N-S direction

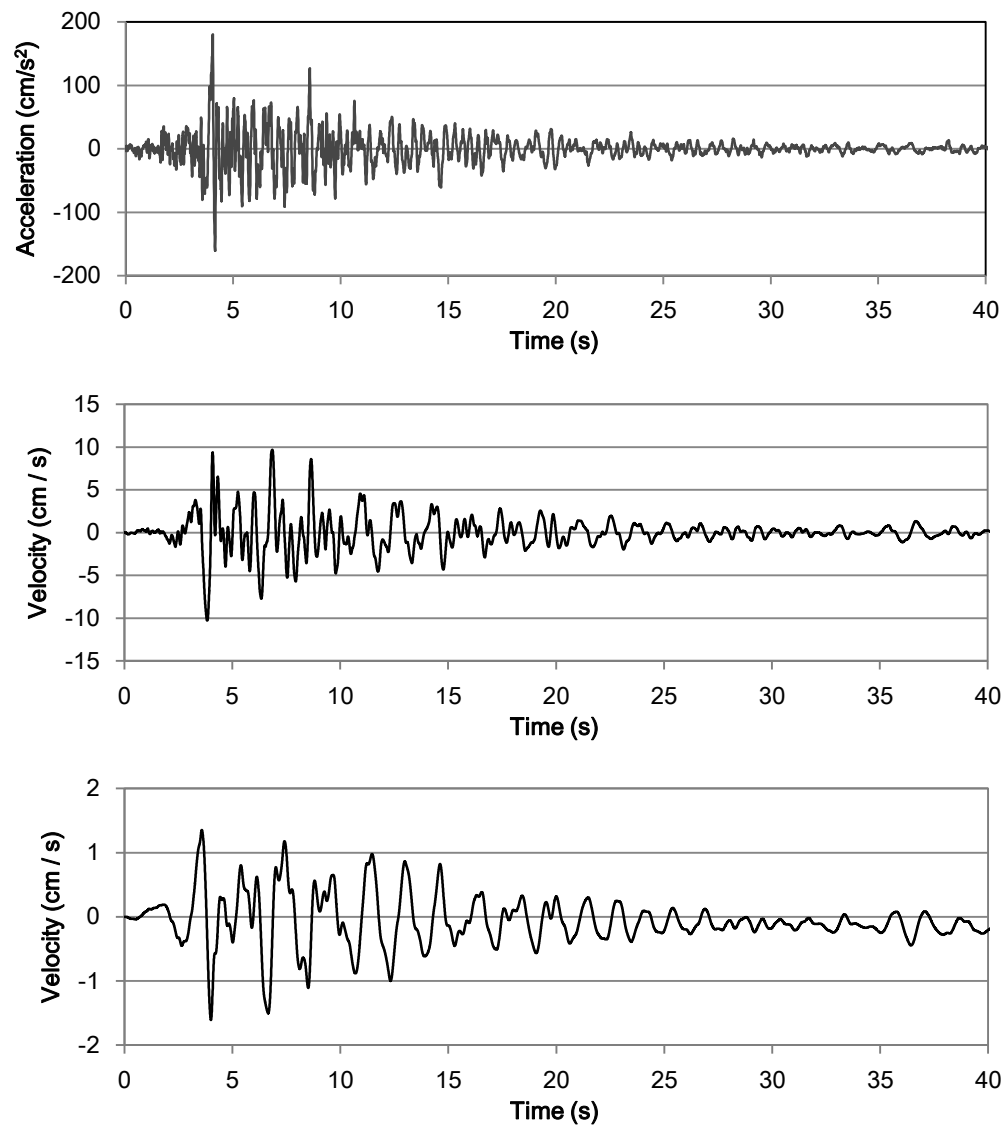


Fig. 5-6 Time histories of A) acceleration, B) velocity and C) displacement of Corinth motion in E-W direction

5.5 Analysis Results

In the model, the point which showed the maximum response acceleration and displacement was column-63 (see fig. 5-7) for Sep. 2010 motion and column-671 (see fig.5-7) for Corinth motion. Moreover, the distributions of maximum response values along the height of column-63 and column-671 are presented in fig. 5-8 and fig.5-11 respectively. Fig. 5-9 and fig. 5-12 show the response displacement of the column along the height of the column at the time when the column reached the peak displacement during seismic excitation. Figs. 5-10 and fig 5-13 show the maximum shear coefficients of the along the height of the column-63 and column-671, respectively. Maximum shear coefficient was 0.40 while the friction coefficients between the marble drums were 0.36 to 0.80 measured by Y. Mabuchi [6].

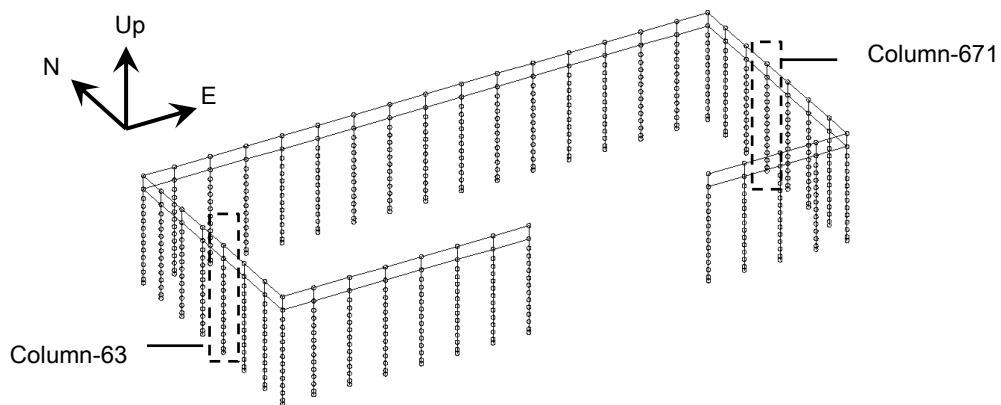


Fig. 5-7 Position of the columns

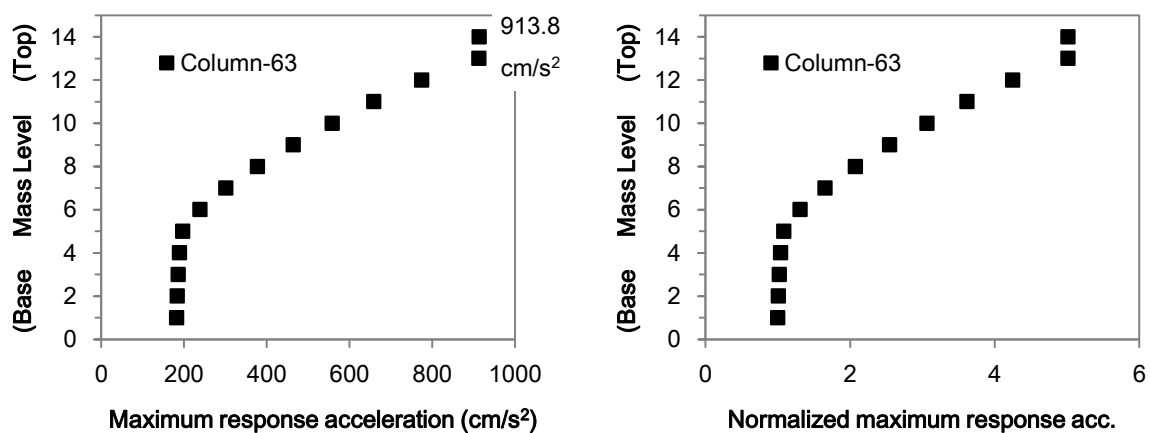


Fig. 5-8 Distribution of the maximum response acceleration at Sep. 2010 motion

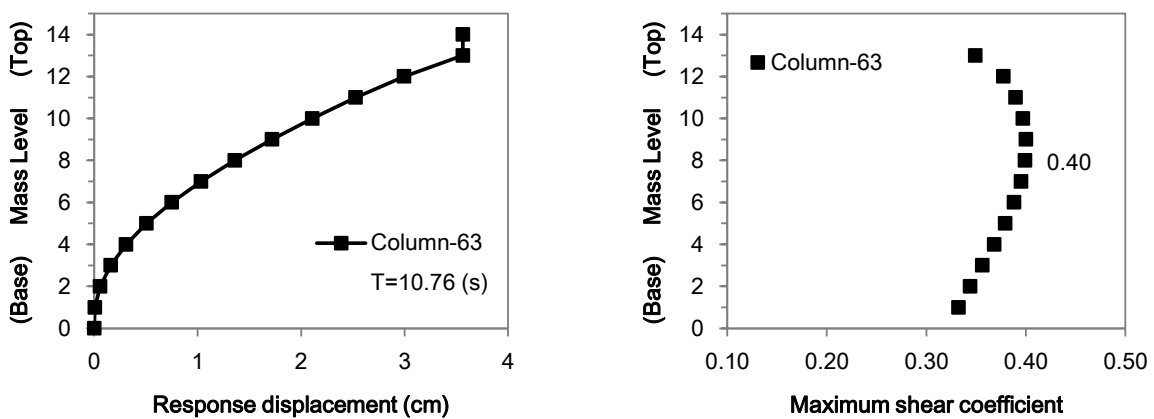


Fig. 5-9 Response displacements along the height of the model at Sep. 2010 motion

Fig. 5-10 Distribution of the maximum shear coefficient at Sep. 2010 motion

The maximum response acceleration was almost the same for 2 input motions. The maximum displacement response at Sep. 2010 motion was larger than one at Corinth motion. This result indicated that the long-period seismic wave cause less displacement of marble members than short-period one. However, in this analysis, the model was elastic one, so it didn't seem to show the actual response of the monument. In the near future, it would be necessary to conduct structural analysis with non-linear model.

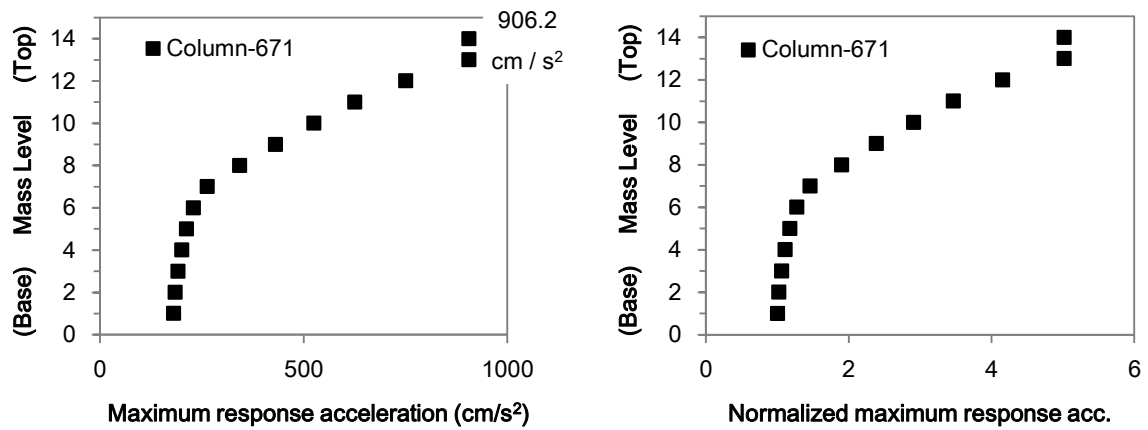


Fig. 5-11 Distribution of the maximum response acceleration at Corinth motion

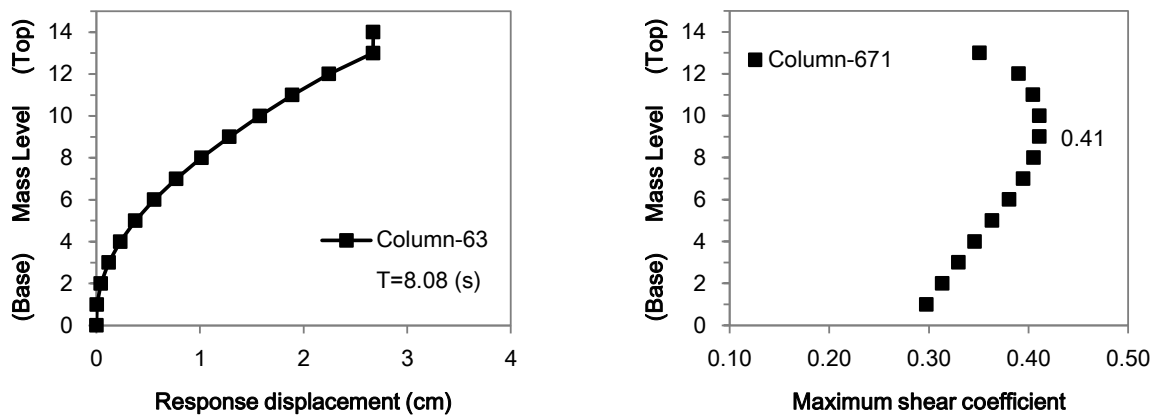


Fig. 5-12 Response displacements along the height of the model at Corinth motion

Fig. 5-13 Distribution of the maximum shear coefficient at Corinth motion

Table 5-8 Base shear

| | Direction | Time [s] | Base shear [tf] | Base shear coefficients |
|-----------|-----------|----------|-----------------|-------------------------|
| Sep. 2010 | N-S | 10.76 | 11446.76 | 0.21 |
| | E-W | 10.51 | 14257.95 | 0.26 |
| Corinth | N-S | 4.045 | 13389.56 | 0.24 |
| | E-W | 4.05 | 9928.84 | 0.18 |

Table 5-8 present the base shear and base shear coefficients.

5.5.1 Mechanical Reason of Residual Displacement

Following figs 5-14 and 5-15 show the shear forces acting on the springs between architrave and frieze. The shear force at the northwest and southwest corners mainly acted on N-S direction while the Sep. 2010 motion caused larger excitation in E-W direction than in N-S direction or while Corinth motion caused almost the same excitation in E-W and N-S direction. These forces at the corners might affect the behavior of the corners toward outside of the model.

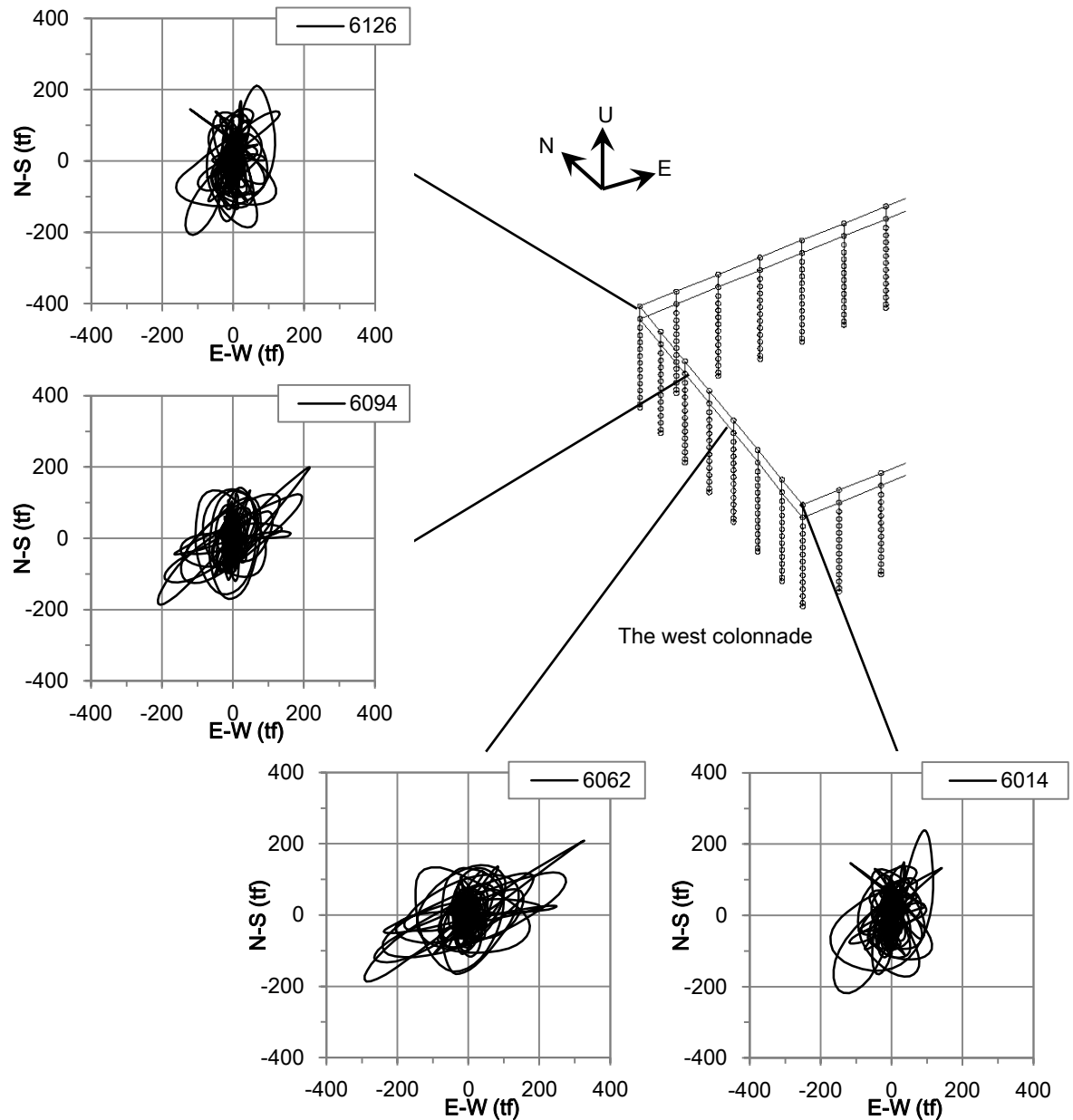


Fig. 5-14 Shear forces acting on the west colonnade at Sep. 2010 motion

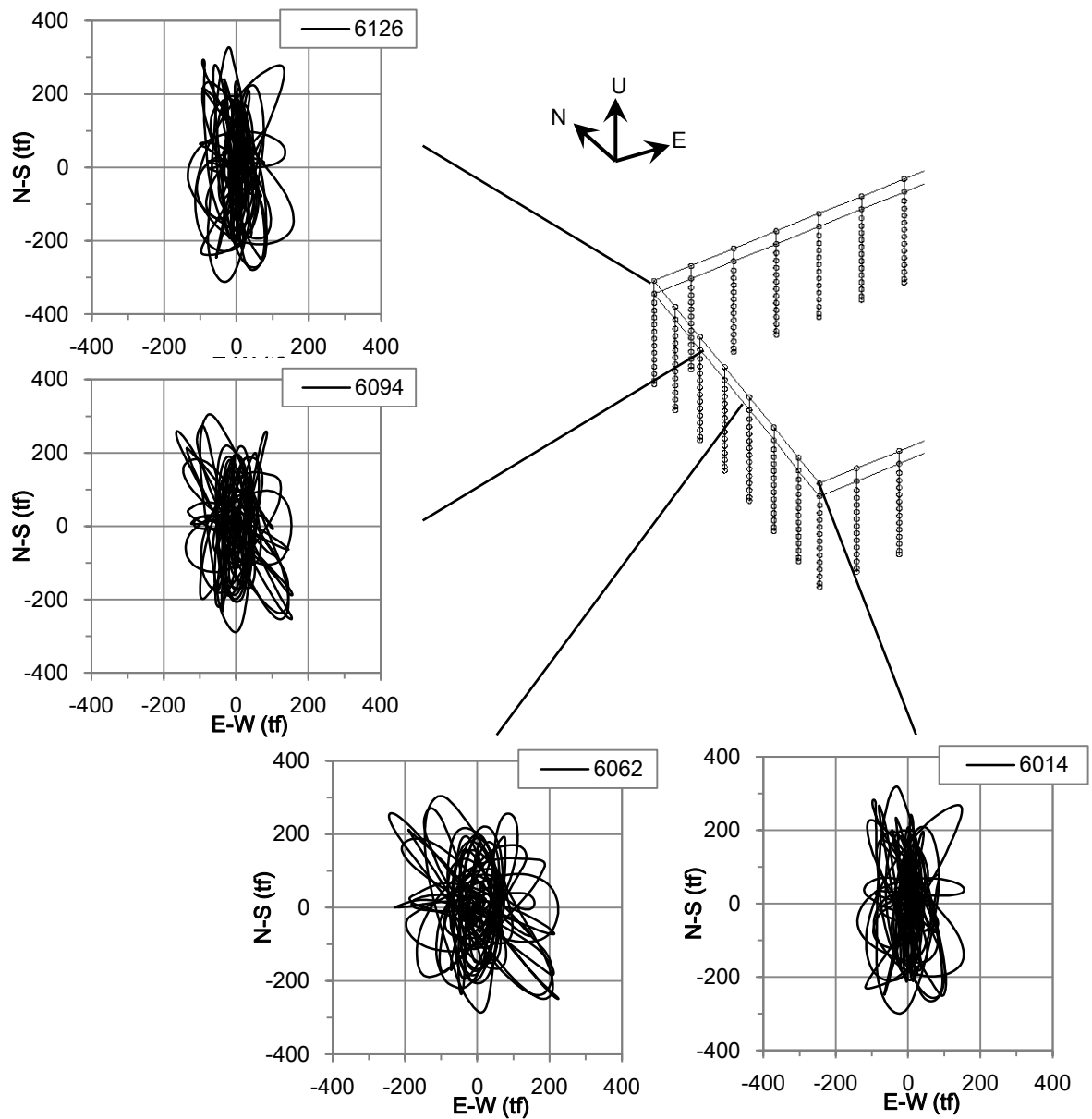


Fig. 5-15 Shear forces acting on the west colonnade at Corinth motion

5.6 Concluding Remarks

The dynamic behaviors of whole peripteral structure of the monument subjected to the simulated ground motions were evaluated and the shear force which was capable to deform the corners of the monument outward was shown.

This analysis simulated the behavior of the monument just at the linear level, it would be necessary to estimate the seismic performance of the monument at non-linear level.

Chapter 6 Conclusions

6.1 Summary of the Study

In the present research collaborated with Greek experts, the fundamental dynamic behaviors of the Parthenon Athens were studied to assess them at linear level by the field survey and by the dynamic structural analysis using the equivalent elastic model. Furthermore, the seismic behaviors at non-linear level were studied by the shaking table tests.

As results of the field survey by microtremor measurements the natural frequencies of the colonnades of the Parthenon Athens were clarified. The natural frequencies of the west colonnade were 2.4 Hz at in-plane direction and 3.3 Hz at out-of-plane direction. At the east colonnade, 2.7 Hz and 3.7 Hz were obtained as the natural frequencies at in-plane and out-of-plane direction, respectively. The natural frequencies of the north colonnade were affected by the location of microtremor sensors in out-of-plane direction, but significant spectral peaks were observed in the range of 2.7 to 3.7 Hz. On the other hand, the value of 3.7 Hz was obtained in in-plane direction.

One earthquake record was obtained at the base of the monument in Sep. 2010 by the seismometers installed by the authors in 2008, however, it was too small to study the seismic performance of the monument during earthquake ground motions. It is necessary to record earthquake data which is enough to know the actual behaviors of the monument under the seismic excitation as well as to revise the analysis model.

Simulated ground motions at the past earthquakes: Athens earthquake of 1999 and the Corinth earthquake of 1981 was synthesized by fitting acceleration response spectra to the target ones. The peak ground accelerations were estimated to be 112.7 cm/s^2 for 1999 and 90.1 cm/s^2 for 1981. In this study, however, the time histories of acceleration just at the base of the Acropolis hill where the monument is standing were simulated. Further study is needed to evaluate the ground motions affected by the topographical effect of the hill.

Shaking table tests were conducted with the simplified miniature model of the Parthenon Athens. The deformation of the actual monument caused by the earthquake of 1981 was reproduced quite well. Furthermore, the dynamic behaviors of the model with high non-linearity were assessed. As results, it was supposed that the deformation depended on such high non-linear response. Moreover, the following 2 methods of reinforcement were discussed. Method 1: additional beams were installed in the south colonnade of which a part has been missing. Method 2: connection between beams was ensured by using metal tie-bands or tie-rods, which was expected to be effective in improvement of seismic performance. By shaking table tests, the effects of the methods were examined. As results, in case of method 1, the model was as unstable as the non-reinforced model. In case of the other method, the reinforcement produced the effect on confinement of the structure and prevention of the residual displacement. The maximum displacement during excitation, however, became larger than that of non-reinforced model.

Although the residual displacement of the actual monument caused by the earthquakes was reproduced in our experiments and at the same time, the effect of the anti-seismic restoration techniques were examined, the test model structures were just miniature ones. Therefore, it should be recognized that there is limitation to understand the actual behaviors because of similarity low. It would be necessary to carry out tests with more accurate model of larger size. Furthermore, it would be expected to record the seismic behaviors of the actual monument as we continue earthquake monitoring.

Seismic response analysis was carried out by employing the linear equivalent frame model. The elastic rigidity of the model was successfully evaluated from the system identification procedure. This identification analysis was performed so that the calculated natural frequencies of the colonnades could agree with the microtremor measurements. As results of response analysis, the behavior of the model subjected the simulated ground motions was evaluated. It also indicated that the shear forces acting on the beams might induce the outward displacement of entablatures.

6.2 Future Studies

In this research, fundamental characteristics of the Parthenon Athens were studied. However, these were the characteristics at linear level. To discuss the dynamic behavior at non-linear level, shaking table tests were conducted, but even by the shaking table tests, the model might not recreate the actual behavior of the monument entirely. In order to study the characteristics of the monument in non-linear level, more accurate laboratory test or non-linear structural analysis model would be necessary.

The study for topographic effect is also important to estimate input ground motions. In this study, the acceleration at the base of the Acropolis hill when the past earthquakes were generated. In further study, the ground motions should be synthesized by taking into account the topographical effect of the hill.

It is important to get the record of both the monument and the ground during earthquake by the monitoring systems. These record or data is essential to understand the accrual behavior of the monument and the topographical effect. It is necessary to continue the earthquake monitoring in the future.

Acknowledgment

The author sincerely thanks to prof. T. Hanazato for his schooling. The author is deeply grateful to Dr. H. P. Mouzakis from the National Technical University of Athens, Dr. M. Ioannidou from the Acropolis Restoration Office and Dr. A. Miltiadou from Hellenic Ministry of Culture and Tourism for their kind cooperation in the international investigation.

At the field survey, the author was supported by Dr. C. Minowa and Dr. T. Nakagwa. At the laboratory tests, prof. Niitsu from Tokyo Denki University, Dr. Hirabayashi, contract assistant professor from Mie University and all the members of Hanazato laboratory gave me their kind help and encouraged me. The author would like give a special thanks to them.

References

- [1] N. Theofanopoulos, T. Hanazato, and M. Watabe, "Seismic Response Analysis of Parthenon Columns," Proc. of STREMAH 89, pp339-348, 1989.
- [2] T. Hanazato, Y. Mabuchi, N. Theofanopoulos and M. Watabe "EARTHQUAKE RESISTANT CAPACITY OF PARTHENON," Proc. of the 9th Japan Earthquake Engineering Symposium, pp. 2007-2012, 1990.
- [3] M. Watabe, H. Aoki, and T. Hanazato, "Earthquake Resistant Capacity of the Parthenon," Proc. of the International Association for Bridge and Structural Engineering Symposium (IABSE), pp.345-352, 1993.
- [4] N. Theofanopoulos, T. Hanazato, K. Matsukawa and M. Watabe, "Analysis of Microtremor Records at Zeus-Olympeion Athens and Assessment of its Safety by Employing Dynamic Response Analysis", Proc. of STREMAH 89, pp319-328, 1989.
- [5] N. Theofanopoulos, T. Hanazato and M. Watabe, "Probabilistic Approach to Generate the Reference Motion for the Protection of Historical Monuments Against Earthquakes," Proc. of the 1st International Conference on Structural Repair and Maintenance of Historical Buildings (STREMAH 89), pp289-298, 1989.
- [6] Y. Mabuchi, T. Hanazato and M. Watabe, "Static shear friction tests on the model marble columns of the Parthenon for the aseismic retrofitting," Proc. of STREMAH 99, pp475-482, 1999.
- [7] G. C. Manos, "The dynamic performance of models of ancient columns and colonnades with and without the insertion of wires made of shape memory alloy," Proc. of STREMAH VI, pp281-290, 1999.
- [8] H. P. Mouzakis, I. N. Psycharis, D. Y. Papastamatiou, P. G. Carydis, C. Papantonopoulos and C. Zambas, "Experimental investigation of the earthquake response of a model of a marble classical column," Earthquake engineering and Structural Dynamics, 2002; 31: 1681-1698.
- [9] C. Papantonopoulos, I. N. Psycharis, D. Y. Papastamatiou, J. V. Lemos and H. P. Mouzakis, "Numerical prediction of the earthquake response of classical columns using the distinct element method," Earthquake engineering and Structural Dynamics, 2002; 31: 1699-1717.
- [10] S. Caddemi, I. Calio, F. Cannizzaro, M. Marletta and B. Panto, "Seismic Vulnerability of the Concordia Temple," Advanced Materials Research, Vols. 133-134 (2010), pp795-764, Trans Tech Publications, Switzerland.
- [11] P. G. Cardis, N. R. Tilford, G. E. Brandow, and J. O. Jirsa, "THE CENTRAL GREECE EARTHQUAKES OF FEBURUARY-MARCH 1981," A Reconnaissance and Engineering Report, Washington, D. C., NATIONAL ACADEMY PRESS, 1982.
- [12] 関隆司 編, "都市と文化財—アテネと大阪：大阪市立大学国際学術シンポジウム," 東信堂, 1998.

- [13] N. Oyaizu, “Earthquake Ground Motions and Structural Damage at the Parthenon Athens,” Bachelor thesis, Department of Architecture, Faculty of Engineering, Mie University, 2011.
- [14] N. N. Ambraseys, K. A. Simpson and J. J. Bommer, “PREDICTION OF HORIZONTAL RESPONSE SPECTRA IN EUROPE,” Earthquake engineering and Structural Dynamics, VOL. 25, 371-400, 1996.
- [15] 中央防災会議，東南海・南海地震等に関する専門調査会，“断層のモデル化，”
<http://www.bousai.go.jp/jishin/chubou/nankai/26/sankousiryoku2.pdf#search='断層のモデル化'>，
2011 年 12 月 11 日閲覧.

Appendix

The plan of the simplified miniature model of the Parthenon Athens

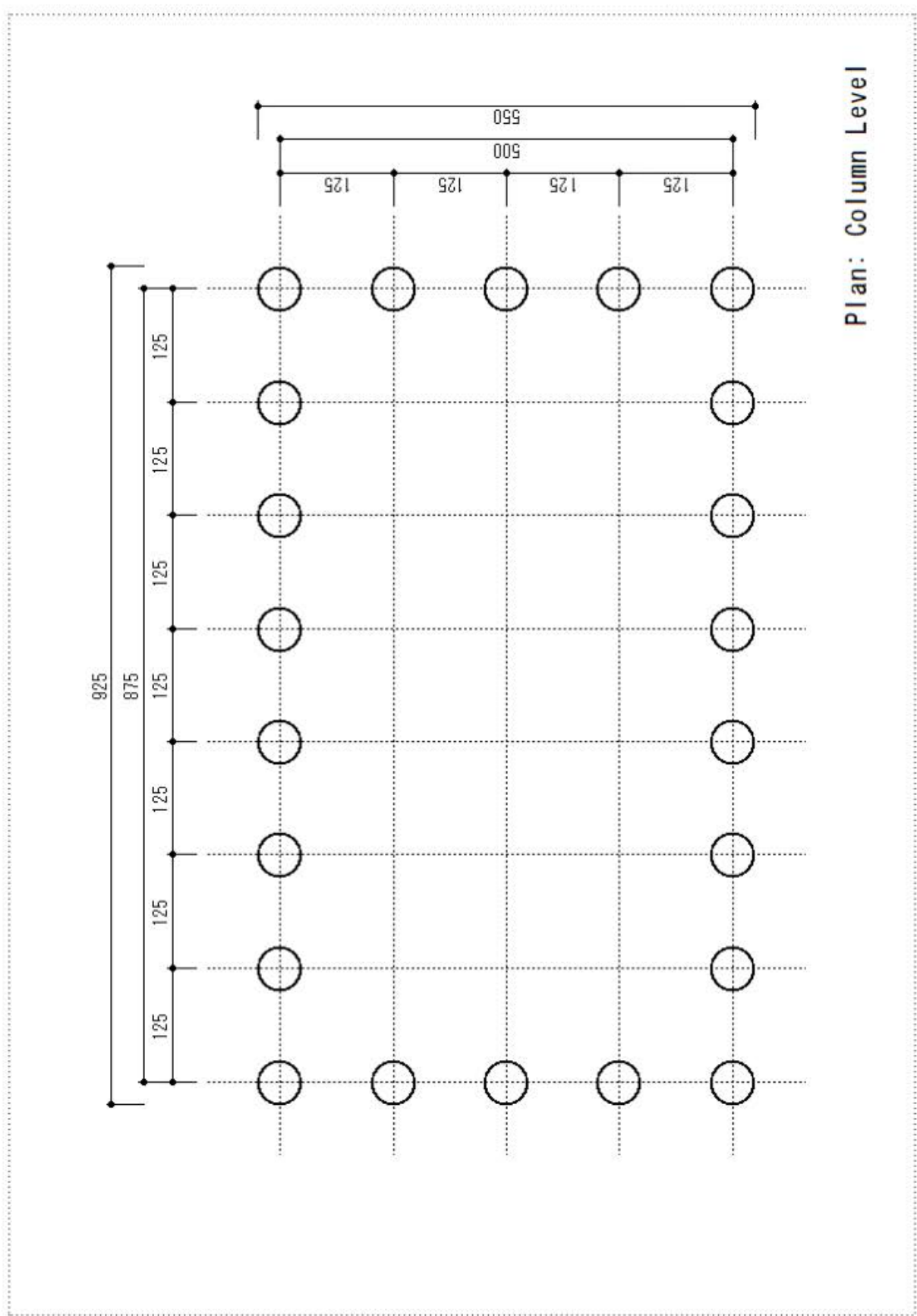


Fig. 84 Plan of the simplified miniature model (Dimension in *mm*)

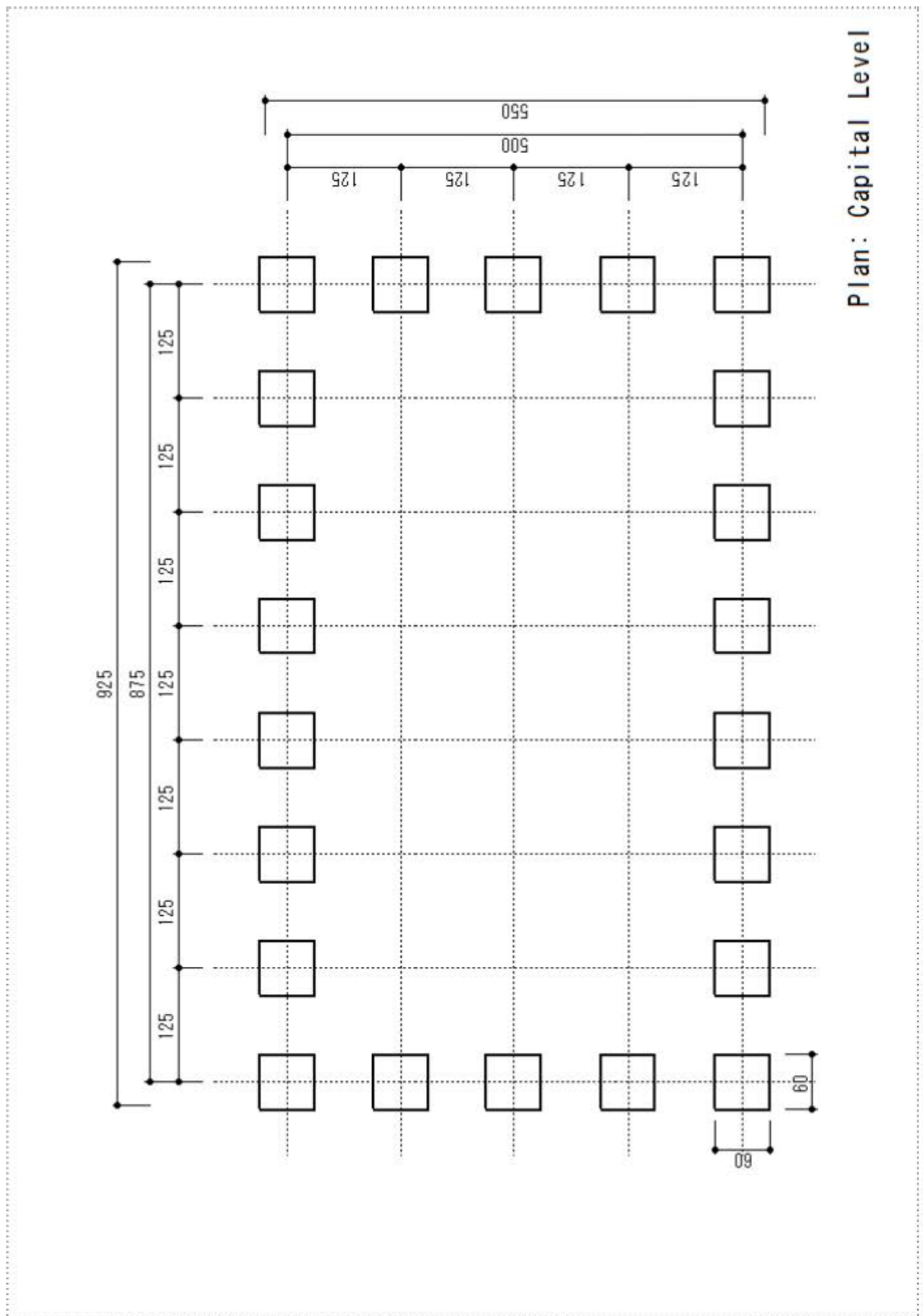


Fig. 85 Plan of the simplified miniature model (Dimension in *mm*)

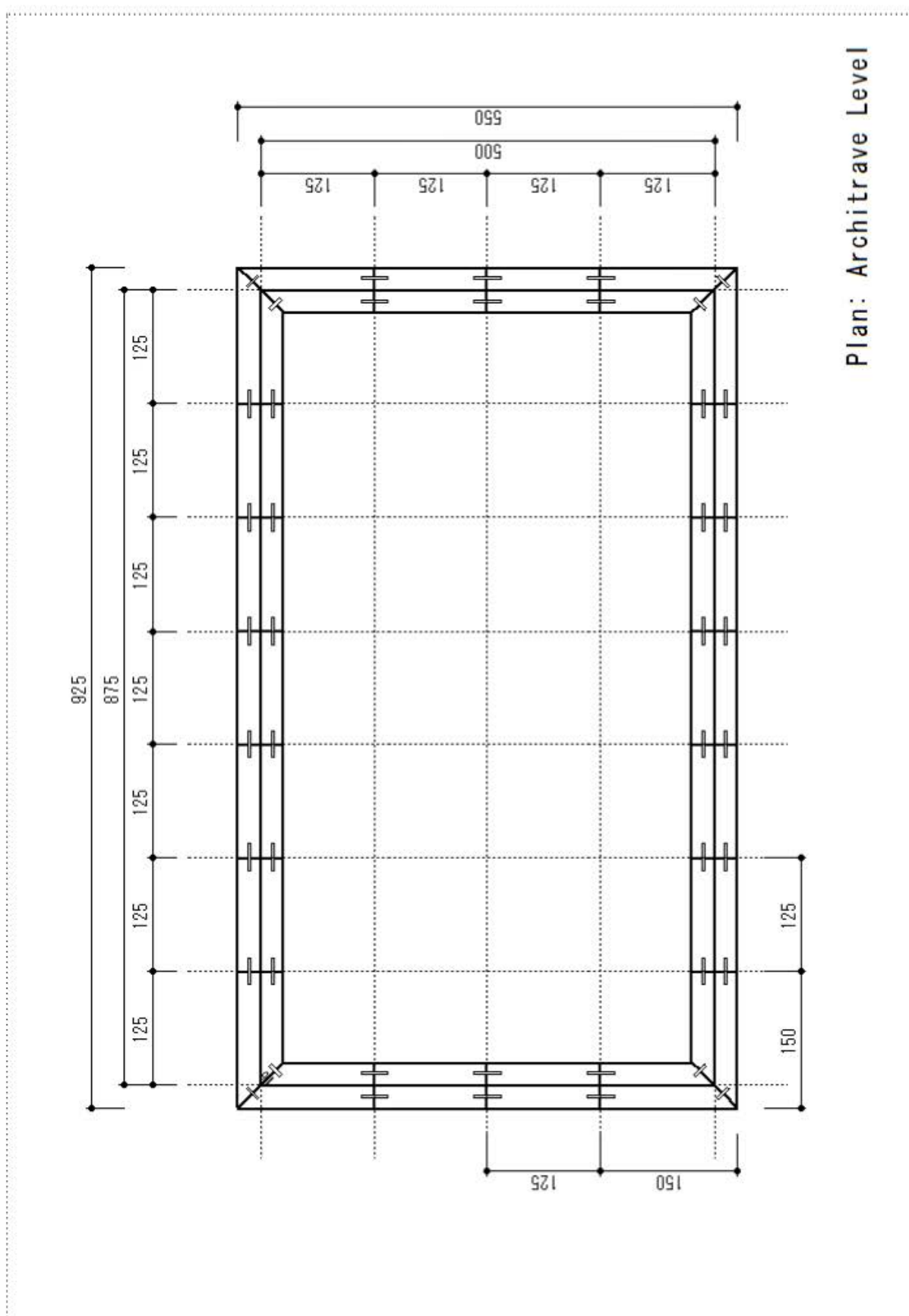


Fig. 86 Plan of the simplified miniature model (Dimension in *mm*)

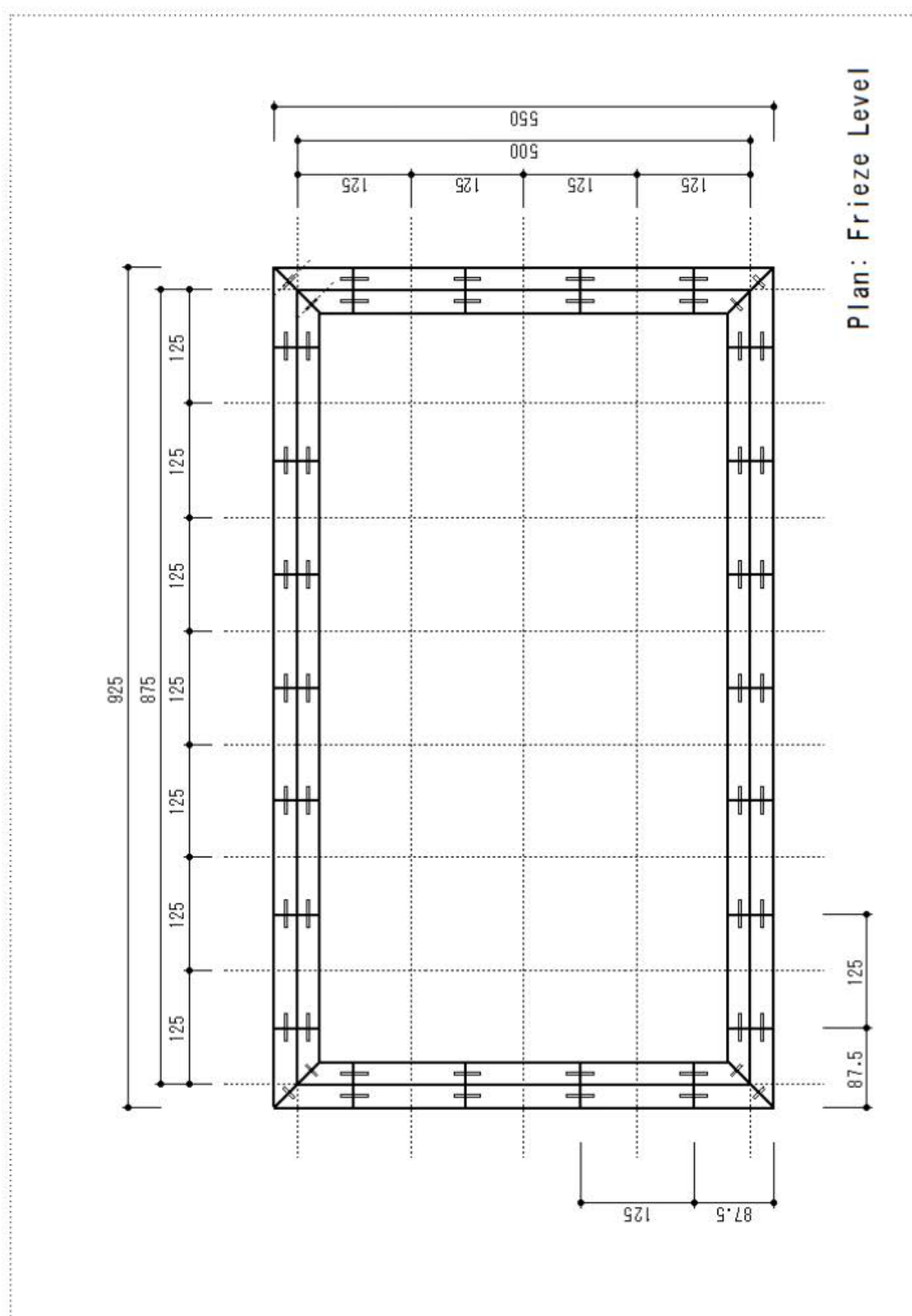


Fig. 87 Plan of the simplified miniature model (Dimension in *mm*)

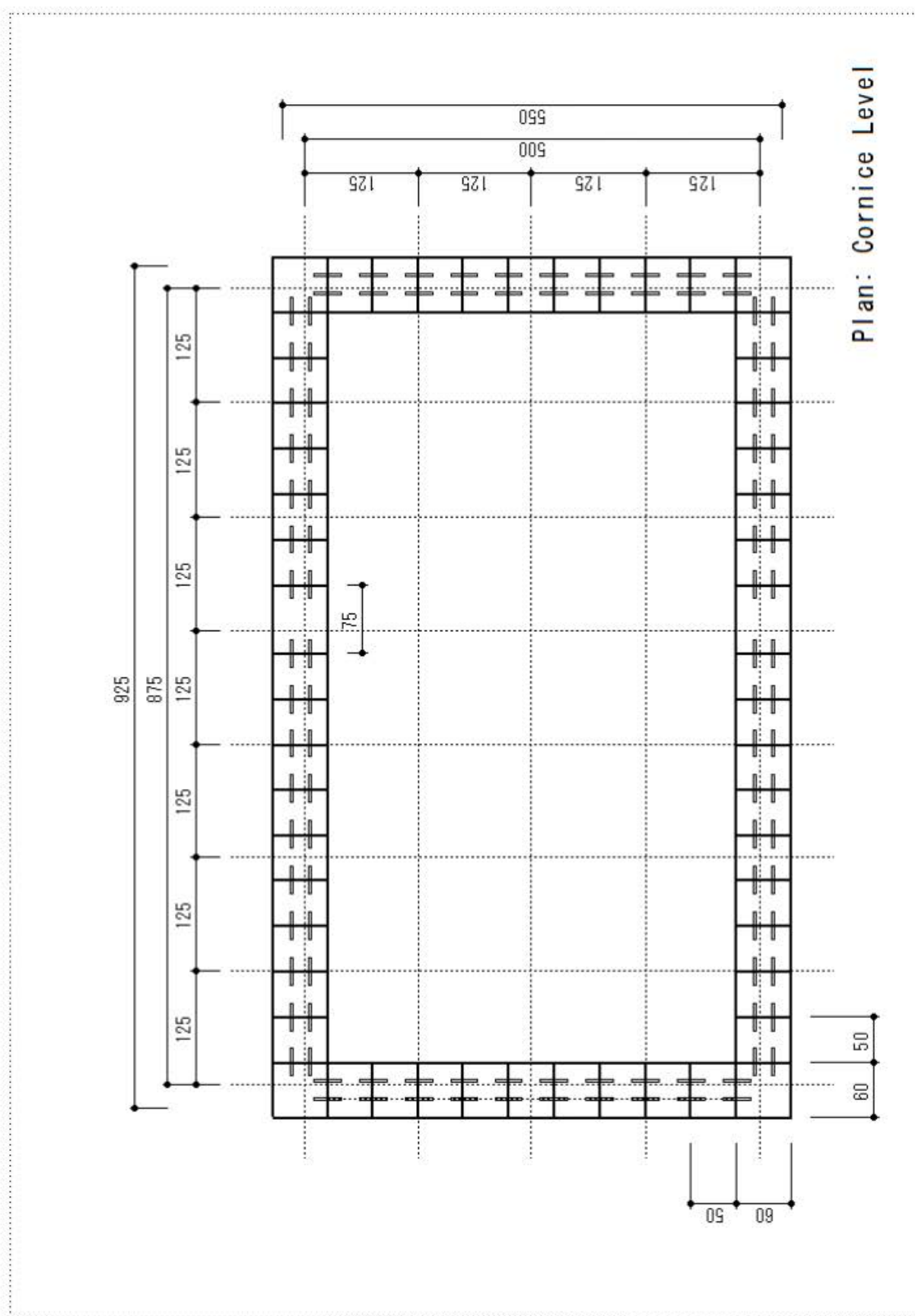


Fig. 88 Plan of the simplified miniature model (Dimension in *mm*)

Friction Coefficient Tests

Table 9 Friction coefficient between the capital and the architrave

| Weight (g) | Friction Coefficient | | | | | | | | | |
|------------|----------------------|-----------------|-----------------|-----------------|-----------------|------|-------|------|-------|------|
| | 1 st | 2 nd | 3 rd | 4 th | 5 th | | | | | |
| 91.1 | (33) | 0.36 | (40) | 0.44 | (44) | 0.48 | (54) | 0.59 | (45) | 0.49 |
| 223.1 | (116) | 0.52 | (139) | 0.62 | (185) | 0.83 | (135) | 0.61 | (174) | 0.78 |
| 355.5 | (194) | 0.55 | (201) | 0.57 | (206) | 0.58 | (238) | 0.67 | (221) | 0.62 |
| 487.7 | (286) | 0.59 | (263) | 0.54 | (252) | 0.52 | (243) | 0.50 | (245) | 0.50 |

()....Force (Dimension in g)

Average = 0.50

Table 10 Friction coefficient between the frieze and the cornice

| Weight (g) | Friction Coefficient | | | | | | | | | |
|------------|----------------------|-----------------|-----------------|-----------------|-----------------|------|-------|------|-------|------|
| | 1 st | 2 nd | 3 rd | 4 th | 5 th | | | | | |
| 127.7 | (41) | 0.32 | (40) | 0.31 | (54) | 0.42 | (56) | 0.44 | (64) | 0.50 |
| 259.7 | (118) | 0.45 | (116) | 0.45 | (113) | 0.44 | (133) | 0.51 | (136) | 0.52 |
| 392.1 | (213) | 0.54 | (206) | 0.53 | (208) | 0.53 | (208) | 0.53 | (234) | 0.60 |
| 524.3 | (281) | 0.54 | (308) | 0.59 | (292) | 0.56 | (318) | 0.61 | (275) | 0.52 |

()....Force (Dimension in g)

Average = 0.57